Title
Evaluation of Muscle Quality and Disease Severity in Individuals with Hip Osteoarthritis

Author
Bird, Alyssa

Publication Date
2022

Peer reviewed|Thesis/dissertation

Evaluation of Muscle Quality and Disease Severity in Individuals with Hip Osteoarthritis

by
Alyssa Bird

DISSERTATION
Submitted in partial satisfaction of the requirements for degree of
DOCTOR OF PHILOSOPHY

in

Rehabilitation Science

in the

GRADUATE DIVISION
of the
UNIVERSITY OF CALIFORNIA, SAN FRANCISCO

Approved:

DocuSigned by:
Victor Cheuy
CA6C3440E6CB456...

Victor Cheuy
Chair

DocuSigned by:
Sharmila Majumdar
[illegible]

Sharmila Majumdar

DocuSigned by:
Diane D. Allen
B6D079BF87ED421...

Diane D. Allen

Committee Members

EVALUATION OF MUSCLE QUALITY AND DISEASE SEVERITY IN INDIVIDUALS WITH HIP OSTEOARTHRITIS

Alyssa Bird

Abstract

Recent evidence suggests that muscle quality may play an important role in the pathogenesis of hip osteoarthritis (OA). Muscle quality describes the extent of adipose tissue accumulation, or fatty infiltration, within skeletal muscle, as adipose tissue stored within the muscle has the capacity to impair muscle function. The hip abductors are important pelvic stabilizers during gait; therefore, dysfunction of these muscles may impact joint loading and lead to degeneration of cartilage and bone. Despite evidence of increased fatty infiltration in individuals with hip OA, minimal research has evaluated muscle quality in a population with mild-to-moderate OA, and relationships of muscle quality with physical function, joint loading, and cartilage health have been sparsely characterized. In this study, chemical shift-based water-fat separated magnetic resonance (MR) imaging was used to quantitatively evaluate hip abductor muscle quality in a cohort of individuals with and without mild-to-moderate hip OA. Measures of hip abductor muscle quality were related to various disease outcomes including radiographic OA severity, patient-reported disability, functional performance, isometric strength, gait kinematics and kinetics, semi-quantitatively evaluated morphological cartilage degeneration, and biochemical cartilage composition evaluated using quantitative MR imaging. Hip abductor fatty infiltration was found to be significantly associated with worse patient-reported outcomes, functional impairment, cartilage

lesions, muscle weakness, and increased frontal plane joint loading. These findings suggest that hip abductor fatty infiltration may contribute to an abnormal mechanical loading environment at the joint, potentially leading to greater cartilage degeneration and disability. These findings are clinically relevant, as muscle quality may be a modifiable risk factor for OA which can be targeted through exercise intervention to improve disease outcomes.

Table of Contents

List of Figures

List of Tables

List of Abbreviations

30CRT	30-second Chair Rise Test
3D	Three-Dimensional
ADL	Activities of Daily Living
ANOVA	Analysis of Variance
B_0	Main Magnetic Field
B_1	Radiofrequency Field
BMI	Body Mass Index
CNN	Convolutional Neural Network
CSA	Cross-Sectional Area
CV	Coefficient of Variation
ECM	Extracellular Matrix
FF	Fat Fraction
FSE	Fast Spin Echo
GEE	Generalized Estimating Equation
GMED	Gluteus Medius
GMIN	Gluteus Minimus
GRF	Ground Reaction Force
HAM	Hip Adduction Moment
HOOS	Hip disability and Osteoarthritis Outcome Score
ICC	Intraclass Correlation Coefficient

IDEAL-IQ	Iterative Decomposition of Water and Fat with Echo Asymmetry and Least-Squares Estimation
IP	In Phase
KL	Kellgren-Lawrence
LV	Lean Volume
MAPSS	Magnetization-Prepared Angle-Modulated Partitioned K-Space Spoiled Gradient Echo Snapshots
MR	Magnetic Resonance
MRI	Magnetic Resonance Imaging
OA	Osteoarthritis
OP	Out of Phase
OR	Odds Ratio
PD	Proton Density
PDFF	Proton Density Fat Fraction
PG	Proteoglycan
QOL	Quality of Life
RF	Radiofrequency
SBP	Subchondral Bone Plate
SCT	Stair Climb Test
SEM	Standard Error of Measurement
SHOMRI	Scoring Hip Osteoarthritis with Magnetic Resonance Imaging
SNR	Signal to Noise Ratio
SPGR	Spoiled Gradient-Recalled Echo

SPM	Statistical Parametric Mapping
Sport	Recreation Function
STB	Subchondral Trabecular Bone
TE	Echo Time
TFL	Tensor Fascia Lata
TSL	Spin-Lock Time

1 Overview

Chapters 2-6 are intended as a general introduction to the epidemiology, pathophysiology, anatomy, and scientific methods relevant to this dissertation. Chapters 7-10 are presented as independent scientific studies which include study-specific background, methods, results, discussion, and conclusions. Chapter 11 serves as a synopsis of the important findings of the research presented in this dissertation and summarizes the clinical implications of this work.

2 Osteoarthritis

Osteoarthritis (OA) is degenerative disease of synovial joints primarily characterized by a degradation or loss of hyaline articular cartilage.[1] This chapter briefly discusses the epidemiology of the disease, risk factors for development and progression of OA, and current treatment options.

2.1 Prevalence and Burden

OA is a leading cause of disability worldwide, with approximately 27 million US adults estimated to have clinically defined OA.[2] OA is typically defined based on radiographic evidence of joint degeneration using standardized grading systems. Symptomatic OA, however, is defined by the presence of both radiographic evidence of OA and symptoms, thus the prevalence of symptomatic OA is often observed to be lower than that of radiographic OA. It is widely recognized that a discordance exists between structural and symptomatic disease, as several studies have demonstrated weak relationships between radiographic OA severity and pain; though, these relationships are stronger in cases of severe radiographic disease.[3–7]

Symptomatic OA in the hip and knee—the most common large joints affected by OA—poses a significant burden to the patient, as disease of these weight-bearing joints

significantly impacts an individual's ability to locomote, carry out activities of daily living, and diminishes overall quality of life.[2,8] It is estimated that approximately 40% of individuals aged 65 or older may have symptomatic hip or knee OA.[9,10] Economically, the impact of OA is substantial at both the individual and societal level due to direct costs of healthcare utilization, as well as indirect costs associated with lost productivity. In 2015, OA was estimated to account for approximately $40 billion in national hospital expenditures in the US.[11] Additionally, OA is related to a greater probability of work absenteeism, with aggregate costs estimated to be higher than any other major chronic disease at approximately $10 billion per year.[12]

2.2 Risk Factors

Increasingly, OA is recognized as a multifactorial process influenced by numerous local and systemic factors. While age is by far the most important risk factor for OA, genetic predisposition, obesity, female sex, increased bone mineral density, and joint laxity, malalignment, or injury have also been identified as risk factors.[13] Mechanical joint loading is widely accepted as a factor contributing to the development and progression of OA. Mechanical stress at the joints produces an imbalance of catabolic and anabolic processes which leads to cartilage degradation. Both underloading and overloading have been linked to OA-related degeneration suggesting that appropriate mechanical loading is important for cartilage health, while abnormal loading may be detrimental.[14] Obesity plays an important role in knee OA, and to a lesser extent in hip OA, as it not only imposes increased mechanical loads on joint

tissues, but also contributes to low-grade systemic inflammation through the release of proinflammatory mediators from adipose tissue (discussed in Chapter 3).[14]

2.3 Current Treatment Options

Current treatment options for OA are limited. In the hip and knee, therapies are aimed at reducing pain, improving mobility, and preventing progression of structural degeneration.[15] These treatment options include non-pharmacological, pharmacological, and surgical approaches. Non-pharmacological modalities include patient education, physical therapy, use of assistive devices, weight reduction or management, as well as aerobic, strengthening, or range of motion exercises. Pharmacological treatments include the use of analgesics and non-steroidal anti-inflammatory drugs, corticosteroid injections, and opioids when pain is unresponsive to more conservative management. Surgical options include joint replacement, osteotomy, lavage, and arthroscopic debridement depending on severity of disease and disability. While these treatment recommendations are evidence-based and have been developed by an expert consensus,[15] no treatments currently exist which halt the progression of cartilage and bone degeneration or reverse existing structural joint damage. A better understanding of risk factors and biomarkers of early-stage disease is needed to develop and tailor treatment plans aimed at preventing or slowing joint degeneration.

3 Musculoskeletal Tissue in Osteoarthritis

Although articular cartilage has received the most attention in the context of OA research, the disease is increasingly recognized as a whole-organ condition which involves all joint tissues including subchondral bone and periarticular soft tissues such as muscle.[16,17] Tissue structure, function, and OA-related degenerative changes relevant to the work discussed in this dissertation are described in this chapter.

3.1 Articular Cartilage

Articular cartilage is a smooth, viscoelastic tissue which covers the ends of long bones of articulating joints whose primary function is to provide a low-friction surface for articulation and to facilitate load transmission.[18] The articular cartilage is approximately 2 to 4 mm thick and is avascular and non-innervated, receiving its nutrients via diffusion from the synovial fluid and subchondral bone.[18] Cartilage consists of a dense extracellular matrix (ECM) and low density of highly specialized chondrocytes which continually remodel cartilage by synthesizing components of the ECM.[19] The ECM is primarily composed of water (up to 80% of cartilage weight), type II collagen, and proteoglycans (PG). These components allow for water retention in the ECM, which is essential to maintaining its mechanical properties.[20]

Articular cartilage can be divided into zones as shown in Figure 3.1: superficial, middle (transitional), deep, and calcified zones. The thin superficial zone consists of tightly packed type II collagen fibrils oriented parallel to the articular surface. This zone primarily acts to resist shear forces and is critical to maintaining the health of deeper zones.[18] The middle zone contains a higher density of PG and thicker collagen fibrils oriented oblique to the articular surface and mainly acts to resist compressive forces.[18] The deep zone provides the greatest resistance to compressive forces, as it contains the greatest density of PG, lowest water content, and has the thickest collagen fibrils which are oriented perpendicular to the articular surface. The calcified zone is separated from the deep zone by the tidemark and plays an important role anchoring cartilage to subchondral bone. This zone is permeable to small molecules and allows for biochemical interaction between the non-calcified articular cartilage and subchondral bone.[21]

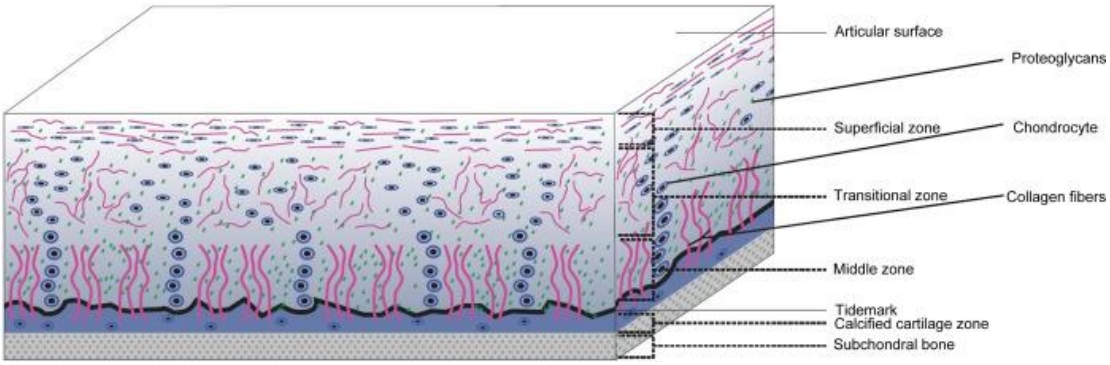

Figure 3.1. Schematic of cartilage extracellular matrix (ECM) and subchondral bone structure. Middle and deep zones labeled as “transitional” and “middle”, respectively. Figure reproduced with permission of Elsevier, from Comparative Kinesiology of the Human Body.[22]

While not fully understood, OA is thought to occur as a result of an imbalance of synthesis and degradation of ECM components.[23] This imbalance leads to a

deterioration in the structural integrity and material properties of the cartilage. In early stages of OA, degenerative changes to articular cartilage include increased hydration, PG loss, and thinning or disruption of the collagen network.[24,25] In later stages of disease, cartilage becomes dehydrated and fibrillated, resulting in a partial or full thickness loss of cartilage which may expose subchondral bone.[26] These changes are shown in Figure 3.2. Due to a low density of chondrocytes and lack of blood vessels, lymphatics, and nerves, articular cartilage has a limited capacity for intrinsic healing and repair[27]; thus, early identification and prevention of degenerative changes to the tissue is critical for maintaining joint health. Evaluation of these early signs of OA-related degeneration will be discussed in Chapter 4.

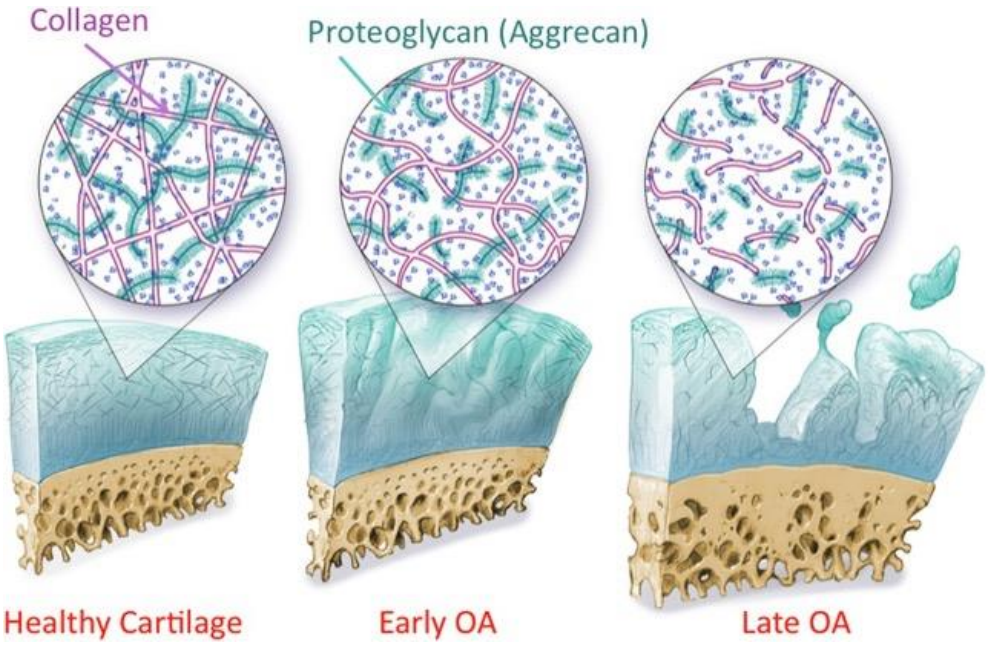

Figure 3.2. Stages of osteoarthritis (OA)-related articular cartilage degeneration. Early-stage OA degeneration includes increased hydration, proteoglycan loss, and thinning or disruption of the collagen network. Late-stage OA degeneration includes decreased hydration and extensive fibrillation and cartilage thinning. Figure reproduced with permission of Wiley, from Quantitative MRI of articular cartilage and its clinical applications.[28]

3.2 Subchondral Bone

Similar to articular cartilage, the function of subchondral bone is to absorb, distribute, and transfer loads across the joint.[29] Subchondral bone refers to the bone components lying deep to the calcified cartilage zone including the subchondral bone plate (SBP) and the cancellous subchondral trabecular bone (STB). Immediately beneath the calcified cartilage zone lies the SBP, a thin cortical lamella which contains channels that allow for direct chemical signaling between chondrocytes and subchondral bone cells.[30] Deep to the SBP is the subchondral trabecular bone (STB). The STB is highly porous and metabolically active, as it contains blood vessels, nerves, and bone marrow. The STB serves as a shock-absorbing and supportive tissue and may also be important for supplying cartilage with nutrients to support metabolism.[21] Subchondral bone is dynamic and able to adapt to mechanical forces transmitted across the joint by adjusting trabecular orientation and scale in relation to stress over time.[31] As such, mechanical stress plays an important role in modifying subchondral bone by way of modeling (formation of new bone) and remodeling (changes to tissue organization and composition).[29]

Along with cartilage degeneration, OA is characterized by changes to the subchondral bone including sclerosis, remodeling of the trabeculae, formation of new bone at the joint margins (osteophytes), and development of bone marrow lesions and subchondral cysts.[23,32] These changes may lead to increased bone stiffness which minimizes the capacity for bone to absorb shock.[30] Together, degenerative changes to the subchondral bone and articular cartilage contribute to joint space narrowing. The

hallmarks of OA such as joint space narrowing, osteophyte formation, and sclerosis will be discussed further in Chapter 4.

3.3 Skeletal Muscle

The structure and function of skeletal muscle is a growing area of interest in OA research. Biomechanically, the primary function of muscle is to convert chemical energy into mechanical energy in order to generate force needed to produce movement.[33] Skeletal muscle is a complex, highly organized tissue composed primarily of contractile tissue, though it also contains connective tissue, blood vessels, and nerves.[34] Muscle (Figure 3.3) is composed of bundles of long, threadlike muscle fibers (myofibers). Each muscle fiber is made up of many myofibrils composed of overlapping thick and thin filaments that are arranged longitudinally into sarcomeres. Sarcomeres are responsible for the shortening and lengthening contractions of muscle.[35]

Bundles of myofibers make up the fascicles, and bundles of fascicles form the muscle. Muscle fibers, fascicles, and muscles are encased in a non-contractile ECM referred to as the endomysium, perimysium, and epimysium, respectively.[34] The ECM enables uniform distribution and transmission of force within the muscle and from muscle to tendon.[35] The force produced by muscle contraction is transmitted via this connective tissue network and tendons to the skeletal system in order to produce or control movement. The capacity for a muscle to generate force is dependent on many factors including muscle size, architecture of muscle fibers and the angle at which they insert into the tendon (pennation angle), and the quality of the interaction between the cellular elements.[33]

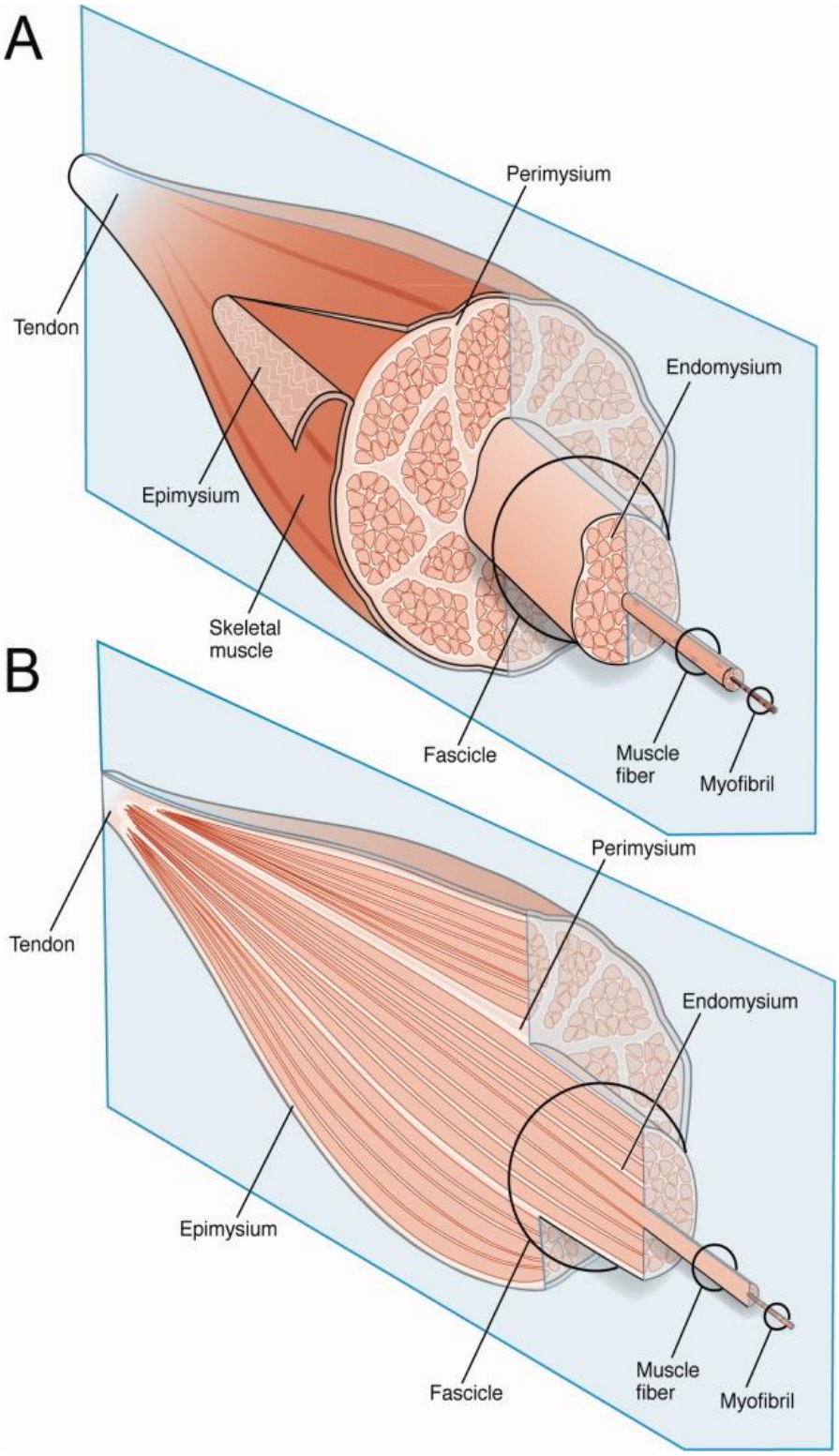

Figure 3.3. Schematic diagram of gross organization of muscle tissue. Figure reproduced with permission of Wiley, from Structure and Function of the Skeletal Muscle Extracellular Matrix.[34]

It is now well-established that a loss of muscle mass and an accumulation of adipose tissue in skeletal muscles are common features of aging and disease.[36,37] While the cause of increased accumulation of adipose tissue is not well-understood, mounting evidence suggests that these changes may be important in the OA disease process, as several recent studies have demonstrated increased fatty infiltration and/or decreased muscle size in individuals with hip and knee OA.[38–43] These changes are of particular interest in OA, as reduced muscle size and accumulation of fat in ectopic depots may have important implications for periarticular muscle function and joint health (further discussed in Chapter 5). However, minimal research has investigated the relationship between fatty infiltration and disease severity or functional impairment, particularly in the context of OA.

Fatty infiltration of skeletal muscle refers to the storage of lipids deep to the fascia of the muscle.[37] This includes accumulation of lipids stored directly within the muscle fibers themselves (intramyocellular), as well as within adipocytes which accumulate in the skeletal muscle between muscle fibers (intramuscular) or between muscle fascicles or muscle groups (intermuscular) as shown in Figure 3.4. Accumulation of adipocytes in these ectopic depots may arise from adipogenic differentiation of various stem cell populations in the skeletal muscle such as satellite cells and fibroadipogenic progenitors.[44] Adipose tissue stored in skeletal muscle releases proinflammatory cytokines which are thought to contribute to local inflammation of muscle,[45–48] as well as systemic, whole-body inflammation.[45] Increased levels of systemic and local (to locomotor muscles) proinflammatory cytokines have been linked to reduced muscle force and mobility impairment.[48–51] Additionally,

proinflammatory cytokines not only have the capacity to impair muscle function, but may also directly contribute to degradation of surrounding joint tissues such as the cartilage ECM.[52–54]

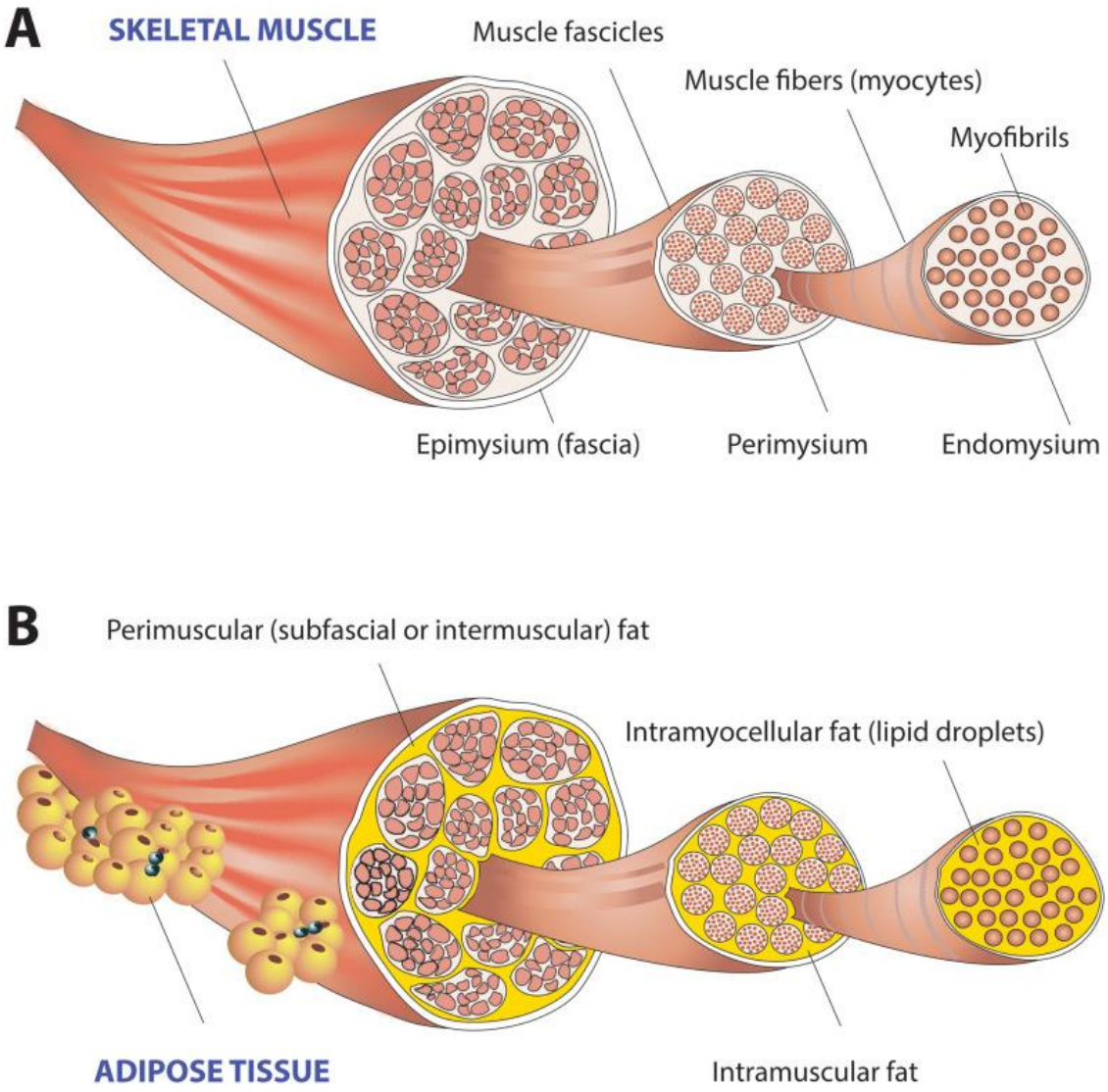

Figure 3.4. Schematic diagram of (A) skeletal muscle and (B) fatty infiltration of skeletal muscle. Fatty infiltration may be classified as intramyocellular, intramuscular, or intermuscular. The term inter-muscular fat is also commonly used to describe adipose tissue stored between muscle groups. Figure reproduced with permission of Altajar and Baffy, from Skeletal Muscle Dysfunction in the Development and Progression of Nonalcoholic Fatty Liver Disease.[55]

Fatty infiltration is thought to alter the metabolic environment of muscle fibers by stimulating local catabolic processes and inhibiting anabolic processes, leading to a loss of muscle mass and impaired muscle function.[37,44,56] Proinflammatory cytokines released by adipose tissue are linked to decreased insulin sensitivity which can impair protein synthesis in muscle.[57] Additionally, adipose tissue may contribute to a shift in muscle fibers from type II to type I.[58] Mechanically, adipose tissue occupies space in the muscle and may alter muscle fiber pennation angle and elasticity.[59–61] Together, the negative metabolic and mechanical effects of fatty infiltration are thought to contribute to muscle dysfunction via reduced force generation per unit of cross-sectional area (CSA) of muscle. Thus, the ratio of adipose tissue to lean muscle has come to be described by the term “muscle quality”. Evaluation of muscle quality will be discussed in Chapter 4.

4 Imaging Joint Tissues in Osteoarthritis

Biomedical imaging represents one of the most useful tools for evaluating OA degeneration, as it is non-invasive and can provide detailed information about the morphology and composition of tissues affected in the disease process. This chapter describes the imaging modalities used to evaluate joint tissues such as those discussed in Chapter 3. The strengths and limitations of these modalities will be addressed with an emphasis on applications relevant to the work presented in this dissertation.

4.1 Radiography

Radiography or x-ray imaging is one of the most cost-effective and widely available imaging tools used to evaluate OA in both clinical and research applications. Radiographs are primarily used to evaluate features such as joint space width and other bone abnormalities such as osteophytes, sclerosis, and subchondral cysts which may indicate the presence of OA. Grading systems such as the Kellgren-Lawrence (KL) score[62] may be used to semi-quantitatively evaluate these features and indicate presence and severity of OA on a scale from 0 to 4, with 0 indicating no radiographic evidence of OA and 4 indicating severe OA. Radiography also has several limitations including an inability to directly visualize cartilage and other non-calcified structures; therefore, cartilage thickness and degeneration can only be inferred from joint space narrowing and presence of other bone abnormalities. Additionally, because radiography is a projection method, this modality is subject to morphological distortion, magnification, and superimposition of overlapping structures which may affect joint measures.[63] Furthermore, x-ray imaging exposes patients to harmful ionizing radiation.

4.2 Magnetic Resonance Imaging

Although comparatively expensive and time-intensive, magnetic resonance (MR) imaging or MRI provides excellent contrast and spatial resolution for multiplanar tomographic imaging of tissues not visible on radiographs. This imaging modality is relatively safe as it does not expose patients to ionizing radiation and instead transfers energy in the form of heat. MR imaging is used to map signals from tissues which are high in hydrogen nuclei (protons) such as water and fat. Various MR sequences can be utilized to provide different image contrasts which allow for targeted evaluation of specific tissues such as cartilage or muscle.

MR sequences differ depending on how the net magnetization of tissue changes or relaxes in the presence of a strong external magnetic field (B_0) after the application of a radiofrequency (RF) pulse (B_1). Common contrast mechanisms used in musculoskeletal applications include T_1-weighted, T_2-weighted, and proton density (PD) or intermediate-weighted sequences. T_1 relaxation describes the time it takes for protons to return to ~63% of their initial longitudinal magnetization; T_2 relaxation is the time it takes for protons to regain ~37% of their transverse magnetization and is characterized by an exponential decay.[64] T_2* relaxation is the effective T_2 which incorporates magnetic field inhomogeneities from the scanner and tissue susceptibility and is thus faster than T_2.[64] PD sequences reflect the density of protons per volume of tissue. The relaxation time of a tissue varies based on its structure and biochemical composition which affect its magnetic properties. Additionally, various forms of fat suppression can be used to exclude signal from fat to highlight other tissues. These

principles form the foundations for MR imaging and the development of specialized sequences which may be used to evaluate joint tissue morphology and composition.

4.2.1 Clinical Cartilage Imaging

Articular cartilage is primarily composed of water and is therefore an excellent target for MR evaluation. MR imaging may be utilized to provide both morphological and compositional information about articular cartilage. Clinical evaluation of articular cartilage is typically performed using intermediate-weighted fast spine-echo (FSE) sequences with or without fat suppression. Fat suppression allows for improved contrast between cartilage and surrounding tissue such as bone, however this process results in a loss of signal. Thus, non-fat suppressed images offer higher spatial resolution and better signal to noise ratio (SNR) for visualizing articular cartilage.[28] Multiple systems for standardized, semi-quantitative grading of cartilage morphology and other degenerative changes in OA have been developed for 1.5T and 3T MR imaging.[65,66] The Scoring Hip OA with MRI (SHOMRI) system described in Chapter 9 has shown good intra- and inter-rater reliability and sensitivity for detecting cartilage lesions in acetabular and femoral cartilage.[66,67] These scoring systems are highly valuable in research applications which evaluate disease severity and track OA progression. However, there are limitations of morphological cartilage grading including the requirement for trained clinicians to evaluate images which can be a time-intensive manual process.

4.2.2 Quantitative Cartilage Imaging

MR imaging can also be employed to provide quantitative information on the biochemical composition of articular cartilage using biomarkers of cartilage ECM

composition such as $T_{1\rho}$ and T_2 relaxation. This advanced application of MR imaging involves long scan times with intensive image processing requirements and therefore is not yet feasible for clinical applications. Nonetheless, quantitative MR imaging of articular cartilage is a rapidly growing area of interest in OA research given its ability to quantify early degenerative changes to cartilage composition which may precede morphological changes.[28]

$T_{1\rho}$-weighted MR sequences use a spin-lock pulse to lock magnetization in the transverse plane while applying a continuous RF pulse. $T_{1\rho}$ relaxation probes the slow-motion interactions between motion-restricted water molecules and their macromolecular environment.[68] A loss of macromolecules such as PG in the cartilage ECM which restrict motion of water molecules can be reflected by $T_{1\rho}$ measures.[28] T_2 relaxation reflects the mobility and energy exchange of free water protons inside the cartilage matrix. Damage to the collagen-PG matrix such as collagen disruption and increased hydration that occurs in cartilage degeneration can be reflected by T_2 measures.[28] Due to the curvature of cartilage on articular surfaces and its layered structure with varying collagen fiber orientation, cartilage T_2 measures are susceptible to the magic angle artifact. The magic angle effect describes a localized increase in T_2 relaxation time in regions of collagen fibrils which are aligned 55° relative to B_0.[69] Quantification of $T_{1\rho}$ and T_2 relaxation times is performed by fitting each voxel of the $T_{1\rho}$- or T_2-weighted images acquired at different spin-lock times (TSLs) or echo times (TEs) to an exponential decay function (described in Chapter 10). Image segmentation can then be performed to define the cartilage region of interest, visualize cartilage relaxation maps as shown in Figure 4.1, and quantify relaxation times in specific regions.

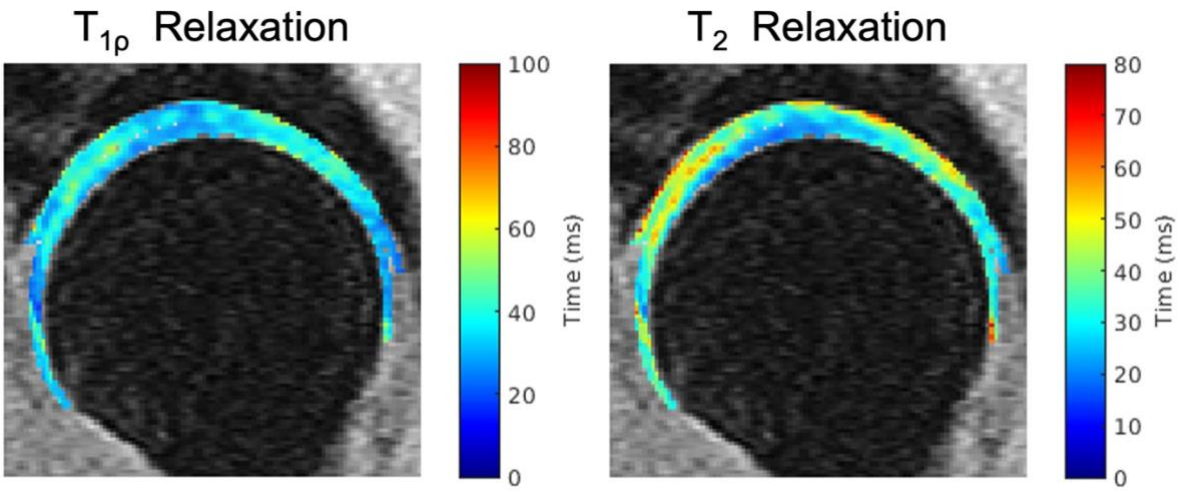

Figure 4.1. $T_{1\rho}$ and T_2 relaxation maps of hip cartilage showing the spatial distribution of relaxation times in the acetabulum and femoral head.

Both $T_{1\rho}$ and T_2 relaxation times provide indirect measures of cartilage ECM composition. Ex vivo studies have shown $T_{1\rho}$ relaxation to be sensitive and specific to PG content in articular cartilage, with $T_{1\rho}$ relaxation times increasing linearly with decreasing PG content.[70–72] In vitro studies have shown that T2 correlates with water content but poorly with PG content.[71] However, T_2 relaxation can provide specific information about collagen organization[73] with increased T_2 relaxation times indicating increased water content and greater disorganization of the collagen network.[73,74] In vivo, elevated $T_{1\rho}$ and T_2 have been observed in individuals with OA and have been associated with OA severity.[75–77] In individuals with no visible signs of morphological cartilage degeneration, elevated $T_{1\rho}$ has also been observed.[75] These findings highlight the capability for $T_{1\rho}$ to detect early compositional changes. Thus, these imaging biomarkers may allow for the development of treatment strategies which target early-stage disease and prevent or slow the progression of OA.

4.2.3 Clinical Muscle Imaging

MR imaging is widely used for visualizing muscle tissue and evaluating muscle quality. For clinical evaluation of muscle, T_1-weighted MR images are commonly acquired[78] and the degree of fatty infiltration of the muscle may be semi-quantitatively graded for clinical or research purposes. The most common grading system used in the evaluation of fatty infiltration of muscle is the Goutallier classification system, originally developed for evaluation of computed tomography images and adapted for use in MR imaging.[79–81] The Goutallier classification system is a relatively fast and simple method for evaluating muscle quality in which fatty infiltration of skeletal muscle is graded on a scale from 0 to 4. However, these semi-quantitative methods have been shown to have poor reproducibility and overestimate fat content.[82–84]

4.2.4 Quantitative Muscle Imaging

Using standard T_1-weighted MR sequences, muscles may be segmented to obtain measure of muscle CSA or volume. However, T_1-weighted images are not recommended for quantifying fatty infiltration, as the signal intensity of the image is not directly related to fat content in the muscle and this imaging method is susceptible to B_1 and B_0 inhomogeneities.[85] Thus, highly specialized water-fat separated MR sequences have been developed which allow for accurate quantification of fat content within the muscle with high spatial resolution. These techniques, known as chemical shift-based water-fat separation methods, exploit the difference in precessional frequencies between water and fat protons and can be implemented with advanced algorithms which allow for the accurate quantification of fat content. Chemical shift-based water-fat

separation techniques separate the MR signal into its water and fat components by acquiring images at two or more TEs after excitation. In the most basic dual-echo approach, two echoes are acquired—one at a TE in which water and fat are “out of phase” (OP) and one at a TE in which water and fat are “in phase” (IP). This method is considered a magnitude-based approach, as the magnitude of the signals from these images is combined to produce water-only and fat-only images using the equations below, where S represents the image signal:

$$S_{Water} = |S_{IP} + S_{OP}|$$

$$S_{Fat} = |S_{IP} - S_{OP}|$$

Then, the signal fat fraction (FF), η, can be calculated as the signal from fat divided by the combined signal from fat and water:

$$\eta = \frac{S_{Fat}}{S_{Water} + S_{Fat}}$$

Notably, the signal FF is confounded by several factors. Specifically, the spectral complexity of fat, T_2* decay, and T_1 bias effects must be considered when determining fat content in tissue.[86–90] Only when all of these confounding factors are addressed in the separation of water and fat does the signal FF equate to the proton density fat fraction (PDFF) where PDFF is defined as the fraction of mobile protons attributable to triglyceride fat relative to the total density of mobile protons that are MR visible.[90] To address this, more advanced methods for separating water and fat signals have been developed which consider these confounding factors. One such implementation of this is pulse sequence and image reconstruction software known as GE’s (GE Healthcare, Waukesha, WI) IDEAL-IQ (iterative decomposition of water and fat with echo

asymmetry and least-squares estimation). The IDEAL-IQ approach uses multiple asymmetrically spaced TEs and performs water-fat separation using an iterative least-squares decomposition algorithm.[91] This approach estimates and corrects for T_2* decay, models the spectral profile of fat as multiple peaks rather than a single peak, uses a low flip angle to minimize T_1 bias, and accounts for other confounding factors such as noise bias, and eddy currents in its decomposition algorithm.[91–94] IDEAL-IQ generates FF maps as seen in Figure 4.2 in which the signal FF is equal to the PDFF, and thus the signal intensity of each voxel is directly related to its fat content.

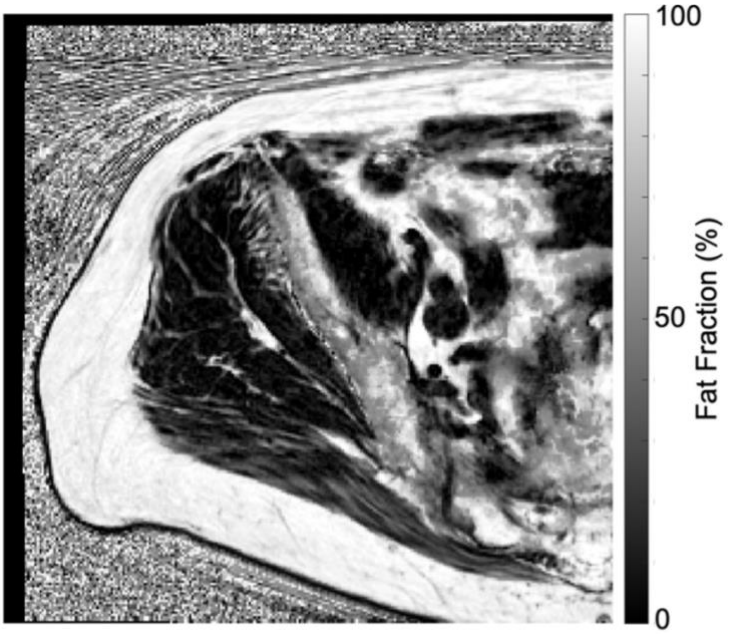

Figure 4.2. IDEAL-IQ axial fat fraction map of the gluteal muscles.

Though this FF measure provides only a relative estimate of fat content which may be affected by the presence of edema or fibrosis, it has been shown to strongly correlate with MR spectroscopy and fat mass in several tissues including skeletal muscle.[88,95,96] These images can then be segmented and muscle quality can be

characterized as the average FF of the voxels in the segmented region. Additionally, lean volume (LV) of each voxel can be calculated by subtracting the fat volume from the voxel using the equation below, where ν is the volume of the image voxel:

$$LV_{voxel} = (100 - FF_{voxel}) \cdot \nu$$

Then, the sum of the LV of all voxels in the segmented region can be calculated to determine overall LV of the muscle. IDEAL-IQ provides a method to evaluate both muscle quality and muscle size with the ability to quantify not only the overall volume of the muscle, but also its FF and LV.

5 Muscle Quality in Hip Osteoarthritis

Thus far, OA and its affected tissues have been discussed in the context of both the hip and knee joints. The focus of the remainder of this dissertation is the hip joint. The hip is a ball and socket synovial joint formed by the articulation between the acetabulum of the pelvis and the head of the femur. Currently, there is a paucity of research investigating the relationship between muscle quality and hip OA. Given the capacity for adipose tissue stored in the muscle to release proinflammatory mediators and impair muscle function, there is a growing interest in the role of muscle structure and function in the development, progression, and severity of hip OA.

5.1 Hip Abductor Muscles

The hip abductor muscles play a critical role in gait as they act to stabilize the hip and pelvis in the frontal plane during single-limb stance.[97] This action generates an internal abduction moment which balances the external hip adduction moment caused by the external ground reaction force which acts medial to the hip joint.[98] Pathology of these muscles is implicated in the OA disease process, as individuals with hip OA commonly demonstrate hip abductor weakness.[99,100]

The gluteus medius (GMED), gluteus minimus (GMIN), and tensor fascia lata (TFL) form the hip abductor muscle group (Figure 5.1). The GMED is the largest of the hip abductors and accounts for approximately 70% of the total abductor volume.[101] The GMED attaches proximally on the upper external surface of the ilium and distally to the lateral and superior-posterior aspects of the greater trochanter.[102] The GMIN lies deep and slightly anterior to the GMED, making up approximately 20% of the total abductor volume.[101] Its proximal attachment also arises from the external surface of the ilium and it attaches distally on the anterior-lateral aspect of the greater trochanter. The GMIN tendon has also been described as having attachments on the anterior and superior hip joint capsule and may play a role in modulating capsule stiffness.[103] Both the GMED and GMIN are multipennate muscles. The TFL is the smallest of the hip abductors, making up approximately 10% of the total abductor volume.[101] The TFL arises from the lateral aspect of the anterior superior iliac spine and attaches distally into the iliotibial band which inserts on the lateral condyle of the tibia.

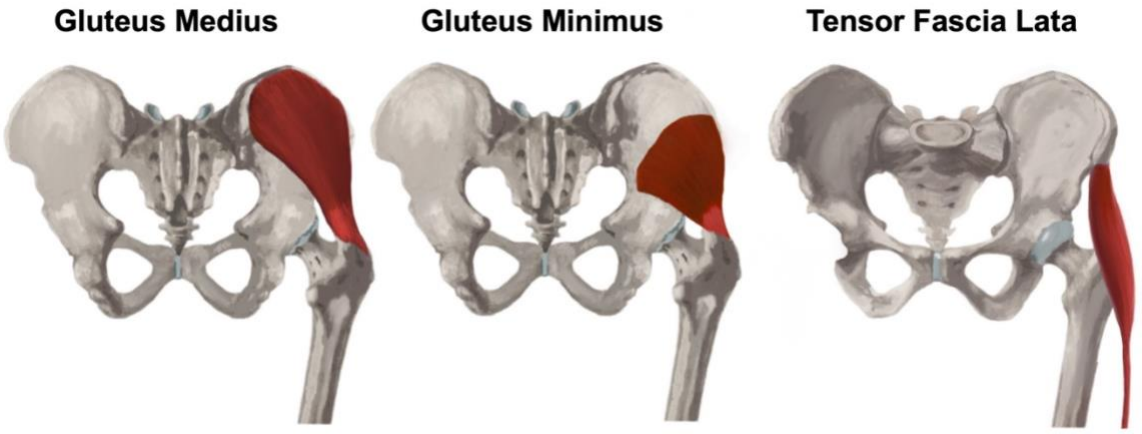

Figure 5.1. Illustration of the hip abductor muscles. Insertion of iliotibial band on the lateral condyle of the tibia not shown.

5.2 Muscle Function and Joint Health

The mechanical loading environment of the joint plays an important role in the development and progression of OA.[14] The function of the joint as a load-bearing structure is dependent on the structural and functional integrity of all its components including articular cartilage and the periarticular muscles which act at the joint. As discussed in Chapter 3, the primary function of muscles is to generate forces which produce movement. In doing so, these forces press the articular surfaces together at joints such as the hip. Thus, forces produced by muscles account for most forces transmitted by the joint. In normal gait, muscles contribute to approximately 95% of the resultant contact force acting at the hip with large contributions from the hip abductors—primarily GMED—throughout the stance phase.[104]

Both underloading[105,106] and overloading[107,108] have been shown to contribute to degenerative changes associated with OA. Intuitively, weakness of the hip abductor muscles would be expected to reduce joint contact forces, as less force is generated by the muscles and transmitted by the acetabulum and femoral head. However, simulations of hip abductor muscle weakness in normal walking have demonstrated that compensatory forces from other muscles may lead to increased joint contact forces in the presence of weakness.[109] Additionally, hip abductor weakness is thought to contribute to a contralateral pelvic drop during single-limb stance resulting in a shift of the body's center of mass away from the stance limb. This shift may result in an increased external hip adduction moment and increased loading of the hip joint.[110] Therefore, muscle weakness or impaired muscle function may contribute to abnormal joint loading, potentially placing the joint at greater risk for OA-related degeneration.[111]

Given the capacity for adipose tissue stored within the muscle to metabolically and mechanically impair muscle function and the close link between muscle quality and muscle weakness[112,113], hip abductor muscle quality may be of great importance in modulating the mechanical loading environment of the hip joint.

With increasing evidence that muscle quality may play a role in the function of skeletal muscle in aging and disease processes,[37,44,113,114] studies have recently begun to explore relationships between hip abductor muscle quality and hip OA. These studies have primarily focused on establishing differences in hip abductor muscle size and fatty infiltration between individuals with and without radiographically defined OA, and have largely consisted of end-stage hip OA cohorts.[40–43,115,116] While several of these studies have demonstrated increased fatty infiltration[40–43] and decreased muscle volume[40,42,115] associated with radiographic and symptomatic hip OA, few studies have explored the functional implications of hip abductor muscle quality on mobility and joint loading in hip OA[117] or relationships with cartilage health.[118] In individuals with knee osteoarthritis, there is evidence that increased fatty infiltration of periarticular muscles may be associated with worse physical function and mobility,[38,119] as well as cartilage degeneration.[38,39,120] Further research is needed to better understand the role hip abductor muscle quality in hip OA, particularly in early-stage disease before the onset of severe disability and disuse-related atrophy which may lead to secondary changes in muscle quality.

5.3 Muscle as a Modifiable Tissue

One of the primary drivers of muscle quality research in OA is its promise as a potentially modifiable risk factor for disease. Several studies have demonstrated that muscle quality may be modified through diet, exercise, or a combination of both.[37] The effects of exercise on muscle quality have been explored using various interventions including low-intensity walking programs, high-intensity resistance training, and combined aerobic and resistance training programs.[121–124] The superiority of either aerobic or resistance training for improving muscle quality remains unclear. Additionally, whether muscle quality improvements observed with intervention are due to a loss of fat mass, an increase in lean muscle mass, or a combination of both is not well-understood. In a cohort of healthy adults, a reduction in vastus medialis fatty infiltration associated with increased physical activity and weight loss has been linked to cartilage volume preservation in the tibia and patella.[125] Though these findings are promising for developing strategies aimed at preventing or slowing OA-related cartilage degeneration, further research is needed to determine whether muscle quality is a significant risk factor leading to the onset or progression of hip OA, or a consequence of disease that results from disability and disuse.

6 Scientific Rigor

The work described in this dissertation utilized several methods—described in detail in preceding and subsequent chapters—for evaluating muscle quality and size, cartilage health, patient-reported outcomes, and physical function. This chapter provides various metrics of validity and reliability for these methods.

6.1 Muscle Evaluation

In Chapters 7-10, muscle quality and size were quantified using IDEAL-IQ MRI. Several studies have shown strong agreement between chemical shift-based water-fat separated IDEAL-IQ MRI and MR spectroscopy.[88,95,96] IDEAL-IQ MRI has also been shown to produce FF estimates which are directly proportional to fat mass.[95] Absolute fat mass derived from IDEAL-IQ FF maps was compared to chemical assay and showed strong correlation and agreement (r^2 = 0.98, slope = 1.01, intercept = 1.99g, mean difference = 2.17±3.40g) with fat mass evaluated in several tissues (i.e., organs, muscle, subcutaneous and visceral adipose tissue). Specifically in skeletal muscle, fat mass derived from IDEAL-IQ MRI was strongly correlated with chemical assay (r^2 = 0.97, slope = 1.19, intercept = -2.84g). Scan-rescan reproducibility of FF from IDEAL-IQ MRI has been evaluated in bone marrow of vertebral bodies, with coefficient of variation

(CV) = 0.86 ± 0.25%.[96] As part of the work presented in this dissertation, reliability of manual muscle segmentation was evaluated. Manual segmentation of GMED, GMIN, and TFL was performed across all slices of the image volume from iliac crest to greater trochanter by a single researcher in a sample of 5 subjects segmented on two separate occasions more than two weeks apart. Intra-rater reliability was assessed using intraclass correlation coefficient (ICC). ICC was determined to be 0.99, 0.97, 0.99 for volume and 0.99, 0.94, 0.99 for FF of GMED, GMIN, and TFL, respectively. This corresponds to a standard error of measurement (SEM) of 3.16 cm^3, 1.62 cm^3, and 0.13 cm^3 for volumetric measures and 0.14%, 0.50%, and 1.17% for FF measures of GMED, GMIN, and TFL, respectively.

6.2 Cartilage Evaluation

Semi-quantitative morphological grading of acetabular and femoral cartilage lesions as described in Chapter 9 was performed using the SHOMRI scoring system.[66] SHOMRI has previously been validated against arthroscopic findings and showed a sensitivity of 95.7% and a specificity of 84.8% for detecting cartilage lesions.[67] Excellent inter- (ICC = 0.93-0.98) and intra-reader (ICC = 0.91-0.94) agreement have been shown for morphological joint features graded by SHOMRI.[66]

Cartilage biochemistry was quantified using relaxation time mapping with fully automatic segmentation in Chapter 10. Reproducibility for relaxation time mapping is given by the CV which represents the short-term precision of this technique. The CV of the combined region of the femoral head and acetabulum mean relaxation times ranges from 2.03 to 5.89% for $T_{1\rho}$ and T_2, respectively.[126]

6.3 Physical Function

Mobility and physical function were evaluated in Chapter 8 using measures including 30-second chair rise test (30CRT) and 12-step stair climb test (SCT). These protocols have been previously described and utilized as clinically meaningful measures of mobility and function in individuals with lower extremity OA.[127,128] The 30CRT has been shown to have excellent reproducibility, with intra- and inter-rater ICC of 0.94 and 0.92, respectively.[129] Similarly, excellent test-retest reliability has been demonstrated for SCT in patients with total hip arthroplasty with ICC = 0.98.[130]

6.4 Gait Biomechanics

In Chapter 10, gait biomechanics were evaluated by three-dimensional (3D) motion analysis performed using optoelectronic stereophotogrammetry in which infrared cameras track the 3D position of a set of retroreflective markers placed on the body. The 3D coordinates of each marker were reconstructed based upon data from two or more cameras. Instrumentation noise error of the system is estimated between 0.5, 0.8, and 2 mm in the X, Y, and Z directions.[131] Soft tissue artifact was mitigated using rigid marker clusters and bony landmarks. Within our research group, intra-rater reliability was evaluated. This measure of reliability takes into consideration both system error and marker placement error. Hip joint angle SEM was found to be 1.56°, 1.01°, and 0.71° for X, Y, and Z, respectively. Hip joint moment SEM was 0.13 $Nm \cdot kg^{-1}$, 0.15 $Nm \cdot kg^{-1}$, and 0.08 $Nm \cdot kg^{-1}$ for X, Y, and Z, respectively.

6.5 Strength

Maximal isometric hip abduction strength testing as described in Chapter 10 was performed according to a previously described standardized protocol which was shown to be valid and reliable for assessing unilateral hip abductor strength.[132] This protocol involves placing the subject in a side-lying position with the hip in neutral alignment with the axis of the dynamometer aligned with the hip joint center in the frontal plane. Test-retest reliability for this protocol in terms of CV is shown to be 3.7% with ICC of 0.90.[132]

6.6 Patient-Reported Outcomes

The Hip disability and Osteoarthritis Outcome Score (HOOS) questionnaire was used to evaluate patient-reported pain and disability as described in Chapter 8. HOOS subscales have been compared to various metrics of hip-related pain and disability such as the Short Form 36, the Oxford Hip Score, the Lequesne Index, and the visual analog scale and have shown good construct validity.[133–135] HOOS test–retest reproducibility evaluated using ICC has been shown to range from 0.75 to 0.97.[136]

7 Automatic Evaluation of Hip Abductor Muscle Quality and Size in Hip Osteoarthritis

7.1 Introduction

The primary hip abductors, consisting of the gluteus medius (GMED), gluteus minimus (GMIN), and tensor fascia lata (TFL), act to stabilize the pelvis relative to the femur during single-limb stance phase of gait and account for most of the compressive force generated between the femoral head and acetabulum during this phase.[103,104] Several studies have found evidence of hip abductor muscle atrophy characterized by decreased muscle size and increased fatty infiltration in individuals with hip osteoarthritis (OA).[40–43,115,116] Given the critical role of the hip abductors in controlling loading at the hip joint, atrophy or dysfunction of these muscles is a growing area of interest for better understanding the development and progression of hip OA.

Fatty infiltration of skeletal muscle has been linked to mobility impairment and functional deficits.[38,114,119] Thus, fatty infiltration has come to be described by the term “muscle quality”, with worse muscle quality indicated by greater fatty infiltration. Despite a growing body of work demonstrating the negative implications of fatty infiltration and muscle atrophy, few studies have quantitatively evaluated muscle quality and size of the

hip abductors in individuals with hip OA. Additionally, due to the time-intensive nature of muscle evaluation which involves laborious manual segmentation of periarticular tissues in 3D medical images, limited research has characterized fatty infiltration and muscle size throughout the entire length of the hip abductors. To save time and allow for large cohort analyses, many studies elect to use abbreviated methods which may involve semi-quantitative or quantitative evaluation of the muscle over only a few slices of the image volume. Recent work has shown that muscle quality varies along the length of the hip abductors.[137,138] However, it is unclear whether specific regions of these muscle are affected in hip OA and, in the case of methods which analyze only a subset of the muscle volume, which regions of the muscle might be most useful for estimating fatty infiltration of the overall muscle. Thus, the time required to segment muscle and variability of muscle quality and size across the length of the muscle present significant barriers to clinical adoption of these emerging biomarkers. Automation of the muscle segmentation process will allow for a better understanding of the role of muscle quality in disease and could greatly enhance translation of muscle quality metrics to clinical practice.

As emerging disease biomarkers such as fatty infiltration are identified, the need for extracting quantitative information from 3D medical images is growing. Advanced techniques such as deep learning enable extraction of image features and can be used to develop automatic segmentation methods for magnetic resonance imaging (MRI).[139] Convolutional neural networks (CNNs) are a type of deep learning algorithm which do not require manual feature extraction and have shown excellent performance for automatic image classification and segmentation.[140,141] Therefore, the goal of this study

was to develop an automatic hip abductor segmentation method using deep learning which would enable automatic estimation of GMED, GMIN, and TFL fatty infiltration and muscle volume throughout the length of the muscles in individuals with hip OA. Additionally, we aimed to identify the regions of these muscles which may provide best estimates of overall muscle fatty infiltration to inform future studies with limited ability to evaluate the full muscle.

7.2 Methods

7.2.1 Study Participants

Forty-four participants with and without varying degrees of mild-to-moderate radiographic hip OA were randomly selected from an ongoing longitudinal study. All subjects signed informed consent as approved by our institution's Committee on Human Research. Participation eligibility was determined at baseline using Kellgren-Lawrence (KL) grading.[62] KL grading was performed by a musculoskeletal radiologist on bilateral anterior-posterior and lateral radiographs. Exclusion criteria included end-stage OA (KL = 4), contraindications to MRI, history of hip surgery, hip trauma within the previous 3 months, joint replacement of any lower extremity joint, pain or OA of any other lower extremity joint, self-reported inflammatory arthritis, and immobility or assistance requirements that limit the ability to walk.

7.2.2 MR Image Acquisition

Unilateral hip MR images were acquired using a 3.0T MR scanner (GE Healthcare, Waukesha, WI) with a 32-channel cardiac coil (GE Healthcare, Waukesha,

WI). Coverage area was prescribed from the iliac crest to the greater trochanter using a 3-plane gradient echo localizer. Muscle MR sequences (Table 7.1) included axial T_1-weighted fast spin echo and 3D axial Iterative Decomposition of water and fat with Echo Asymmetry and Least-squares estimation (IDEAL-IQ)[91,93] spoiled gradient-recalled echo (SPGR) with multi-peak fat spectrum modeling and single T_2* correction.[142] T_1-weighted images and IDEAL-IQ fat fraction (FF) maps were then used for muscle segmentation, and FF and volume were quantified on the FF maps.

Table 7.1. Magnetic resonance sequences and acquisition parameters.

MR Sequence	Acquisition Parameters
3-plane gradient echo	-
Axial T_1-weighted FSE	TR/TE = 785/8.9 ms, ETL = 2, FOV = 16 × 16 cm, matrix size = 288 × 224, slice thickness = 6 mm
3D IDEAL-IQ SPGR	TR = 9.3 ms, ETL = 2, number of echoes = 6, FA = 3, FOV = 16 x 16 cm, matrix size = 192 × 192, slice thickness = 6 mm

MR, magnetic resonance; FSE, fast spin echo; 3D, three-dimensional; IDEAL-IQ, Iterative Decomposition of water and fat with Echo Asymmetry and Least-squares estimation; SPGR, spoiled gradient recalled echo; TR, repetition time; TE, echo time; ETL, echo train length; FOV, field of view; FA, flip angle

7.2.3 Manual Muscle Segmentation

Manual segmentation of GMED, GMIN, and TFL was performed on all slices of T_1-weighted images from iliac crest to greater trochanter in 44 hip MR image volumes. Borders of the muscles were traced with image segmentation software developed in-house using MATLAB (MathWorks, Natick, MA). Segmentation masks were then transferred to volumetric FF maps. Manual segmentation was performed by a single trained researcher. Intra-rater reliability of muscle segmentations was evaluated in a sample of 5 subjects segmented on two separate occasions more than two weeks apart using intraclass correlation coefficient (ICC). ICC was determined to be > 0.94 for FF

and volumetric measures of GMED, GMIN, and TFL. Time-to-segment all muscles on a single image volume ranged from 2-3 hours per volume depending on number of slices acquired from iliac crest to greater trochanter.

7.2.4 Automatic Segmentation Network

The 44 manually segmented FF maps and their corresponding muscle masks were divided into training (29 volumes), validation (8 volumes), and testing (7 volumes) sets, ensuring no significant differences in age, gender, body mass index (BMI), or proportion of individuals with (KL ≥ 2) and without (KL < 2) radiographic hip OA across the splits. The dataset was used to train and validate a 3D V-Net CNN.[140] In this approach, a 3D V-Net is trained end-to-end on MR image volumes, and the network learns to generate voxel-wise prediction masks for the entire image volume at once. The test set was treated as a holdout dataset which was never used for network optimization and served only as a measure of final network performance. Image volumes and muscle masks were augmented to train the model to be invariant to anatomical heterogeneity in muscle shape and size. Augmentation transforms were randomly applied to images and their corresponding masks and included various combinations of 3D rotation, 3D affine deformation, and 3D B-spline deformations. To train the 5-level V-Net comprising 1, 2, 3, 3, and 3 consecutive convolutions per level, a combination of weighted cross-entropy (class weights = 0.85, 1, 2, 0.005 for tissue GMED, GMIN, TFL, and background, respectively) with Dice loss minimized, using Adam optimizer, learning rate = $1x10^{-4}$, 0.05 dropout probability and batch size =1. Training to convergence required 92 epochs for 15 hours on an NVIDIA Titan X GPU

(NVIDIA, Santa Clara, CA) and was implemented in Python 3.6.5 utilizing TensorFlow v1.8.0 (Google, Mountain View, CA).

To train the V-Net, labeled FF map image volumes were used as input to the V-Net and the network generated a corresponding 4-class prediction mask for GMED, GMIN, TFL, and background on each of the input image slices. All prediction masks automatically generated by the model underwent post-processing in MATLAB 2020b which involved removal of extra pixels from the mask by keeping only the largest connected component, extraction and dilation of the perimeter of the mask using a structuring disk element (radius = 1), and any remaining holes in the mask were filled. The final trained segmentation network allows for input of unlabeled IDEAL image volumes and automatically outputs prediction masks for GMED, GMIN, and TFL which then undergo post-processing (Figure 7.1).

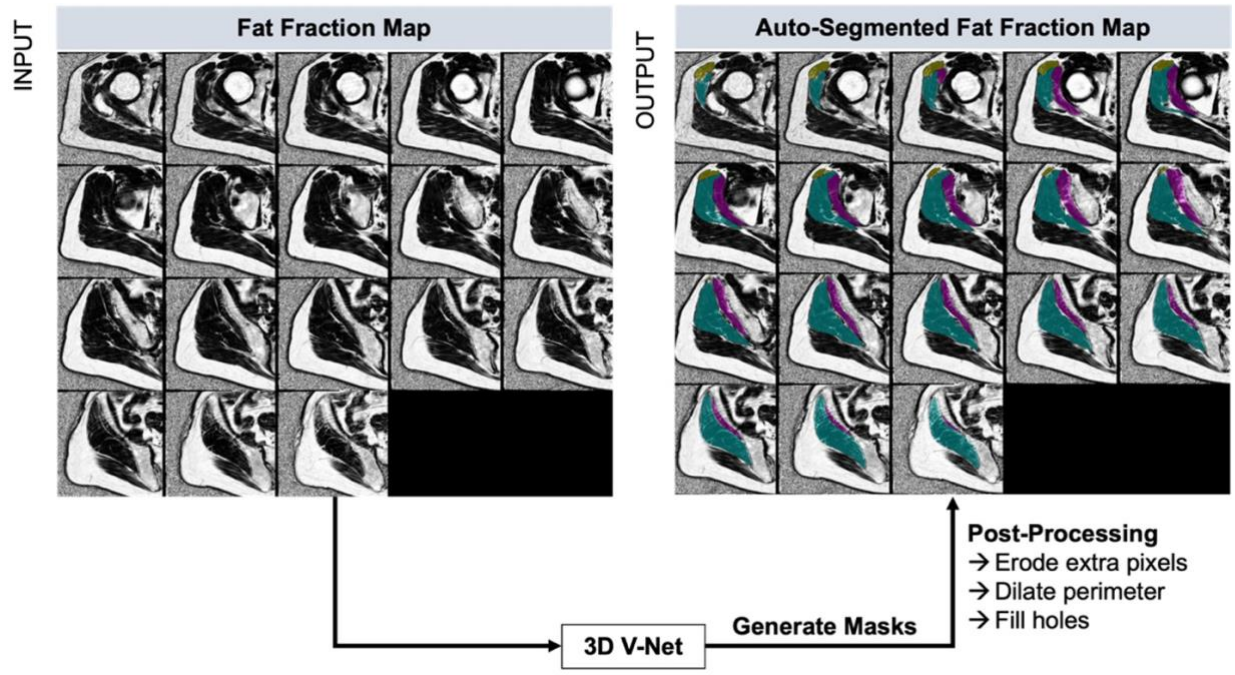

Figure 7.1. Processing pipeline for automatic muscle segmentation using the 3D V-Net showing steps from input of unlabeled images to output of fully segmented images.

7.2.5 Muscle Fat Fraction and Volume Quantification

For manually and automatically segmented image volumes, the overall FF and volume in the segmented region of each muscle was quantified. FF was calculated by taking the average signal intensity of the FF map in the segmented region. Total volume of each muscle was calculated by taking the sum of the segmented cross-sectional area (CSA) of each slice multiplied by slice thickness where CSA was the sum of all the pixels in the segmented region multiplied by pixel spacing.

7.2.6 Characterization of Axial FF and CSA Across Muscle Length

Using methods previously described,[137] FF and CSA were characterized across the length of the muscle from proximal to distal in all 44 manually segmented image volumes. This was performed by normalizing the length of each muscle to 101 points. With this approach, axial profiles of slice-wise muscle FF and CSA are generated in which 0% represents the most proximal aspect of the muscle and 100% represents the most distal aspect of the muscle. Mean FF and muscle CSA were determined at each slice and approximated at every 1% of the muscle length using spline interpolation.

7.2.7 Statistical Analysis

Differences in demographics and group characteristics for training, validation, and test sets were evaluated using one-way analysis of variance (ANOVA) for continuous variables and Chi-square test for dichotomous variables. All evaluations of network performance were performed on the holdout test set. Descriptive statistics were used to evaluate spatial overlap between manual and automatic segmentation. This was quantified with the Dice similarity coefficient using the equation below where T is

the ground truth manual segmentation map and P is the predicted segmentation map generated by the network.[143]

$$Dice = \frac{2|T \cap P|}{|T| + |P|}$$

Agreement between the manual and automatic FF and volume of each muscle was evaluated using Pearson's correlation and Bland-Altman[144] plots in R Studio v4.0.2 (R Core Team, Vienna, Austria). Statistical Parametric Mapping (SPM) was then used to evaluate locations across the length of the muscle at which the axial FF was significantly associated with and most strongly associated with overall muscle FF. SPM is a topological data analysis technique in which hypothesis testing is performed at each point along a 1-dimensional curve. Using this approach, a linear regression was performed in MATLAB 2020b using open source spm1d code [SPM spm1d version 0.4; http://www.spm1d.org]).[145] At each 1% of the length of the muscle, a t-statistic, correlation coefficient, and corresponding *P*-value was output to determine locations of the muscle from proximal to distal at which axial FF was most strongly associated with overall FF. A higher t-statistic indicates greater confidence in the ability of axial FF to predict overall FF. A *P*-value < .05 was considered significant.

7.3 Results

7.3.1 Demographic Data

Demographics and group characteristics for training, validation, and test groups are shown in Table 7.2. No significant differences were found in age, sex, BMI, or proportion of radiographic OA cases included between groups.

Table 7.2. Demographics and characteristics for training, validation, and test sets.

	Train (N = 29)	Val (N = 8)	Test (N = 7)	*P* Value
Age, years (Mean ± SD)	52.2 ± 16.8	51.9 ± 17.0	55.6 ± 13.6	.879
Male:Female (N)	9:20	3:5	2:5	.923*
BMI, kg/m^2 (Mean ± SD)	23.6 ± 3.6	24.1 ± 3.9	23.9 ± 2.6	.935
OA:Control (N)	15:14	2:6	3:4	.401

**P*-value from Chi-square test. BMI, body mass index; OA, osteoarthritis (Kellgren-Lawrence grade ≥ 2); train, training group; val, validation group; test, testing group.

7.3.2 Automatic and Manual Segmentation Comparison

The automatic segmentation network resulted in a mean Dice coefficient of 0.94, 0.87, and 0.91 for GMED, GMIN, and TFL, respectively. An example of side-by-side manual and automatic segmentation masks across all axial slices of the IDEAL FF image volume can be seen in Figure 7.2.

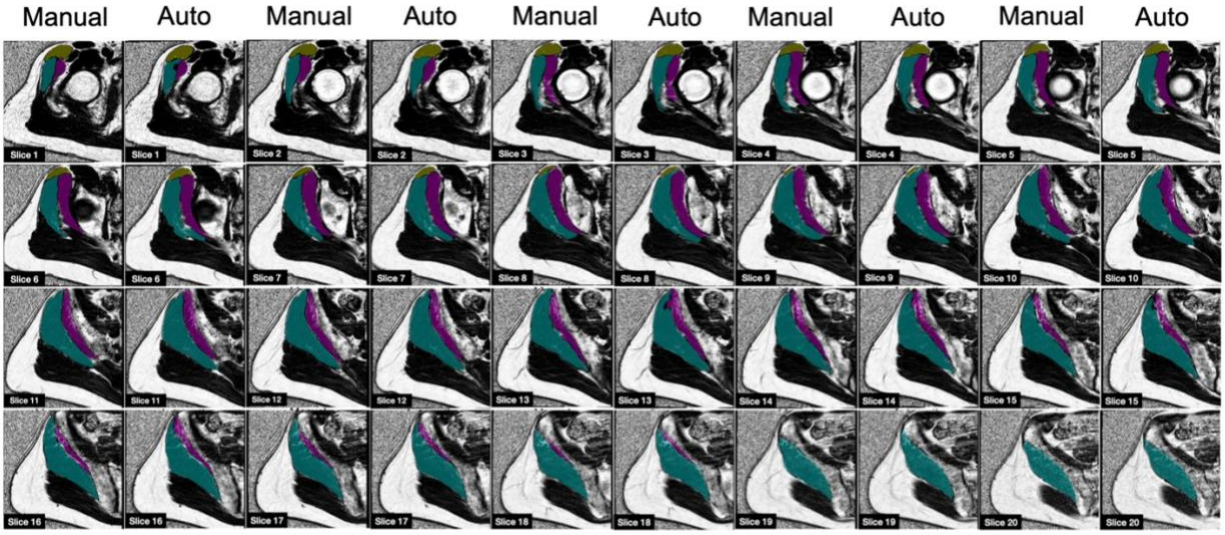

Figure 7.2. Comparison of manual and automatic muscle segmentation. Manual and automatic segmentation masks generated by the 3D V-Net are shown overlaid on the IDEAL-IQ sequence fat fraction maps. Gluteus Medius (GMED) is shown in teal, gluteus minimus (GMIN) in magenta, and tensor fascia lata (TFL) in dark yellow.

Correlations between manual and automatic segmentation methods are shown in Figure 7.3. FF and volume measures derived from manual and automatic segmentation methods were strongly correlated and all relationships were statistically significant. For FF measures, Pearson's correlations coefficients were 0.99, 0.92, and 0.99 for GMED, GMIN, and TFL, respectively. For total muscle volume, Pearson's correlations coefficients were 0.99, 0.98, and 0.95 for GMED, GMIN and TFL, respectively. Bland-Altman agreement plots for manual and automatic FF and volume measures are shown in Figure 7.4. The 95% upper and lower limits of agreement and mean absolute differences for all measures are shown in Table 7.3. All values fell within the limits of agreement.

Table 7.3. Bland-Altman agreement between fat fraction and volumetric measures derived from manual and automatic segmentation methods.

	95% Limits of Agreement		Mean Absolute Difference
	Lower	Upper	
Fat Fraction (%)			
GMED	-0.52	1.51	0.50
GMIN	-1.99	1.93	0.68
TFL	-1.25	2.89	1.06
Volume (cm^3)			
GMED	-9.79	17.43	6.16
GMIN	-7.23	4.52	2.74
TFL	-3.81	3.45	1.41

GMED, gluteus medius; GMIN, gluteus minimus; TFL, tensor fascia lata.

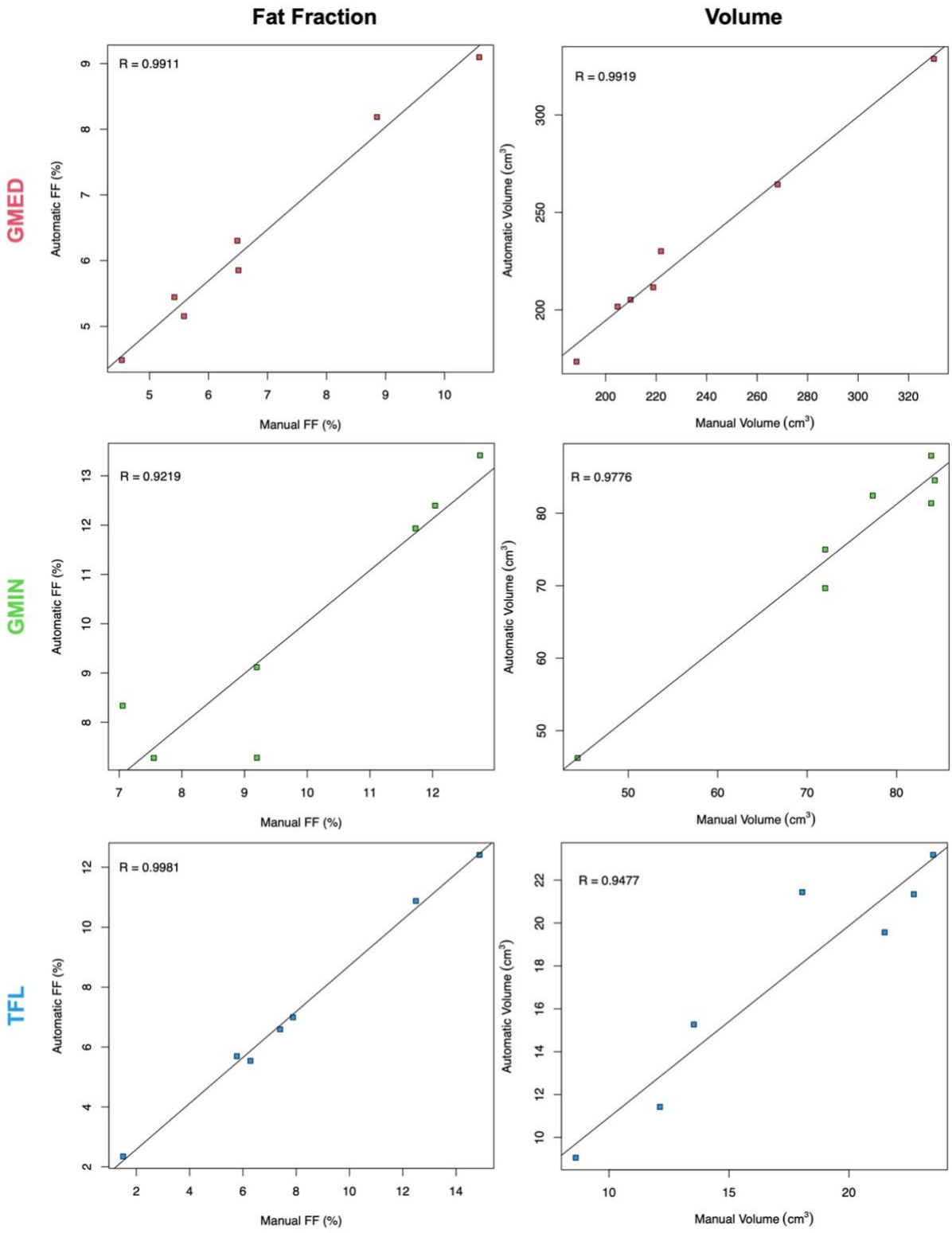

Figure 7.3. Correlation between manual and automatic segmentation for (left) fat fraction and (right) volume measures. (Top) gluteus medius, (middle) gluteus minimus, and (bottom) tensor fascia lata.

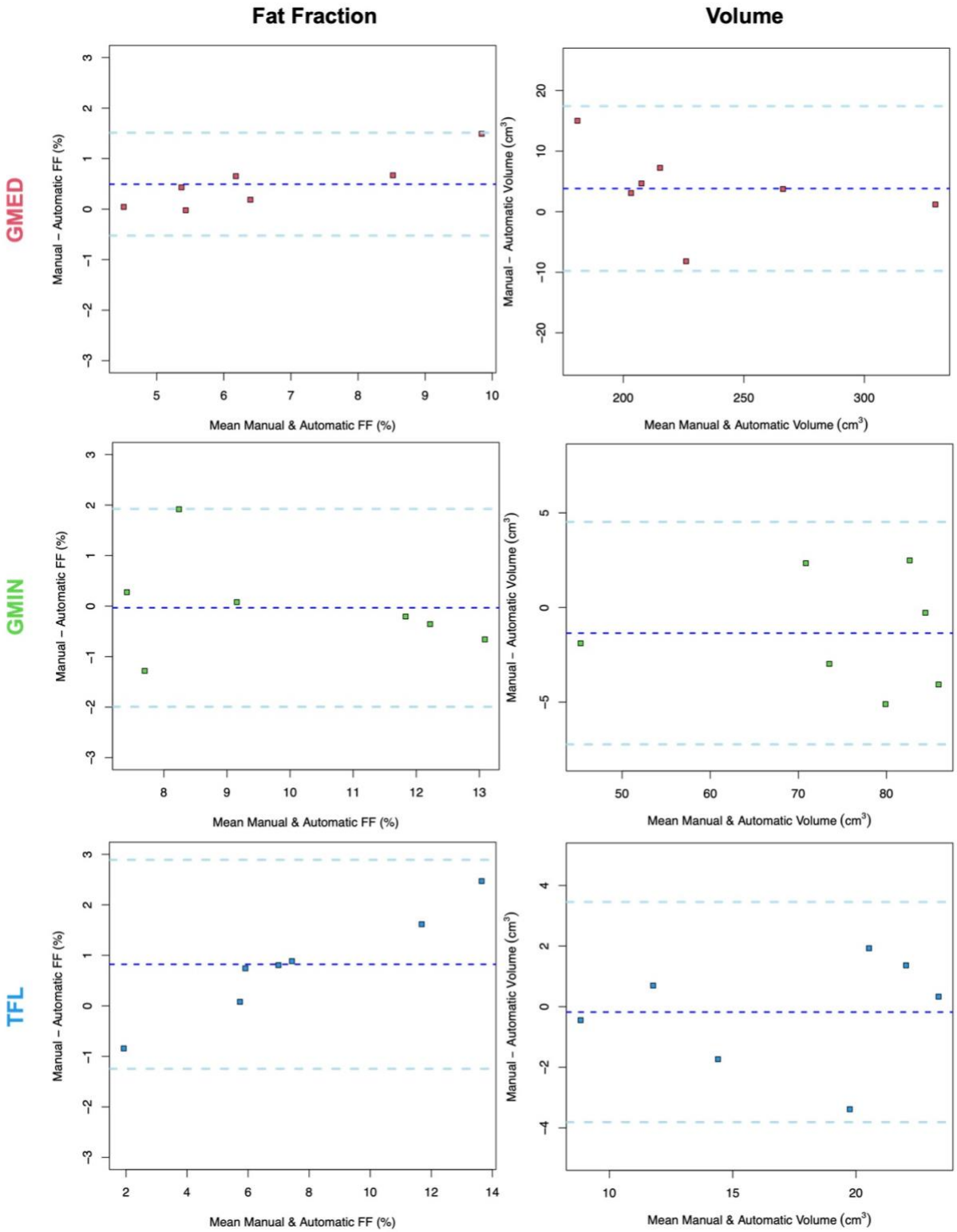

Figure 7.4. Bland-Altman agreement between manual and automatic segmentation for (left) fat fraction and (right) volume measures. (Top) gluteus medius, (middle) gluteus minimus, and (bottom) tensor fascia lata. Mean of manual and automatic measures is plotted on the x-axis and the difference between measures is plotted on the y-axis.

7.3.3 Associations of Axial Fat Fraction with Overall Fat Fraction

Localized associations of mean axial FF with overall FF were evaluated using SPM (Figure 7.5) in 44 subjects (age 52.7 ± 16.1 years, BMI 23.7 ± 3.4 kg/m^2, 14 males). Across the length of the muscle, axial FF was significantly associated with overall FF at all portions of the GMED, GMIN, and TFL except for a small region of the distal GMIN. In GMED, the correlation coefficient was highest at 50% the length of the muscle with r = 0.94. In GMIN, the correlation coefficient was highest at 50% with r = 0.93 and in TFL at 65% with r = 0.97. T-statistics were similarly high in these regions indicating greater confidence in associations at these points.

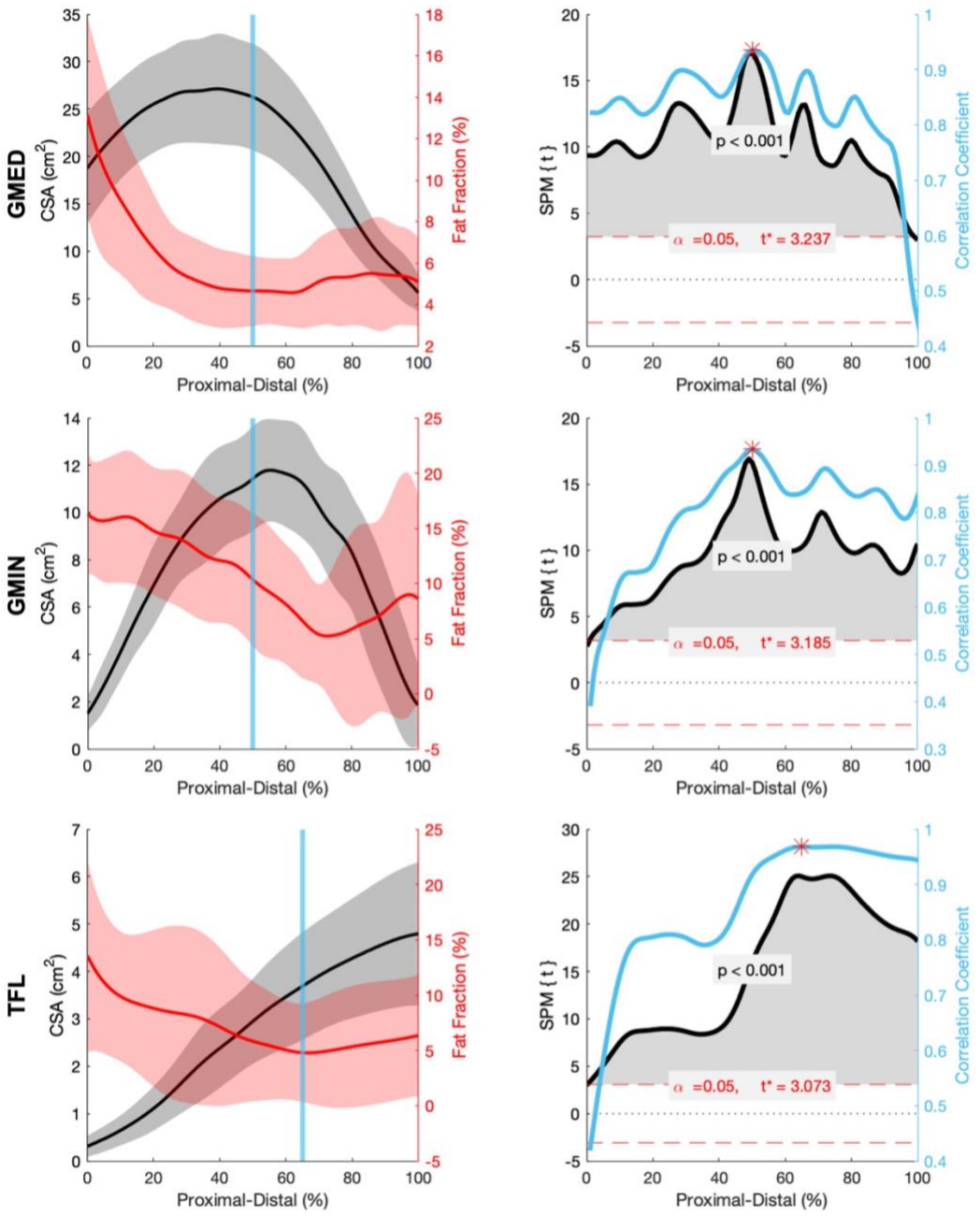

Figure 7.5. Characterization of muscle fat fraction (FF) [red] and cross-sectional area (CSA) [black] across the length of the muscle (Left) for GMED (top), GMIN (middle), and TFL (bottom). Statistical parametric mapping (SPM) results (right) show t-statistics [black] and regression coefficients [blue]. Regions which were significantly associated with overall FF are shaded in grey with corresponding *P*-values. Regions with highest correlation coefficient for predicting overall FF from axial FF are shown with a blue bar on the CSA-FF plots and red asterisk on the SPM-Regression plots.

7.4 Discussion

In this study, we developed an automatic segmentation network that allows for streamlined estimation of hip abductor muscle quality and size across a large image volume in individuals with and without radiographic hip OA. Our data suggest that the FF and volumetric measurements derived from automatic segmentation were highly correlated and showed strong agreement with manual methods. This network provides estimation of GMED and GMIN FF and volume from muscle origin to insertion. While the full length of the TFL muscle belly was not acquired in our imaging protocol, this network allows for automatic segmentation of all available slices of TFL at or above the level of the greater trochanter. Additionally, we characterized FF and CSA from proximal to distal ends of the hip abductors and found regions of the muscle which may be most useful in estimation of overall muscle quality using only a subset of axial image slices.

Previous work by Tibrewala et al demonstrated strong performance of an automatic segmentation network for evaluation of GMED, GMIN, and TFL FF and volume across 6 consecutive slices of IDEAL FF image volumes.[118] This previous study showed Dice performance of 0.90, 0.88, 0.91 for GMED, GMIN, and TFL, respectively. Additionally, the previously described 6-slice network had 95% upper and lower limits of agreement of [-2.1%, 3.5%] for FF and [-7.5 cm^3, 10 cm^3] for volume. Our results showed very similar performance in both spatial overlap and Bland-Altman agreement using all available image slices which ranged from 16 to 24 slices depending on subject size. However, given that our network evaluated muscle size over a much larger volume of muscle, the volumetric discrepancy of our network may provide size estimation superior to that of previous work. Our results demonstrate that similarly strong

performance for estimating hip abductor FF and volume can be achieved while capturing a large volume of the hip abductor muscles.

Recent work has demonstrated that hip abductor fatty infiltration is variable across the length of the muscle from proximal to distal,[137,138] and that specific regions of these muscles may be more responsive to exercise interventions[137]. Our work similarly demonstrates variability in fatty infiltration across the length of the muscle, with fatty infiltration generally decreasing from proximal to distal in GMED, GMIN, and TFL. These results highlight the utility of our segmentation network which is capable of estimating muscle quality across the length of the hip abductors in an efficient and fully automatic manner. This segmentation network may serve to further research aimed at better understanding aging and disease processes which lead to localized changes in fat distribution across the length of the hip abductor. Furthermore, this segmentation network will accelerate our understanding of the role of hip abductor muscle quality in hip OA and make clinical translation of these findings more viable.

While automatic segmentation provides the ability to rapidly estimate overall FF and muscle volume, acquisition and segmentation of the full length of the hip abductors may not be feasible for all studies aiming to evaluate muscle quality in individuals with hip OA. Therefore, we examined regions of the muscle which provide the greatest predictive ability for estimating overall muscle quality. These data may inform studies wishing to select a small subset of slices of the hip abductors to evaluate overall muscle quality. Our results indicate that for GMED and GMIN muscle quality estimation, FF of axial cross-sections at 50% the length of the muscle is strongly associated with overall muscle quality. The large CSA of the muscles in these regions may provide less error in

segmentation and better estimation of overall muscle quality. Given that the imaging volume used to capture the full length of GMED extends beyond the origin of GMIN, the 50% points for GMED and GMIN correspond to different slices within the image volume for each muscle. In the TFL, regions of the muscle with the best predictive ability for estimating overall muscle quality may correspond to smaller, more proximal cross-sections of the muscle rather than the larger, more distal region. These data suggest that slice selection should be tailored to the individual muscle being evaluated, as a one-size-fits-all approach may not provide best estimates of overall muscle quality.

Limitations of this study should be considered. First, our cohort consisted of individuals with relatively healthy BMI and excluded those with end-stage hip OA. Hip abductor fatty infiltration has been shown to be BMI-dependent[146] and greater atrophy of these muscles has been associated with clinical severity of disease.[147] Therefore, the performance of this segmentation network may not be generalizable to individuals with higher BMI or more severe disease. Additionally, TFL muscle quality was characterized in only a portion of the muscle, as the MR coverage area used in this study does not capture the full TFL muscle belly distal to the greater trochanter. Thus, the performance of this segmentation network on the full volume of TFL has not been tested. Furthermore, regions of the TFL which showed strongest association with overall muscle quality are reported relative to the length of muscle acquired. Further research is needed to fully characterize overall TFL muscle quality throughout the entire length of the muscle and determine regions of the muscle which provide best estimates of overall muscle quality.

7.5 Conclusions

These results demonstrate that hip abductor FF and volume can be accurately estimated across nearly the entire muscle length without requiring time-intensive manual segmentation. The ability to automatically estimate hip abductor muscle quality will allow future studies to further explore relationships between muscle quality and joint health in large cohorts of individuals with hip OA, where the time cost of manual image segmentation would otherwise be prohibitive. For studies in which automatic segmentation is not possible and an abbreviated approach is adopted, our results provide evidence that specific regions of the GMED, GMIN, and TFL can be selected to estimate overall muscle quality.

8 Hip Abductor Muscle Quality is Associated with Symptomatic and Functional Disease Severity in Hip Osteoarthritis

8.1 Introduction

Osteoarthritis (OA) is a leading cause of disability worldwide, with over 27 million US adults estimated to have clinically-defined OA.[2] Hip OA is a highly debilitating form of disease given its impact on weight-bearing joints in which severe pain may limit basic daily activities.[8] It is estimated that one in four people will develop hip OA by the age of 85.[148] Current treatment approaches for OA are limited and primarily aim to reduce pain and disability while minimizing progression of structural degeneration.[149] Identification of biomarkers associated with structural and symptomatic OA severity is necessary in order to develop more effective treatment strategies which target factors that lead to OA-related physical and functional decline.

It is well-established that individuals with hip OA have weak hip abductors.[100,150,151] This muscle group, consisting of the gluteus medius (GMED), gluteus minimus (GMIN), and tensor fascia lata (TFL), plays a critical role in stabilizing

the pelvis during functional tasks—particularly during activities which involve single-limb stance.[97] There is also evidence of increased fatty infiltration and decreased muscle size of the hip abductors in individuals with hip OA compared to controls.[41,42,152] Fatty infiltration of skeletal muscle is a growing area of interest in OA research, as adipose tissue within the muscle has been linked to muscle dysfunction and mobility impairment.[37,38,114,119] Accumulation of adipose tissue within the muscle is thought to limit the contractile capacity of the muscle by altering mechanical and metabolic properties of the surrounding muscle fibers.[37,153] Thus, individuals with higher ratios of adipose to lean tissue are described as having worse muscle quality.

Currently, evidence is sparse relating hip abductor muscle quality and size to measures of structural disease severity and functional deficits. Previous work has been limited by the inclusion of individuals with end-stage (severe) hip OA and by the use of coarse semi-quantitative measures of fatty infiltration which have been shown to lack sensitivity for differentiating subjects with varying levels of fatty infiltration.[38,84] Additionally, previous work that has reported muscle size in hip OA has used muscle volume measurements which include both muscle and adipose tissue, and have not isolated lean, contractile tissue. While data suggest that muscle quality and size are associated with hip abductor strength,[40] evidence is lacking regarding the impact of these measures on overall patient function. Given that muscle quality and size have been shown to be modifiable through exercise intervention,[37,137] there is a significant need for data evaluating the relationship of muscle quality and size with structural and functional disease outcomes. This research is specifically needed in individuals with mild-to-moderate disease, a population in which modification of OA risk factors may be

most effective at slowing disease progression. Furthermore, sensitive measures which can differentiate between and quantify contractile lean muscle and non-contractile adipose tissue are needed to better understand the process of muscle atrophy in mild-to-moderate hip OA.

Therefore, the aim of this study was to examine the relationships of quantitatively measured hip abductor muscle fatty infiltration and lean volume with radiographic OA severity as well as patient-reported and physical function in individuals with mild-to-moderate hip OA.

8.2 Methods

8.2.1 Study Participants

Participants were recruited from the community as part of an ongoing study on progression of hip OA. All subjects signed informed consent as approved by our institution's Committee on Human Research. Participation eligibility was determined at baseline and required participants have either no signs of radiographic hip OA (Kellgren-Lawrence [KL] grade 0) or have evidence of mild-to-moderate hip OA (KL grade 1-3), excluding participants with end-stage hip OA (KL grade 4).[62] KL grading was performed by a trained musculoskeletal radiologist on bilateral anterior-posterior and lateral hip screening radiographs. Additional exclusion criteria included contraindications to MRI, history of hip surgery, hip trauma within the previous 3 months, joint replacement of any lower extremity joint, pain or OA of any other lower extremity joint, self-reported inflammatory arthritis, and immobility or assistance requirements that limit the ability to walk. Because muscle imaging was not consistently performed at each visit

for all participants, cross-sectional data were selected from multiple years of the study (1-year, 2-year, and 3-year follow-up) based upon the earliest timepoint at which complete muscle imaging and functional outcome data were available. However, only one set of images (bilateral hips when available) and outcome data were included for a single subject.

8.2.2 Self-Reported and Physical Function

Patient-reported function was evaluated using the Hip Disability and Osteoarthritis Outcome Scores (HOOS) questionnaire.[133] The HOOS questionnaire evaluates five subscales of hip-related disability including pain, symptoms, activities of daily living (ADL), quality of life (QOL), and recreation function (Sport) on a scale from 0-100 with lower scores indicating worse patient-reported disability. This has been shown to be a valid, responsive measure of hip-related disability in the OA population.[133] Physical function was evaluated using (1) the stair climb test (SCT) that records the time to ascend and descend a set of 12 stairs and (2) the 30-second chair rise test (30CRT) in which participants are instructed to stand from a seated position as many times as possible in 30 seconds and the number of repetitions is measured. These protocols have been previously described and utilized as clinically meaningful measures of mobility and function in individuals with lower extremity OA.[127,128]

8.2.3 Imaging Procedures

Hip MR images were obtained using a 3.0T MR scanner (GE Healthcare) with a 32-channel cardiac coil (GE Healthcare). A 3-plane gradient echo localizer was used to identify the greater trochanter and iliac crest and prescribe the coverage area. Muscle

MR images (Table 1) were acquired using a 3-dimensional (3D) axial Iterative Decomposition of water and fat with Echo Asymmetry and Least-squares estimation (IDEAL-IQ)[91,93] spoiled gradient-recalled echo (SPGR) sequence (repetition time [TR] = 9.3 ms, echo train length = 2, number of echoes = 6, flip angle = 3°, matrix size = 256 × 256, slice thickness = 6 mm, field of view = 22 cm) using multi-peak fat spectrum modeling and single T_2* correction.[142] Fat fraction (FF) maps in which the signal intensity of each voxel represents the percentage of fat in that voxel were generated online and used for further image analysis.

8.2.4 Image Analysis

Muscle segmentation was performed on FF maps using the automated hip abductor muscle segmentation network previously described and validated in Chapter 7. This network automatically segments the GMED, GMIN, and TFL on all available image slices. All segmentations generated by the network underwent post-processing using MATLAB 2020b (MathWorks, Natick, MA). Post-processing involved removing extra pixels from the mask by keeping only the largest connected component, extracting and dilating the perimeter of the mask using a structuring disk element (radius = 1), and filling holes within the mask.

Muscle quality was evaluated by determining the overall FF of each segmented muscle throughout the FF map image volume. The FF of each muscle was calculated by taking the average signal intensity of the FF map in the segmented region across all slices of the image volume.

Muscle size was evaluated by computing the total lean volume (LV) of each muscle. First, lean cross-sectional area (CSA) of each slice was calculated by multiplying the number of pixels in the segmented region by pixel size, subtracting the fat area. Next, lean CSA was summed across all slices and multiplied by slice thickness to obtain a measure of LV.

8.2.5 Statistical Analysis

Generalized estimating equations (GEE) were used to evaluate relationships of muscle FF and LV with KL grade, HOOS scores, and functional tasks. GEE methods were selected for their ability to account for correlation of data from bilateral hips within the same subject.[154] For evaluating associations with KL grade, separate models were built for GMED, GMIN, and TFL FF and LV with muscle metric as the outcome variable and age, sex, body mass index (BMI), and KL grade as explanatory variables. For evaluating relationships with patient-reported outcomes and functional performance, the effect of muscle quality and size on HOOS and function was of interest. Therefore, GEE models were built with HOOS scores, SCT, or 30CRT as the outcome variables and GMED, GMIN or TFL FF and LV as the explanatory variables. Age, sex, and BMI were also included in the models as covariates. All statistical analyses were performed in R Studio v4.0.2 (R Core Team, Vienna, Austria) and a P-value < .05 was considered statistically significant.

8.3 Results

8.3.1 Demographics and Characteristics

A total of 85 hips from 48 participants were included in this study (37 bilateral cases and 11 unilateral cases). Participants had an average age of 52.7 ± 14.9 years, BMI of 24.2 ± 3.4 kg/m^2, and consisted of 32 hips from males (38%). The cohort consisted of 21 hips with radiographic KL grade 0, 38 hips with KL grade 1, 13 hips with KL grade 2, and 13 hips with KL grade 3. Demographics and characteristics are shown in Table 8.1. Of the 26 hips included with radiographic OA (KL ≥ 2), 20 had bilateral OA.

Table 8.1. Group Demographics and Characteristics (N = 48, 85 hips).

Characteristic		Value
Demographics	Age (years)	52.7 ± 14.9
	Sex (% Male)	38
	BMI (kg/m^2)	24.2 ± 3.4
HOOS	Pain	92.2 ± 11.8
	Symp	90.9 ± 10.9
	ADL	95.5 ± 7.9
	QOL	88.2 ± 14.8
	Sport	90.6 ± 13.8
Fat Fraction (%)	GMED	5.51 ± 1.7
	GMIN	9.0 ± 3.5
	TFL	5.0 ± 2.5
Lean Volume (cm^3)	GMED	229.1 ± 56.5
	GMIN	71.1 ± 16.0
	TFL	19.1 ± 7.4

Values are mean ± SD unless otherwise specified. BMI, body mass index; HOOS, Hip Disability and Osteoarthritis Outcome Score; Symp, Symptoms; ADL, activities of daily living; QOL, quality of life; Sport; sport and recreation; GMED, gluteus medius; GMIN, gluteus minimus; TFL, tensor fascia lata; OA, osteoarthritis.

8.3.2 Relationships of Muscle Quality and Size with KL Grade

Results from GEE analyses for KL grade are shown in Table 8.2. After adjusting for age, sex, BMI, and within-subject factors, KL score was not significantly associated with FF or LV of any muscle. The distribution of FF and LV for GMED, GMIN, and TFL based on KL groups is shown in Figure 8.1.

Table 8.2. Results from generalized estimating equations for association of KL grade with muscle fat fraction and lean volume adjusted for age, sex, and BMI.

	β	Std. Error	95% Wald CI		Wald Chi-Squared	*P*-Value
			Lower	Upper		
Fat Fraction						
GMED	0.097	0.0885	-0.076	0.271	1.21	.270
GMIN	-0.048	0.2370	-0.512	0.417	0.04	.840
TFL	-0.210	0.2698	-0.738	0.319	0.60	.437
Lean Volume						
GMED	2.747	3.5940	-4.300	9.790	0.58	.445
GMIN	1.594	1.4240	-1.200	4.380	1.25	.263
TFL	0.695	0.5186	-0.321	1.712	1.80	.180

Bold indicates statistical significance at $p < .05$. GMED, gluteus medius; GMIN, gluteus minimus; TFL, tensor fascia lata

8.3.3 Relationships of Muscle Quality and Size with HOOS

Results from GEE analyses for HOOS scores are shown in Table 8.3. GMED FF (β = -2.577, P = .003), GMIN FF (β = -0.981, P = .021), and TFL FF (β = -1.109, P = .017) were significantly negatively associated with HOOS symptoms. GMED FF (β = -3.029, P = .048) was also significantly negatively associated with HOOS QOL. GMED LV showed significant negative associations with HOOS pain (β = -0.221, P = .022). GMED LV (β = -0.088, P = .019), GMIN LV (β = -0.285, P = .022), and TFL LV (β = -0.503, P = .021) were negatively associated with HOOS QOL.

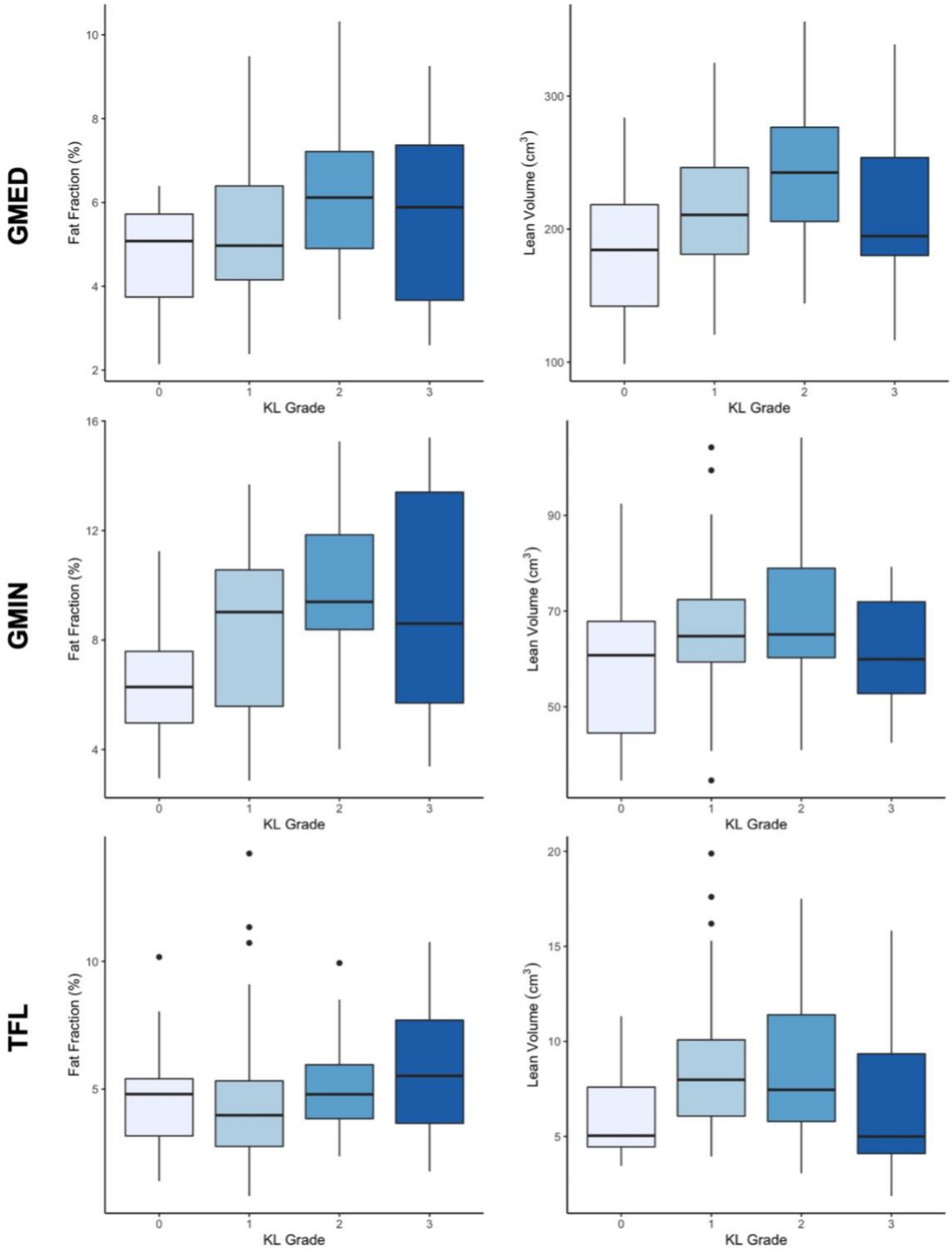

Figure 8.1. Distribution of fat fraction and lean volume across KL grade. Fat fraction (left) and lean volume (right) for gluteus medius (top), gluteus minimus (middle), and tensor fascia lata (bottom). Lines within boxes represent median and error bars represent standard error.

Table 8.3. Results from generalized estimating equations for associations of muscle fat fraction and lean volume with HOOS adjusted for age, sex, and BMI.

	Fat Fraction		Lean Volume	
	β (95% CI)	*P*-	β (95% CI)	*P*-Value
HOOS Pain				
GMED	-1.750 (-3.621, 0.121)	.067	-0.052 (-0.118, 0.014)	.124
GMIN	-0.714 (-1.518, 0.091)	.082	**-0.221 (-0.41, -0.032)**	**.022**
TFL	-0.617 (-1.842, 0.607)	.320	-0.244 (-0.594, 0.107)	.170
HOOS Symp				
GMED	**-2.577 (-4.277, -0.877)**	**.003**	-0.061 (-0.123, 0.002)	.057
GMIN	**-0.981 (-1.817, -0.145)**	**.021**	-0.151 (-0.360, 0.057)	.155
TFL	**-1.109 (-2.020, -0.200)**	**.017**	-0.254 (-0.611, 0.104)	.165
HOOS ADL				
GMED	-1.003 (-2.63, 0.624)	.230	-0.018 (-0.057, 0.021)	.360
GMIN	-0.287 (-0.943, 0.369)	.391	-0.076 (-0.204, 0.052)	.244
TFL	0.132 (-0.635, 0.900)	.735	-0.055 (-0.314, 0.203)	.675
HOOS QOL				
GMED	**-3.029 (-6.026, -0.033)**	**.048**	**-0.088 (-0.162, -0.014)**	**.019**
GMIN	-0.701 (-1.693, 0.292)	.166	**-0.285 (-0.529, -0.040)**	**.022**
TFL	-0.791 (-2.386, 0.803)	.331	**-0.503 (-0.931, -0.074)**	**.021**
HOOS Sport				
GMED	-1.201 (-4.200, 1.800)	.430	-0.038 (-0.108, 0.032)	.290
GMIN	0.158 (-0.909, 1.225)	.771	-0.153 (-0.381, 0.075)	.187
TFL	0.155 (-1.080, 1.390)	.810	-0.307 (–0.696, 0.082)	.120

Bold indicates statistical significance at $P < .05$. GMED, gluteus medius; GMIN, gluteus minimus; TFL, tensor fascia lata; HOOS, Hip Disability and Osteoarthritis Outcome Score; Symp, Symptoms; ADL, activities of daily living; QOL, quality of life; Sport; sport and recreation.

8.3.4 Relationships of Muscle Quality and Size with Physical Function

Results from GEE analyses for physical function outcomes are shown in Table 8.4. GMED FF was significantly positively associated with SCT (β = 0.642, P = .002). GMED FF (β = -1.5, P = .002) and GMIN FF (β = -0.243, P = .03) showed significant

negative associations with 30CRT (Figure 8.2). TFL FF and LV of all muscles were not significantly associated with any physical function outcomes.

Table 8.4. Results from generalized estimating equations for associations of muscle fat fraction and lean volume with physical function adjusted for age, sex, and BMI.

	Fat Fraction		Lean Volume	
	β (95% CI)	*P*-Value	β (95% CI)	*P*-Value
SCT				
GMED	**0.642 (0.241, 1.043)**	**.002**	-0.009 (-0.025, 0.006)	.218
GMIN	0.133 (-0.002, 0.268)	.053	-0.032 (-0.072, 0.009)	.124
TFL	-0.030 (-0.249, 0.190)	.791	-0.037 (-0.113, 0.040)	.342
30CRT				
GMED	**-1.500 (-2.461, -0.536)**	**.002**	-0.008 (-0.039, 0.024)	.633
GMIN	**-0.243 (-0.461, -0.024)**	**.030**	-0.039 (-0.089, 0.010)	.119
TFL	-0.240 (-0.566, 0.085)	.148	-0.049 (-0.169, 0.072)	.426

Bold indicates statistical significance at $P < .05$. GMED, gluteus medius; GMIN, gluteus minimus; TFL, tensor fascia lata; SCT, stair climb test; 30CRT, 30-second chair rise test.

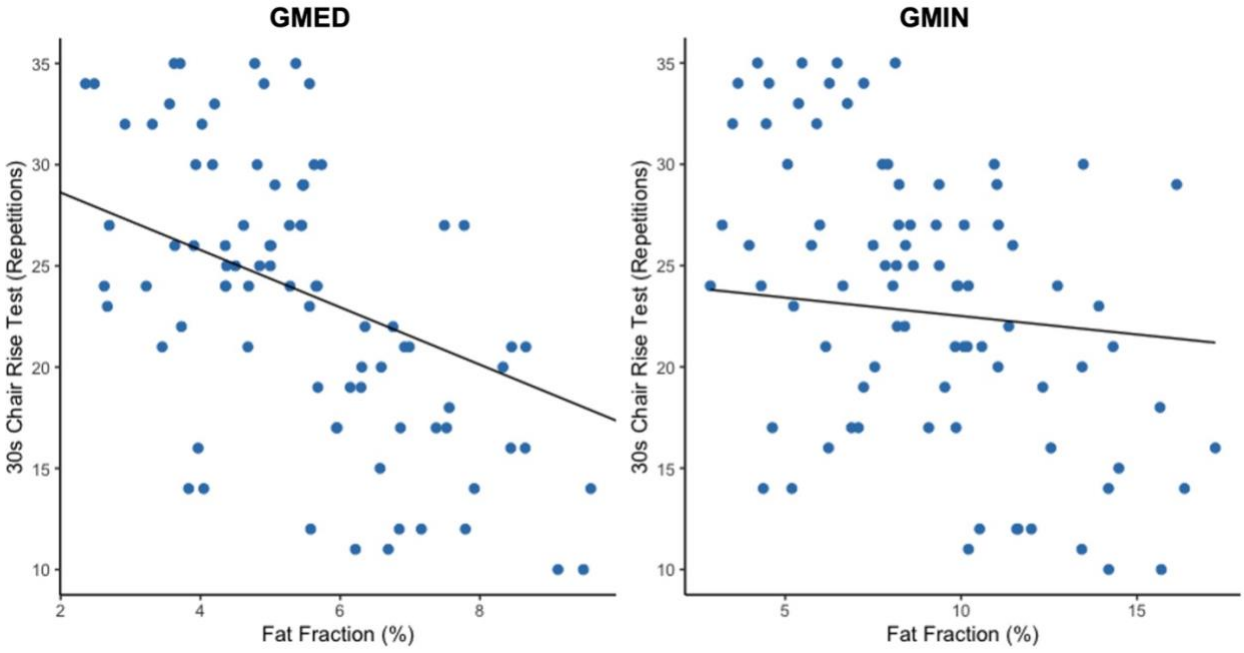

Figure 8.2. Relationship between fat fraction and 30-second chair rise test (30CRT). (Left) gluteus medius and (right) gluteus minimus. Regression lines show the unique contribution of the fat fraction variable of interest to the prediction of 30CRT performance.

8.4 Discussion

This study presents novel data evaluating the relationship between quantitatively measured hip abductor fatty infiltration and lean muscle volume with structural and functional disease outcomes in individuals with mild-to-moderate hip OA. Our findings demonstrate a lack of association of hip abductor FF and LV with radiographic KL grade. However, our results indicate that fatty infiltration of the hip abductors may play an important role in symptomatic and functional disease outcomes, as individuals with greater fatty infiltration reported worse hip-related symptoms and demonstrated greater functional limitations. Decreased LV was not observed in individuals with worse patient-reported outcomes or physical function; in fact, greater LV of the hip abductors was associated with worse patient-reported pain and QOL. These findings suggest that fatty infiltration may occur without a concurrent loss of lean muscle mass and may be more important for patient disability than the size of the muscle alone.

We found no significant association between increasing radiographic OA severity and hip abductor fatty infiltration. While previous research has found that GMED and GMIN fatty infiltration is higher in the hips of individuals with OA compared to controls[41,42] or in the affected versus unaffected limbs of individuals with unilateral OA[40,42,43], this research has largely consisted of studies which included individuals with end-stage disease who may have severe disuse-related atrophy. In one study which compared hip abductor fatty infiltration of individuals with mild-to-moderate radiographic OA to matched controls, greater GMIN, but not GMED or TFL, fatty infiltration was observed.[42] The previous study used semi-quantitative Goutallier classification[155] to grade fatty infiltration of the hip abductors on 3 consecutive MR slices. Goutallier

classification has been shown to overestimate fat content,[83,84] therefore the discrepancy between these findings and those of the present study may be due in part to our use of more accurate quantitative measures and evaluation across a much larger volume of muscle. It is well-established that radiographic OA severity is weakly associated with pain and symptoms[3] and KL grading lacks sensitivity for detecting early degenerative changes.[63] These limitations of radiographic OA classification may explain the lack of association observed between fatty infiltration and KL grade despite significant relationships with patient-reported symptoms and physical. Additionally, muscle quality and size were evaluated approximately 1-3 years after initial KL grading was performed in this study. This time gap may have contributed to the lack of association observed between muscle quality and radiographic OA severity. Further research is needed to evaluate muscle quality in relation to joint health using more sensitive measures of degeneration acquired at the same point in time as muscle data.

Due to a lack of methodological standards for evaluating muscle volume, it has been difficult to draw conclusions regarding muscle size deficits in individuals with hip OA. A recent systematic review with meta-analysis found low quality evidence of reduced muscle size in OA compared to matched controls.[152] Conflicting reports have shown increased, decreased, and no difference in hip abductor muscle volume in individuals with hip OA compared to healthy controls or in the affected versus unaffected limb.[40–43,115] Notably, none of these studies reported true measures of lean muscle volume, as intramuscular fat was not excluded from muscle size measures. While no association was observed between radiographic OA severity and LV in the present study, greater GMED LV was associated with worse patient-reported pain, and

LV of all muscles was associated with worse QOL. Despite the use of statistical methods which adjusted for BMI in our study, this method may not adequately control for differences in muscle volume related to body size. More specific measures of pelvis size or skeletal size may be necessary to accurately control for body size-associated differences in muscle volume and characterize how muscle volume varies with disease severity. Overall, the lack of positive association observed between hip abductor LV and HOOS scores suggests that lean muscle atrophy may not occur until later stages of disease, potentially after the onset of more advanced fatty infiltration.

To our knowledge, this is the first study to report relationships of quantitatively measured hip abductor fatty infiltration with patient-reported disability and physical function in individuals with mild-to-moderate hip OA. Previously, differences in GMED and GMIN fatty infiltration have been reported between individuals with symptomatic hip OA and asymptomatic controls.[41,42] In individuals with mild-to-moderate OA, semi-quantitatively measured GMED and GMIN fatty infiltration was reported to have no association with HOOS scores.[156] In our cohort, more sensitive quantitative measures of fatty infiltration were used and showed that—even at low levels of fatty infiltration—greater GMED, GMIN, and TFL fatty infiltration was associated with worse patient-reported symptoms.

Functional performance tests were used to understand the role of muscle quality and size in physical function. We found that GMED and GMIN fatty infiltration, and not LV, was associated with worse physical function as measured by SCT and 30CRT. These data are in accordance with a previous study which found greater hip abductor fatty infiltration was associated with greater gait variability and poor balance in a

population of older adults where gait variability was measured using temporospatial gait parameters and balance using clinical assessments.[114] Interestingly, only GMED FF was significantly associated with SCT performance. GMIN FF trended toward a positive relationship with SCT, indicating this study may be underpowered for detecting this relationship. However, our results which showed a positive association between GMED FF and SCT indicate that GMED FF may be more important for function in activities which involve single-limb stance. Whereas the 30CRT is a bilateral support activity, the SCT involves a single-limb component. These results suggest that GMIN fatty infiltration may be more closely associated with overall mobility impairment as measured by 30CRT performance, whereas GMED FF may be specific to single-limb function. Previous semi-quantitative reports of hip abductor muscle quality have hypothesized that GMIN fatty infiltration may be a normal process of aging common to both healthy controls and those with end-stage hip OA, whereas GMED fatty infiltration may be a pathological process specific to disease.[157] Our data support this hypothesis and indicate that GMED muscle quality may be a better predictor of disability than GMIN during tasks which involve single-limb stance.

At the knee, fatty infiltration of the quadriceps has been shown to predict patient-reported disability[38] and mobility[38,119] in individuals with knee OA. Beyond simply occupying volume in the muscle, adipose tissue stored in the muscle has the capacity to actively impair the function of remaining muscle fibers by altering muscle fiber pennation angle and elasticity, as well as through the release of proinflammatory cytokines which contribute to local inflammation and impair muscle metabolism.[37] We did not observe a decrease in lean muscle volume associated with increasing KL grade, worsening HOOS

scores, or worse physical function; therefore, it is possible that fatty infiltration may contribute to muscle dysfunction without a concurrent decrease in lean muscle size. A longitudinal study of muscle strength in older adults found that strength deficits were present even in individuals who gained lean muscle mass over a 3-year period.[158] Furthermore, evidence from a single-limb suspension study demonstrated that fatty infiltration may exceed a loss of lean muscle mass due to physical inactivity.[46] Our findings add to a growing body of work which suggests that fatty infiltration plays an important role in disease-related disability and demonstrates that changes in symptoms and function may not be fully captured by measures of muscle size alone.

Compared to radiographic signs of OA or other imaging-related biomarkers such as cartilage thickness or composition, muscle quality represents a potentially modifiable target for disease intervention. Several studies have shown that fatty infiltration of skeletal muscle can be reduced by exercise intervention.[124,137,159] Our data suggest that muscle quality may be an effective target for OA management and prevention strategies, and exercise intervention may be useful for improving symptomatic disease severity and patient function. Future longitudinal studies are needed to explore how changes in muscle quality over time impact disease severity and whether interventions aimed at maintaining or improving muscle quality positively affect disease trajectories.

Limitations of this study must be considered when interpreting the results. Our cohort consisted of high-functioning individuals with relatively healthy BMI, therefore our results may not be generalizable to a larger population with more severe pain, functional limitations, or higher BMI. Another limitation of this study was the use of cross-sectional data acquired at varying lengths of time from original baseline KL assessment. Because

muscle MR images were not acquired consistently at each timepoint, data from 1-year, 2-year, and 3-year follow-up were utilized. Therefore, degeneration may have worsened beyond original baseline KL readings. Additionally, the automatic segmentation method utilized in this study may introduce error beyond that of manual segmentation; however, this tool allowed for the inclusion of more subjects to power the study, as time-to-segmentation was reduced. Finally, the imaging coverage area used was not optimized for TFL analysis given that the muscle belly extends beyond the greater trochanter. This imaging coverage area was selected to optimize analysis of the larger hip abductor muscles while minimizing scan time. Previous work, however, has suggested that TFL fatty infiltration and size is minimally affected in the OA disease process.[42,116,147]

8.5 Conclusions

We found that fatty infiltration of the hip abductors was associated with worse patient-reported symptoms and physical function, but not radiographic OA severity in individuals with mild-to-moderate hip OA. Greater hip abductor lean muscle volume was also associated with worse patient-reported pain and QOL, suggesting a lack of lean muscle atrophy in individuals with greater disability. These findings suggest that hip abductor fatty infiltration may be a feature of mild-to-moderate disease which significantly contributes to patient-perceived and physical disability and this process may occur without a concurrent loss of lean muscle mass. Future studies are needed to evaluate longitudinal changes in hip abductor muscle quality and size related to disease progression using biomarkers of joint health with greater sensitivity to early-stage degenerative changes.

9 Associations of Hip Abductor Muscle Quality with Cartilage Lesions in Hip Osteoarthritis

9.1 Introduction

Osteoarthritis (OA) is increasingly recognized as a whole-joint disease affecting not only articular cartilage and bone, but also soft tissues such as periarticular muscles.[16] While OA research has primarily focused on characterization of degenerative changes in cartilage and bone to date, recent evidence of OA-related muscle atrophy suggests that muscle may play an important role in the OA disease process.[152,160] Muscle atrophy may be characterized by both fatty infiltration of the muscle and a loss of lean muscle mass. The ratio of adipose to lean tissue within the muscle has come to be described by the term “muscle quality” with worse muscle quality indicated by a greater proportion of adipose tissue within the muscle. Adipose tissue stored within muscle releases pro-inflammatory cytokines which may directly affect joint tissues, and may alter or impair the mechanical and metabolic properties of the muscle.[37,56]

In individuals with hip OA, increased fatty infiltration of the hip abductors has been observed[40–43] and, although conflicting results have been reported, some studies have found decreased hip abductor muscle size associated with hip OA.[40,42] However,

most studies have investigated muscle quality and size in relation to radiographic grading of disease severity which can only be used to infer the status of cartilage health through joint space narrowing. At the knee, fatty infiltration of the quadriceps has been associated with severity and progression of cartilage lesions over 3 years in individuals with knee OA.[38,39] In hip OA, there is a paucity of research evaluating relationships between muscle quality and cartilage health. One study has evaluated the relationship between hip abductor fatty infiltration and cartilage composition using quantitative magnetic resonance imaging (MRI), but found mixed results.[118] Thus, further research is needed to evaluate muscle quality and size in relation to direct measures of cartilage health to better understand the impact of muscle atrophy on joint tissues.

Therefore, the objective of this study was to evaluate whether quantitatively measured hip abductor (gluteus medius [GMED], gluteus minimus [GMIN], and tensor fascia lata [TFL]) muscle quality and size is associated with greater cartilage lesions in individuals with and without mild-to-moderate hip OA. The secondary objective of this study was to determine whether hip abductor muscle quality and size is associated with localized patterns of degeneration in the acetabular or femoral cartilage.

9.2 Methods

9.2.1 Study Participants

Subjects were selected from an ongoing study on the progression of hip OA. All subjects signed informed consent as approved by our institution's Committee on Human Research. Study eligibility required subjects have either no signs of radiographic hip OA (Kellgren-Lawrence [KL] grade 0) or have evidence of mild-to-moderate hip OA (KL

grade 1-3)[62]. Participants with end-stage hip OA (KL grade 4) were excluded from the study. KL grading was performed by a trained musculoskeletal radiologist on bilateral anterior-posterior and lateral hip screening radiographs. Additional exclusion criteria included contraindications to MRI, history of hip surgery, hip trauma within the previous 3 months, joint replacement of any lower extremity joint, pain or OA of any other lower extremity joint, self-reported inflammatory arthritis, or mobility assistance requirements.

9.2.2 MR Image Acquisition and Analysis

Hip MR images were obtained using a 3.0T MR scanner (GE Healthcare, Waukesha, WI), with each hip scanned individually. Patients were positioned supine with feet taped together to ensure neutral hip alignment during MR imaging and a 32-channel coil (GE Healthcare, Waukesha, WI) was placed on the hip. MR sequences (Table 9.1) included: (1) 3-plane gradient echo localizer for prescribing the imaging coverage area, (2) 3D axial Iterative Decomposition of water and fat with Echo Asymmetry and Least-squares estimation (IDEAL-IQ)[91,93] spoiled gradient-recalled echo (SPGR) with multi-peak fat spectrum modeling and single T_2* correction[142] for muscle evaluation, and (3) coronal T_2 and 3D fast spin-echo Cube with sagittal, axial, and oblique axial reconstructions for morphological assessment of articular cartilage. IDEAL-IQ fat fraction (FF) maps in which the signal intensity of each voxel represents the percentage of fat in that voxel on a scale from 0 to 100% were generated online. FF map image volumes were acquired from the iliac crest to the greater trochanter to image the full length of GMED, GMIN, and a large portion of TFL. Due to time

constraints during MR scanning, muscle imaging of only a single hip was acquired for some subjects resulting in the inclusion of both bilateral and unilateral cases.

Table 9.1. Magnetic resonance sequences and acquisition parameters.

MR Sequence	Acquisition Parameters	Measurements
3-plane gradient echo	-	Localizer—coverage
3D IDEAL-IQ SPGR	TR = 9.3 ms, ETL = 2, number of echoes = 6, FA = 3, FOV = 22x22 cm, matrix size = 256x256, slice thickness = 6 mm	Muscle segmentation; FF and Lean Volume Quantification
Coronal T2 FS	TR/TE = 3000/57.98 ms, ETL = 18, matrix size = 512x512, FOV=20x20 cm, slice thickness = 4 mm	SHOMRI scoring
3D FSE-CUBE FS	TR/TE = 1200/20, ETL = 30, matrix size = 192x192, FOV = 15.3x15.3 cm, slice thickness = 0.8 mm	SHOMRI scoring

3D, three-dimensional; IDEAL-IQ, Iterative Decomposition of water and fat with Echo Asymmetry and Least-squares estimation; SPGR, spoiled gradient-recalled echo; FS, fat-saturated; FSE, fast spin echo; TR, repetition time; TE, echo time; ETL, echo train length; FA, flip angle; FOV, field of view; SHOMRI, scoring hip OA with MRI

Automatic segmentation of GMED, GMIN, and TFL was performed on IDEAL-IQ FF maps using the automatic muscle segmentation network described and validated in Chapter 7. Automatic segmentations underwent post-processing (removal of extra pixels from the mask by keeping only the largest connected component, extraction and dilation the perimeter of the mask using a structuring disk element (radius = 1), and filling holes within the mask). The FF of each muscle was calculated by taking the average signal intensity of all voxels in the segmented region on the FF map. Lean volume (LV) of each muscle was calculated by taking the sum of all voxels in the segmented region across all slices minus fat volume.

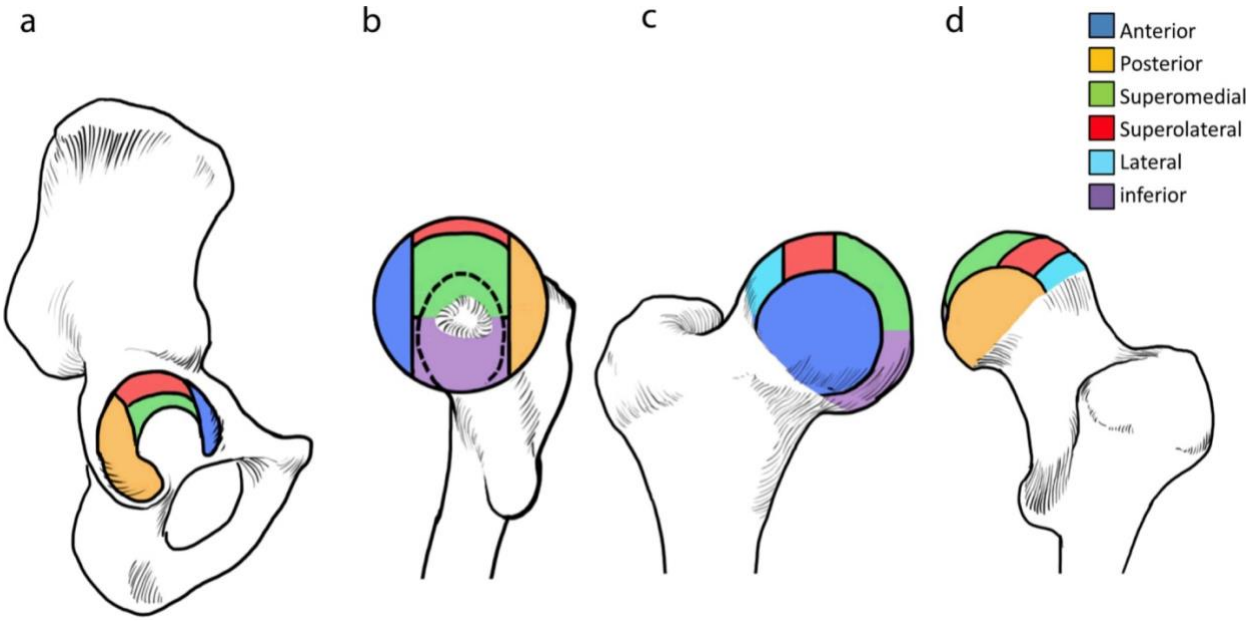

Figure 9.1. Cartilage subregions as defined in the Scoring Hip Osteoarthritis with MRI (SHOMRI) morphological grading system. Subregions include four acetabular regions and six femoral regions. Figure reproduced with permission of Wiley, from Scoring hip osteoarthritis with MRI (SHOMRI): A whole joint osteoarthritis evaluation system.[66]

Semi-quantitative morphological assessment of cartilage abnormalities was performed using the Scoring Hip OA with MRI (SHOMRI) evaluation system[66] by an experienced, board-certified radiologist. SHOMRI has previously been validated against arthroscopic findings[67] and has been shown to have excellent inter- and intra-reader agreement (intra-reader intraclass correlation coefficient [ICC] = 0.93–0.98; inter-reader ICC = 0.91–0.94)[66]. Using the SHOMRI scoring system to assess cartilage morphology, the acetabulum and femoral head were divided into 4 (superolateral, superomedial, anterior, posterior) and 6 (lateral, superolateral, superomedial, inferomedial, anterior, posterior) subregions as shown in Figure 9.1. In each of the 10 subregions, cartilage lesions were graded on a 3-point scale, with 0 indicating no lesion, 1 indicating partial-thickness cartilage loss, and 2 indicating full-thickness cartilage loss. Subregion scores were then dichotomized into presence or no presence of a cartilage lesion in that

subregion. The total acetabulum and femur SHOMRI scores were then calculated by summing cartilage scores across the 6 and 4 subregions, respectively. Finally, the overall SHOMRI total combined cartilage score was calculated as the sum of cartilage scores in all 10 subregions.

9.2.3 Statistical Analysis

Relationships of hip abductor FF and LV with SHOMRI total combined cartilage, total acetabular, and total femoral scores were evaluated using linear regression models with a generalized estimating equation (GEE) approach. In the GEE models, subject identifier and muscle FF or LV served as the within-subjects variables, and SHOMRI score as the dependent variable, with age, sex, and body mass index (BMI) entered as covariates. For subregion analysis, logistic regression using GEE was performed to calculate odds ratios (OR) for incidence of cartilage lesions, with FF or LV as the independent variable, and presence of cartilage lesion as the dependent variable, with age, sex, and body mass index (BMI) as covariates. All statistical analyses were performed in R Studio v4.0.2 (R Core Team, Vienna, Austria) with P-value < .05.

9.3 Results

9.3.1 Demographics and Characteristics

A total of 88 hips from 51 participants (37 bilateral cases and 14 unilateral cases) were included in this analysis with an average age of 53.6 ± 15.6 years, BMI of 24.1 ± 3.4 kg/m^2, and included 34 male hips (39%). A total of 24 hips were KL grade 0, 39 were KL grade 1, 14 were KL grade 2, and 11 were KL grade 3. Demographics and group characteristics are shown in Table 9.2. Frequency of presence of cartilage lesions in acetabular and femoral subregions is shown in Table 9.3.

Table 9.2. Group Demographics and Characteristics (N = 51, 88 hips).

Characteristic		Value
Demographics	Age (years)	53.6 ± 15.6
	Sex (% Male)	39
	BMI (kg/m^2)	24.1 ± 3.4
Fat Fraction (%)	GMED	5.6 ± 1.8
	GMIN	9.12 ± 3.5
	TFL	5.3 ± 3.1
Lean Volume (cm^3)	GMED	223.4 ± 54.2
	GMIN	70.3 ± 16.8
	TFL	18.8 ± 7.7
SHOMRI	Total Combined Cartilage	3.8 ± 2.8
	Total Ace	1.8 ± 1.5
	Total Fem	2.0 ± 1.8

Values are mean ± SD unless indicated otherwise. BMI, body mass index; GMED, gluteus medius; GMIN, gluteus minimus; TFL, tensor fascia lata; SHOMRI, scoring hip OA with MRI; Ace, acetabular; Fem, femoral.

Table 9.3. Frequency of lesions in cartilage subregions.

Cartilage Region	Subregion	Frequency, n
Acetabular	Superolateral	61
	Superomedial	31
	Anterior	30
	Posterior	4
Femoral	Lateral	51
	Superolateral	59
	Superomedial	11
	Inferomedial	11
	Anterior	14
	Posterior	1

Presence of lesion determined by SHOMRI score > 0 in cartilage subregion.

9.3.2 Relationships of Muscle Fat Fraction with SHOMRI Cartilage Scores

Results for correlations between muscle FF and SHOMRI cartilage scores are shown in Table 9.4. GEE analysis revealed that GMED FF was significantly positively associated with SHOMRI total combined cartilage scores (β = 0.747, *P* < .001) with significant positive associations observed for both total acetabular (β = 0.349, *P* = .009) and femoral (β = 0.420, *P* < .001) scores. GMIN FF was significantly positively associated with SHOMRI total combined cartilage scores (β = 0.203, *P* = .025), with significant positive associations observed only for total femoral cartilage scores (β = 0.112, *P* = .034). TFL FF was not significantly associated with SHOMRI total combined cartilage or total acetabular and femoral scores. Relationships of GMED and GMIN FF with SHOMRI total combined cartilage scores are shown in Figure 9.2 with an example of subject differences shown in Figure 9.3.

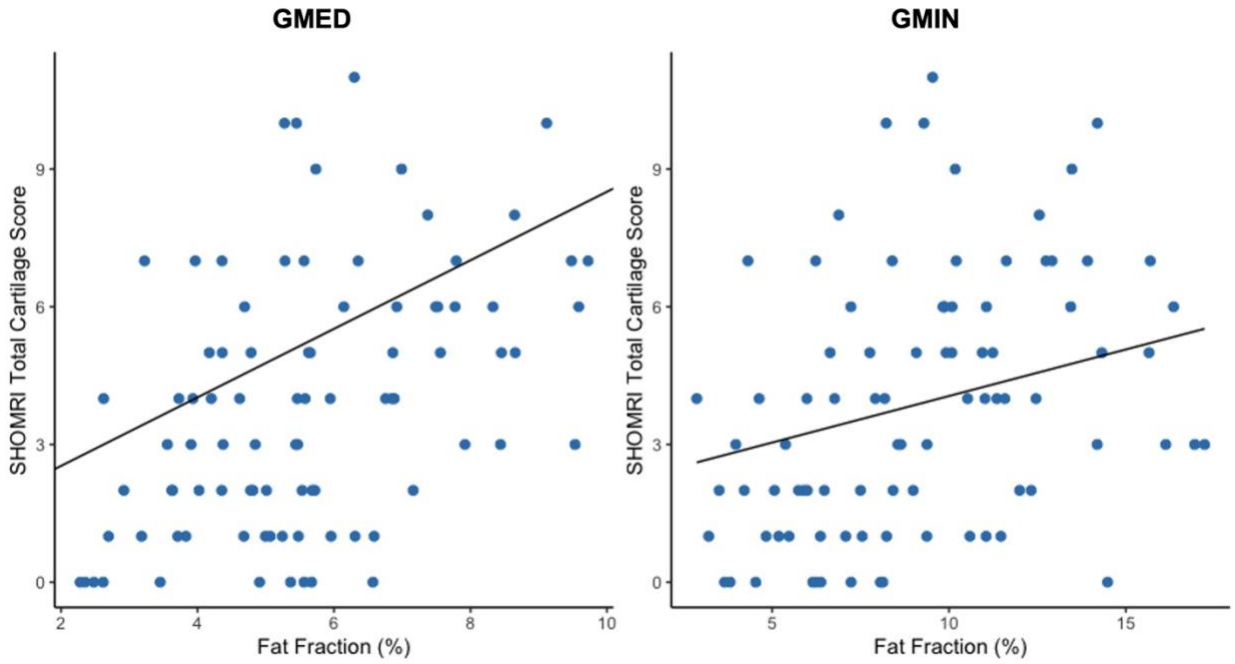

Figure 9.2. Relationships between fat fraction and SHOMRI total combined cartilage score. (Left) gluteus medius and (right) gluteus minimus. Regression lines show unique contribution of fat fraction variable of interest to the prediction of SHOMRI scores.

Subregion analysis using logistic regression (Table 9.5) revealed that GMED FF was significantly associated with greater odds of superolateral acetabular (OR = 2.0, *P* = .007) and femoral (OR = 1.71, *P* = .006) cartilage lesions. Relationships of GMIN FF with presence of cartilage lesions did not reach statistical significance for any subregion. However, greater TFL FF was associated with increased odds of superolateral acetabular cartilage lesions (OR = 1.65, *P* = .022). Less than 5% of hips had a cartilage lesion in either the posterior acetabular or femoral cartilage regions, therefore results were not reported for these subregions.

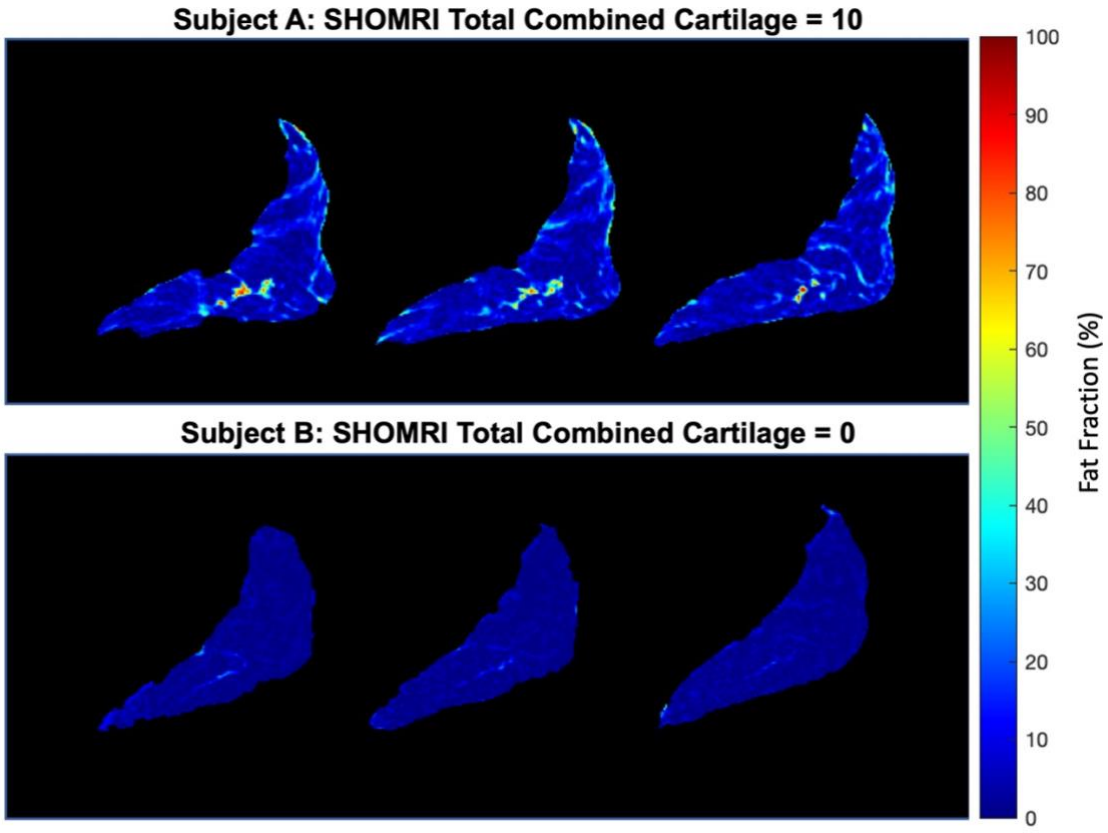

Figure 9.3. Comparison of GMED fat fraction (FF) maps for subjects with high and low SHOMRI total combined cartilage scores. Image slices selected from approximately the same proximal to distal region in both subjects. Subject A (top) had overall GMED FF of 9.1% and SHOMRI total combined cartilage score of 10. Subject B (bottom) had overall GMED FF of 2.4% and SHOMRI total combined cartilage score of 0.

9.3.3 Relationships of Muscle Lean Volume with SHOMRI Cartilage Scores

TFL LV was significantly negatively associated with SHOMRI total combined cartilage scores (β = -0.069, 95% CI [-0.135, -0.004], *P* = .039). However, no other significant relationships were observed between LV and total cartilage scores, and logistic regression revealed no significant relationships of LV with presence of lesions in cartilage subregions (data not shown).

Table 9.4. Generalized estimating equation results for associations of fat fraction with SHOMRI cartilage scores adjusted for age, sex, and BMI.

	GMED FF		GMIN FF		TFL FF	
	β (95% CI)	*P*-Val	β (95% CI)	*P*-Val	β (95% CI)	*P*-Val
Total Cartilage	**0.747 (0.345, 1.149)**	**< .001**	**0.203 (0.026, 0.380)**	**.025**	0.157 (-0.029, 0.342)	.098
Total Ace	**0.349 (0.088, 0.610)**	**.009**	0.010 (-0.018, 0.215)	.098	0.059 (-0.047, 0.166)	.280
Total Fem	**0.420 (0.171, 0.668)**	**< .001**	**0.112 (0.009, 0.215)**	**.034**	0.108 (-0.012, 0.229)	.078

Bold indicates statistical significance at $P < .05$. GMED, gluteus medius; GMIN, gluteus minimus; TFL, tensor fascia lata; FF, fat fraction; SHOMRI, scoring hip OA with MRI; Ace, acetabulum; Fem, femoral head.

Table 9.5. Results from generalized estimating equation logistic regression models for classification of subjects with and without subregion cartilage lesions adjusted for age, sex, and BMI.

		GMED FF		GMIN FF		TFL FF	
		OR (95% CI)	*P*-Val	OR (95% CI)	*P*-Val	OR (95% CI)	*P*-Val
Ace	Superolateral	**2.00 (1.210, 3.290)**	**.007**	1.13 (0.927, 1.380)	.220	**1.65 (1.070, 2.530)**	**.022**
	Superomedial	1.30 (0.840, 2.030)	.240	1.16 (0.971, 1.390)	.100	0.98 (0.832, 1.158)	.824
	Anterior	0.99 (0.684, 1.438)	.964	1.20 (0.959, 1.506)	.111	1.10 (0.912, 1.322)	.326
Fem	Lateral	1.34 (0.879, 2.041)	.170	1.15 (0.967, 1.373)	.112	1.25 (0.946, 1.665)	.120
	Superolateral	**1.71 (1.160, 2.510)**	**.006**	1.19 (0.981, 1.433)	.077	1.17 (0.919, 1.499)	.200
	Superomedial	1.58 (0.873, 2.861)	.130	1.14 (0.951, 1.356)	.160	0.99 (0.835, 1.179)	.930
	Inferomedial	1.97 (0.915, 4.228)	.083	1.07 (0.882, 1.304)	.480	1.10 (0.904, 1.342)	.340
	Anterior	1.06 (0.609, 1.844)	.838	1.17 (0.934, 1.468)	.171	1.11 (0.916, 1.336)	.294

Bold indicates statistical significance at $P < .05$. GMED, gluteus medius; GMIN, gluteus minimus; TFL, tensor fascia lata; FF, fat fraction; Ace, acetabulum; Fem, femoral head.

9.4 Discussion

We found that increased fatty infiltration of the hip abductors, particularly the GMED, was associated with greater cartilage degeneration measured by semi-quantitative morphological grading. Additionally, decreased TFL lean volume was associated with greater number and severity of cartilage lesions. Subregion analysis revealed areas of cartilage which may be at greater risk for degeneration with increased fatty infiltration of the hip abductors. Our findings highlight the importance of hip abductor muscle quality and size in cartilage health and suggest that these muscles may serve as a promising therapeutic target for preventing or slowing progression of cartilage degeneration in individuals with hip OA.

To date, hip abductor muscle quality and size have primarily been related to joint health using radiographic OA grading. These methods lack sensitivity for detecting early degenerative changes and do not allow for direct evaluation of cartilage.[63] Our data, obtained from a cohort with mild-to-moderate radiographic OA, provide evidence that the hip abductors play an important role in joint health. Much of the previous work evaluating muscle quality in hip OA has included individuals with end-stage radiographic disease (KL = 4). Several of these studies have demonstrated increased GMED[40,41,43] and GMIN[43] fatty infiltration in individuals with hip OA. However, a study by Zacharias et al which excluded individuals with end-stage disease, found that individuals with hip OA had greater fatty infiltration of GMIN but not GMED.[42] These findings led the authors to hypothesize that GMIN atrophy may precede GMED, with GMED atrophy thought to occur only in late stages of disease. Our results challenge this hypothesis and suggest

that GMED fatty infiltration, even at very low levels of less than 10%, is significantly associated with cartilage degeneration in mild-to-moderate hip OA. The previous study used semi-quantitative Goutallier grading to evaluate hip abductor fatty infiltration, which may have lacked sensitivity for detecting low levels of fatty infiltration as seen in GMED.[38,84] Our results are in accordance with the results of a study by Kumar et al which found that, at the knee, quadriceps fatty infiltration was associated with greater progression of morphological joint degeneration over 3 years, with an average fat fraction of 5.2% in the quadriceps.[39]

Increased GMED fatty infiltration was specifically associated with a greater risk of superolateral acetabular and femoral cartilage lesions. A previous report by Damm et al showed that increased fatty infiltration of the GMED was associated with increased hip joint contact forces 3 months following total hip arthroplasty.[117] Hip joint contact forces have been shown to be transmitted primarily through the anterior superolateral quadrant of the acetabulum during gait.[161] Therefore, it was not surprising that increased hip abductor fatty infiltration and decreased lean volume were linked to degeneration in this region. These data highlight the need for future studies to evaluate joint loading related to muscle quality and size in individuals with mild-to-moderate hip OA, as muscle quality and size may play an important role in controlling loading of articular cartilage and other joint tissues.

The relationships observed between fatty infiltration and cartilage health in this study indicate that hip abductor muscle quality may be a promising biomarker of early degeneration in individuals with hip OA. Several studies have demonstrated that fatty infiltration of skeletal muscle can be mitigated through exercise intervention.[123,124,137]

Therefore, muscle quality represents a promising target for therapeutic interventions. However, whether muscle atrophy is a factor leading to joint degeneration or simply a result of disease onset remains unclear. Longitudinal studies are needed to evaluate whether interventions aimed at altering muscle quality affect longitudinal trajectories of joint degeneration.

Limitations of this study should be considered when interpreting the results. Our cohort consisted of high-functioning, community-dwelling adults, and our study did not use symptomatic criteria for subject recruitment. Therefore, our results may not be generalizable to individuals with more severe, symptomatic disease. Although this cohort was high functioning and did not have significant mobility impairments, physical activity levels were not evaluated or controlled for. Reduced physical activity levels of individuals with greater cartilage degeneration may have contributed to our findings. Additionally, the imaging coverage area used in this study was not optimized for evaluation of the full length of TFL. Further research is needed to evaluate the entirety of this muscle in relation to cartilage health. Finally, relationships with lean volume reported in this study were adjusted for BMI. However, statistically controlling for BMI may not fully control for body size differences. Although no standards currently exist for reporting muscle size, some studies have reported muscle volume normalized to body mass. However, these methods may also have limitations, as muscle volume may be influenced to a greater extent by skeletal size rather than overall body mass. Further exploration of methods which fully account for body size in muscle volume evaluation are needed.

9.5 Conclusions

We have shown that hip abductor fatty infiltration, particularly of the GMED, is associated with greater cartilage degeneration, evaluated using semi-quantitative morphological grading. Subregion analysis revealed that increased fatty infiltration and decreased lean volume of the hip abductors was associated with increased risk of lesions in the superolateral acetabular and femoral cartilage. These results suggest that muscle quality and size may play a role in cartilage degeneration and indicate that these muscles may be useful therapeutic targets for disease intervention.

10 Hip Abductor Muscle Quality is Associated with Altered Frontal Plane Joint Loading and Cartilage Composition in Individuals with Hip Osteoarthritis

10.1 Introduction

Osteoarthritis (OA) is a common degenerative joint disease affecting over 27 million US adults, with this number expected to rise as the population ages.[2] Hip OA is a particularly debilitating form of disease given its impact on weight-bearing joint structures which may significantly impact an individual's ability to locomote and carry out common activities of daily living.[8] Currently, treatment approaches for minimizing tissue damage are extremely limited.[149] Therefore, identification of biomarkers of early-stage disease is critical for the development of more effective treatment strategies which may prevent or slow the progression of disease.

In recent years, muscle quality has been identified as a potential biomarker of disease in OA.[38–40,42,147] Muscle quality has been defined as the proportion of adipose versus lean tissue in the muscle, with a higher ratio of adipose tissue indicating worse

muscle quality. Beyond occupying space within the muscle that would normally be composed of lean contractile tissue, adipose tissue stored within the muscle secretes numerous signaling factors and may alter or impair the mechanical and metabolic function of surrounding muscle fibers.[37,56] Greater fatty infiltration has been observed in individuals with both knee[38,39] and hip[40–43] OA and has been linked to reduced strength, mobility, and function.[38,114,119] Muscle quality represents a promising target for disease prevention and management, as fatty infiltration and lean muscle mass have been shown to be modifiable through exercise intervention.[37,137]

Though OA is increasingly recognized as a multifactorial disease, joint loading has long been hypothesized to play an important role in the pathogenesis of OA.[162,163] Muscle dysfunction caused by fatty infiltration or decreased lean muscle volume may alter load transmission by the joint. At the hip, muscle quality of the hip abductors may contribute to altered frontal plane joint loading, as these muscles act to stabilize the pelvis in the frontal plane during the single-limb stance phase of gait and are often weak in individuals with OA.[97,100] A study in individuals with hip OA following total hip arthroplasty demonstrated higher joint contact forces in individuals with increased fatty infiltration of the hip abductors.[117] Furthermore, increased frontal plane joint loading has been linked to hip OA and progression of disease.[164–166] However, no studies have linked muscle quality to frontal plane gait biomechanics in individuals with mild-to-moderate OA. Further investigation is needed to understand the role of muscle quality in joint loading and joint health using quantitative muscle quality and size assessment, gait analysis, and biomarkers of cartilage degeneration which are sensitive and specific to early degenerative changes.

$T_{1\rho}$ and T_2 relaxation time mapping allows for indirect quantification of cartilage biochemistry and provides insight into the health of articular cartilage in early stages of disease.[28] In articular cartilage, $T_{1\rho}$ relaxation times are negatively correlated with proteoglycan content, with higher $T_{1\rho}$ relaxation times indicating decreased proteoglycan content.[70] T_2 relaxation times correspond to water content and collagen organization, with increased T_2 relaxation times indicating increased water content and greater disorganization of the collagen network.[73,74] To date, there is limited evidence relating hip abductor muscle quality to cartilage composition. One study has investigated this relationship and found mixed results for the relationship of muscle quality with $T_{1\rho}$ relaxation times, and a negative association with T2 relaxation times.[118] Given that cartilage relaxation times have been shown to be sensitive to loading[167–169] and muscle quality may alter joint loading, further evaluation of this relationship with added context regarding subject-specific biomechanics is needed.

Therefore, the purpose of this study was to determine whether hip abductor fatty infiltration and lean volume is associated with hip abductor strength and altered frontal plane gait kinematics and kinetics in individuals with mild-to-moderate OA. The secondary aim was to determine the association of hip abductor fatty infiltration and lean volume with cartilage $T_{1\rho}$ and T_2 relaxation times.

10.2 Methods

10.2.1 Study Participants

Subjects were recruited from the community as part of an ongoing longitudinal study on progression of hip OA. All subjects signed informed consent as approved by

our institution's Committee on Human Research. Subject eligibility was determined using Kellgren-Lawrence (KL) grading to determine radiographic OA severity.[62] KL grading was performed by a trained musculoskeletal radiologist on bilateral anterior-posterior and lateral hip screening radiographs. Subjects with end-stage hip OA (KL grade = 4) were excluded from the study. Additional exclusion criteria included contraindications to MRI, history of hip surgery, hip trauma within the previous 3 months, joint replacement of any lower extremity joint, pain or OA of any other lower extremity joint, self-reported inflammatory arthritis, and immobility or assistance requirements that limit the ability to walk and participate in motion analysis.

10.2.2 MR Image Acquisition and Analysis

Hip MR images were obtained using a 3.0T MR scanner (GE Healthcare, Waukesha, WI) with a 32-channel coil (GE Healthcare, Waukesha, WI) placed over the hip. Patients were positioned supine in the scanner with feet secured to ensure leg rotational neutral alignment. MR sequences (Table 10.1) included: (1) 3-plane gradient echo localizer for prescribing the imaging coverage, (2) 3D axial Iterative Decomposition of water and fat with Echo Asymmetry and Least-squares estimation (IDEAL-IQ)[91,93] spoiled gradient-recalled echo (SPGR) with multi-peak fat spectrum modeling and single T_2* correction[142] for muscle evaluation, and (3) 3D magnetization-prepared angle-modulated partitioned k-space spoiled gradient echo snapshots (3D MAPSS)[170] for combined cartilage $T_{1\rho}$ / T_2 assessment. IDEAL-IQ fat fraction (FF) maps in which the signal intensity of each voxel represents the percentage of fat in that voxel on a scale from 0 to 100% were generated online. Coverage area of muscles was prescribed from

the iliac crest to the greater trochanter to acquire the full length of GMED, GMIN and a large portion of TFL. Due to time constraints during MR scanning, muscle imaging of only a single hip was acquired for some subjects; therefore, this study included unilateral and bilateral cases when available.

Table 10.1. Magnetic resonance sequences and acquisition parameters.

MR Sequence	Acquisition Parameters	Measurements
3-plane gradient echo	-	Localizer—coverage
3D IDEAL-IQ SPGR	TR = 9.3 ms, ETL = 2, number of echoes = 6, FA = 3, FOV = 22x22 cm, matrix size = 256x256, slice thickness = 6 mm	Muscle segmentation; FF and LV Quantification
3D combined $T_{1\rho}$ / T_2 MAPSS	TE = 0/10.4/20.8/41.6 ms; TSL = 0/15/30/45 ms; FOV = 14x14cm; TR = 1.2s; spin lock frequency = 300 Hz; matrix size = 256x128; slice thickness = 4 mm	Cartilage segmentation; $T_{1\rho}$ and T_2 quantification

MR, magnetic resonance; 3D, three-dimensional; IDEAL-IQ, Iterative Decomposition of water and fat with Echo Asymmetry and Least-squares estimation; SPGR, spoiled gradient-recalled echo, TR, repetition time; TE, echo time; ETL, echo train length; FA, flip angle; FOV, field of view; MAPSS, magnetization-prepared angle-modulated partitioned k-space spoiled gradient echo snapshots; FF, fat fraction; LV, lean volume.

Muscle segmentation was performed on all IDEAL-IQ FF maps using an automated hip abductor muscle segmentation network previously described and validated in Chapter 7. The segmentation network automatically generated GMED, GMIN, and TFL segmentations on all slices of the image volume from iliac crest to greater trochanter, and these segmentations underwent post-processing in MATLAB 2020b (MathWorks, Natick, MA). Post-processing involved removing extra pixels from the mask by keeping only the largest connected component, extracting and dilating the perimeter of the mask using a structuring disk element (radius = 1), and filling holes

within the mask. The FF of each muscle was calculated by taking the average voxel signal intensity of the IDEAL FF map in the segmented region across all slices. Total lean volume (LV) of each muscle was calculated by taking the sum of all voxels in the segmented region across all slices minus fat volume.

Cartilage segmentation was performed using a single atlas-based registration technique to automatically segment femoral and acetabular cartilage regions of each subject.[171,172] With this method, the first spin lock time (TSL) = 0 ms of the $T_{1\rho}$-weighted image of each participant was non-rigidly registered to a single reference atlas and this transformation field was then applied to the remaining $T_{1\rho}$- and T_2-weighted images. $T_{1\rho}$ and T_2 relaxation maps were reconstructed by fitting each voxel of the $T_{1\rho}$- and T_2-weighted images using Equations 10.2.1 and 10.2.2 below.[173] Mean $T_{1\rho}$ and T_2 relaxation times were then calculated by taking the average relaxation time of all voxels in the femoral and acetabular cartilage regions.

$$S(TSL) \propto \exp\left(-TSL/T_{1\rho}\right) \quad \text{(Equation 10.2.1)}$$

$$S(TE) \propto \exp\left(-TE/T_2\right) \quad \text{(Equation 10.2.2)}$$

10.2.3 Gait Data Acquisition and Analysis

A previously described 8-segment set of 45 retroreflective markers were adhered to each subject before collection of biomechanical data.[174] Motion analysis was performed using a 10-camera motion capture system (Vicon, Oxford, UK) and two in-ground force plates (AMTI, Watertown, MA). 3D marker position and ground reaction force (GRF) data were collected at 250 Hz and 1000 Hz, respectively. A one-second standing static calibration trial was collected with all markers adhered to the subject.

Next, calibration markers were removed, and subjects completed a series of gait trials with remaining tracking markers. Gait trials required subjects walk at a fixed speed of 1.35 $m \cdot s^{-1}$ ± 5%.[175] A gait trial was considered successful if the subject's target foot landed within the borders of the force plate. A minimum of five successful gait trials were collected for both left and right sides.

Raw marker position and GRF data were filtered using a fourth order, zero-lag, low-pass Butterworth filter with cutoff frequencies of 6 Hz and 50 Hz, respectively (Visual3D; C-Motion Inc., Rockville, MD). From the static calibration trial, an 8-segment, 6 degrees of freedom kinematic model consisting of the torso, pelvis, bilateral thighs, shanks, and feet was created. Joint centers were defined using methods previously described.[174] An unweighted least-squares method was used to describe segment position and orientation[176] and joint coordinates were resolved using an XY'Z'' Cardan sequence.[177] Inverse dynamics was used to calculate external joint moments, with joint angles and moments expressed in the same coordinate system.[178] Frontal plane hip kinematics and kinetics were analyzed during the stance phase of gait which was defined as initial contact to toe-off and time normalized to 101 points. Initial contact and toe-off were determined using a vertical GRF threshold > 20 N to define the point at which the foot first strikes the force plate and the last point at which the foot is in contact with the force plate.

Discrete kinematic variables of interest for this study included peak hip adduction and abduction angles. Kinetic variables of interest included peak external hip adduction moment (HAM) normalized to body mass ($Nm \cdot kg^{-1}$) and HAM impulse which is the integral of the normalized HAM with respect to time ($Nm \cdot s \cdot kg^{-1}$). Positive kinematic and

kinetic values indicate hip adduction. Using a custom written MATLAB program (MathWorks, Natick, MA), discrete biomechanical variables were determined for each trial, and the average of each variable over 5 trials was calculated.

10.2.4 Strength Testing

Peak hip abductor torque was measured during isometric testing using an instrumented dynamometer (Primus RS, BTE, Hanover, MD) sampled at 100 Hz. Testing was performed side-lying with the hip in neutral position. Before maximal strength testing, subjects performed 3 practice trials at progressive effort levels (25%, 50%, 75%) to familiarize subjects with the task. Next, torque data were acquired during 3 maximal effort isometric abduction trials. All trials were separated by 30-second rest periods. Subjects were given standardized instructions and verbal encouragement. For each maximal effort trial, the peak torque was measured and the trial with the highest peak torque across the 3 trials was normalized to body mass ($Nm \cdot kg^{-1}$).

10.2.5 Statistical Analysis

Relationships of muscle quality and size with peak isometric hip abductor strength, frontal plane gait biomechanics, and cartilage relaxation times were evaluated using generalized estimating equations (GEE). GEE methods are able to account for within-subject correlation of bilateral hip data included in this study and allow for datasets that include a combination of unilateral data for some subjects and bilateral for others.[154] In the GEE models, subject identifier and muscle FF or LV were entered into the model as the within-subjects variables, and gait biomechanical variables or cartilage relaxation times as the dependent variable, with age, sex, and body mass index (BMI)

entered as covariates. A *P*-value < .05 was considered statistically significant. All statistical analyses were performed in R Studio v4.0.2 (R Core Team, Vienna, Austria).

10.3 Results

10.3.1 Demographics and Characteristics

This study included a total of 69 hips from 41 participants (28 bilateral cases and 13 unilateral cases). The cohort had an average age of 52.6 ± 16.1 years, BMI of 24.1 ± 3.2 kg/m^2, and included 23 hips from males (33%). A total of 18 hips with radiographic KL grade 0, 30 hips with KL grade 1, 11 hips with KL grade 2, and 10 hips with KL grade 3 were included in this study. Group demographics and characteristics are shown in Table 10.2.

Table 10.2. Group Demographics and Characteristics (N = 41, 69 hips).

Characteristic		Value
Demographics	Age (years)	52.6 ± 16.1
	Sex (% Male)	33
	BMI (kg/m^2)	24.1 ± 3.2
Fat Fraction (%)	GMED	5.6 ± 1.8
	GMIN	9.14 ± 3.5
	TFL	5.2 ± 2.7
Lean Volume (cm^3)	GMED	217.5 ± 47.6
	GMIN	69.8 ± 15.0
	TFL	19.1 ± 7.8

Values are mean ± SD unless indicated otherwise. BMI, body mass index; GMED, gluteus medius; GMIN, gluteus minimus; TFL, tensor fascia lata.

10.3.2 Relationships of Muscle Quality and Size with Strength

Results for relationships of muscle FF and LV with peak isometric hip abduction strength are shown in Tables 10.3 and 10.4. GMED FF (β = -0.019, *P* = .001) and GMIN FF (β = -0.005, *P* = .019) were significantly negatively associated with strength. These relationships are shown in Figure 10.1. GMIN LV (β = 0.001, *P* = .003) was significantly positively associated with strength. No associations were observed for TFL with strength measures.

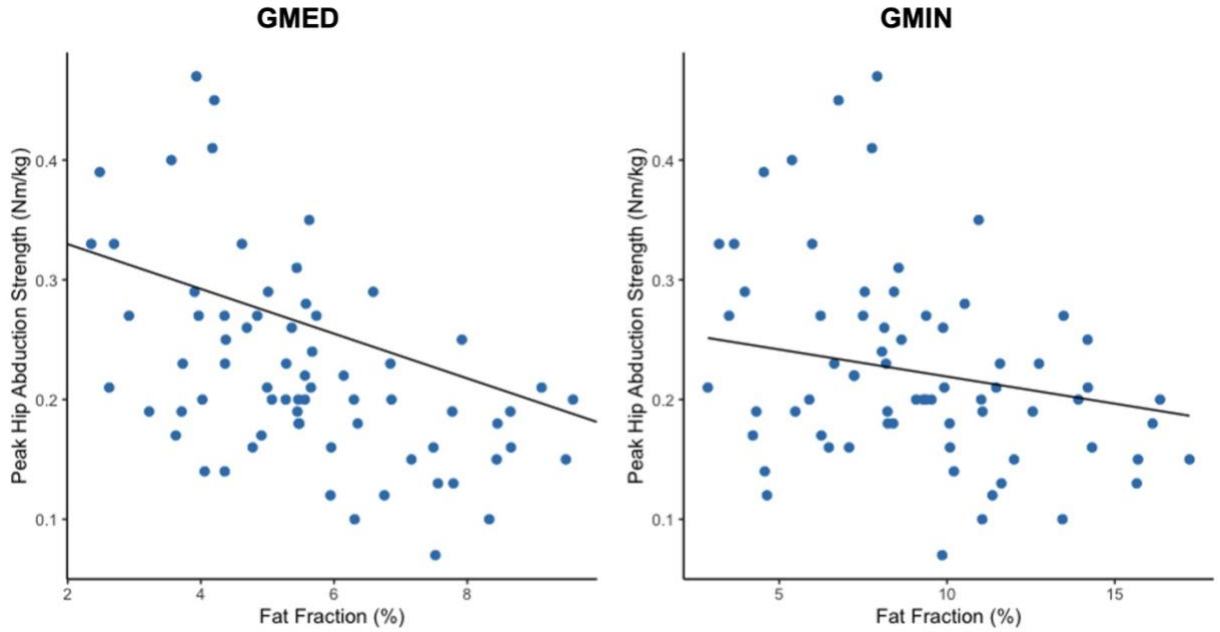

Figure 10.1. Relationship between fat fraction and hip abduction strength.(Left) gluteus medius and (right) gluteus minimus. Peak isometric hip abduction strength is normalized to body mass. Regression lines show unique contribution of fat fraction variable of interest to the prediction of hip abduction strength.

10.3.3 Relationships of Muscle Quality and Size with Frontal Plane Gait Biomechanics

Results for relationships of muscle FF and LV with gait kinematics and kinetics are shown in Tables 10.3 and 10.4. GMED FF was significantly positively associated

with peak HAM (β = 0.038, *P* < .001) and HAM impulse (β = 0.016, *P* =.023). These relationships can be visualized in Figures 10.2 and 10.3. GMIN and TFL FF were not significantly associated with hip frontal plane kinetics during gait, and no significant associations with hip frontal plane kinematics were observed for FF of any muscle. GMIN LV was significantly positively associated with peak HAM (β = 0.002, *P* = .015) and HAM impulse (β = 0.002, *P* = .015). GMED and TFL LV were not significantly associated with hip frontal plane kinetics, and no significant associations with hip frontal plane kinematics were observed for LV of any muscle.

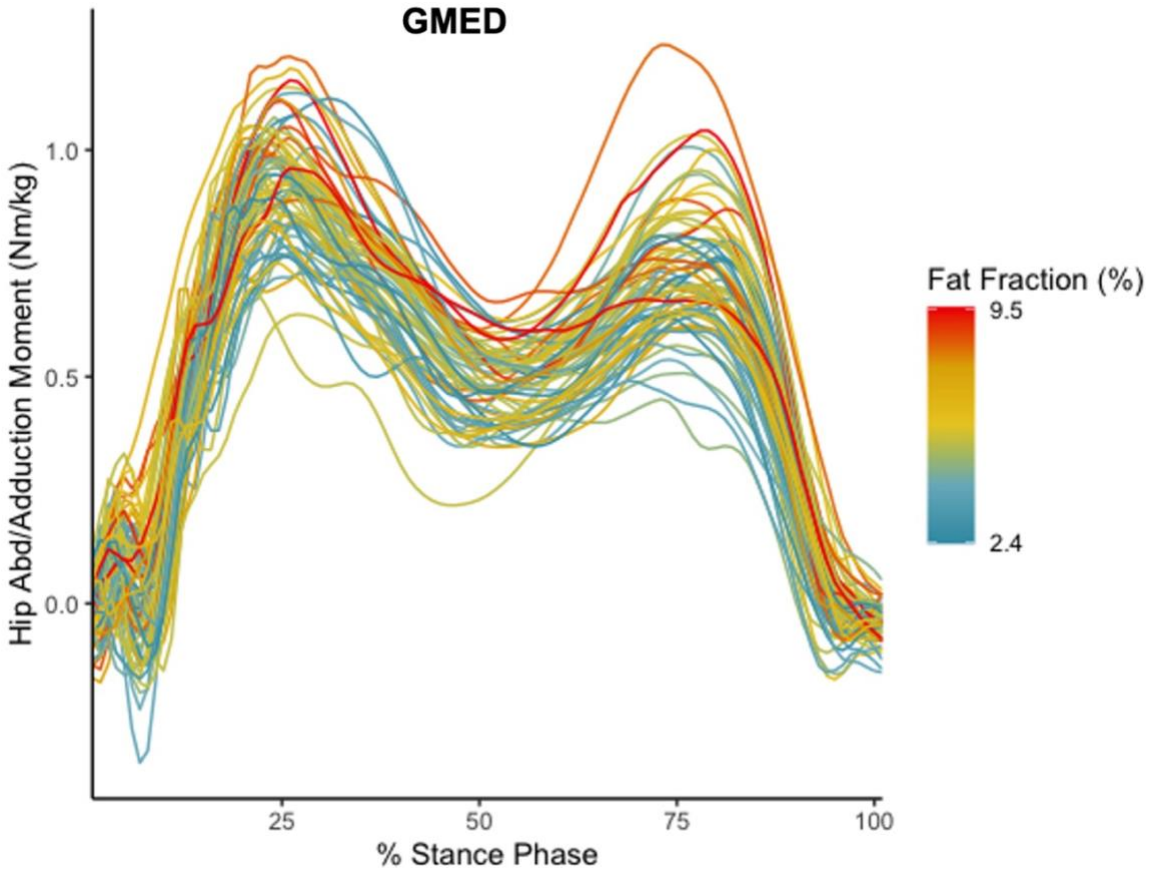

Figure 10.2. Ensemble curves showing frontal plane hip moment during the average of 5 walking trials with each subject's curve colored by their corresponding gluteus medius (GMED) fat fraction.

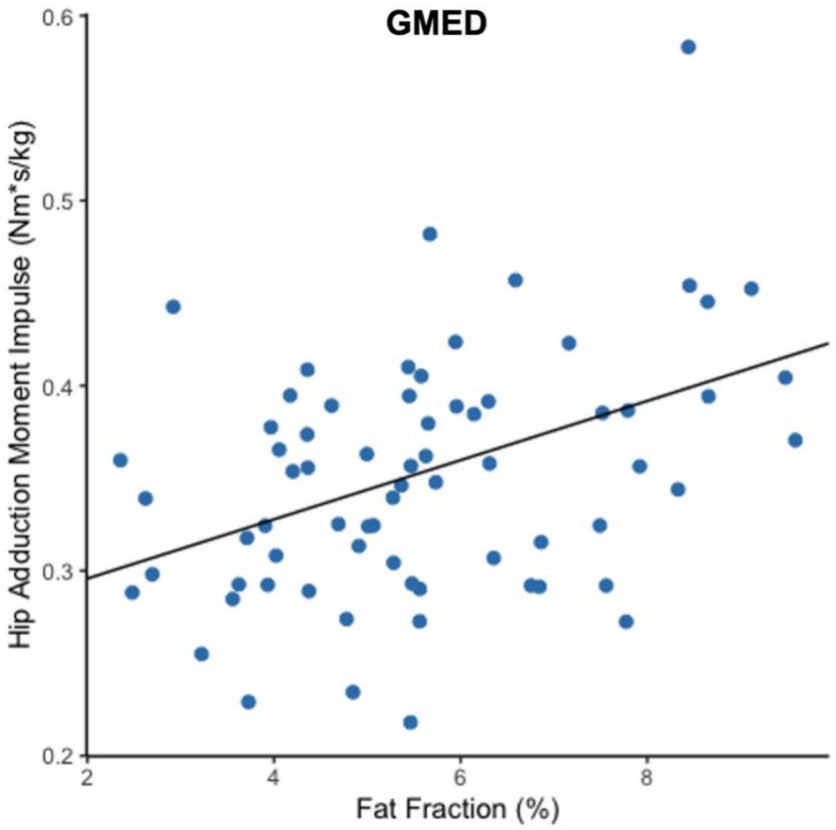

Figure 10.3. Relationship between gluteus medius (GMED) fat fraction and external hip adduction moment impulse (normalized to body mass). Regression line shows unique contribution of GMED fat fraction to the prediction of hip adduction moment impulse.

10.3.4 Relationships of Muscle Quality and Size with $T_{1\rho}$ and T_2 Cartilage Relaxation Times

Results for relationships of muscle FF and LV with cartilage relaxation times are shown in Tables 10.5 and 10.6. GMED FF was significantly negatively associated with mean femoral T_2 relaxation times (β = -1.12, *P* = .008). GMIN and TFL FF and LV of all muscles were not significantly associated with cartilage relaxation times.

Table 10.3. Results from generalized estimating equations for associations of muscle fat fraction with peak isometric strength and frontal plane gait kinematics and kinetics adjusted for age, sex, and BMI.

	GMED FF		GMIN FF		TFL FF	
	β (95% CI)	*P*-Val	β (95% CI)	*P*-Val	β (95% CI)	*P*-Val
Strength						
Pk Hip Abd	**-0.019 (-0.030, -0.007)**	**.001**	**-0.005 (-0.008, -0.001)**	**.019**	-0.004 (-0.010, 0.003)	.269
Kinematics						
Pk Hip Add	0.281 (-0.394, 0.957)	.414	0.054 (-0.222, 0.33)	.702	-0.041 (-0.312, 0.231)	.768
Pk Hip Abd	0.464 (-0.119, 1.047)	.120	0.075 (-0.127, 0.276)	.466	-0.031 (-0.262, 0.200)	.794
Kinetics						
Pk HAM	**0.038 (0.016, 0.061)**	**< .001**	0.009 (-0.004, 0.022)	.160	0.009 (-0.004, 0.022)	.170
HAM Impulse	**0.016 (0.002, 0.030)**	**.023**	0.004 (-0.003, 0.010)	.303	0.002 (-0.005, 0.010)	.541

Bold indicates statistical significance at p < .05. GMED, gluteus medius; GMIN, gluteus minimus; TFL, tensor fascia lata; FF, fat fraction; Pk, peak; Add, adduction; Abd, abduction; HAM, external hip adduction moment.

Table 10.4. Results from generalized estimating equations for associations of muscle lean volume with peak isometric strength and frontal plane gait kinematics and kinetics adjusted for age, sex, and BMI.

	GMED LV		GMIN LV		TFL LV	
	β (95% CI)	*P*-Val	β (95% CI)	*P*-Val	β (95% CI)	*P*-Val
Strength						
Pk Hip Abd	0.0002 (-0.0001, 0.001)	.231	**0.001 (0.0005, 0.002)**	**.003**	-0.001 (-0.002, 0.002)	.919
Kinematics						
Pk Hip Add	-0.002 (-0.0251, 0.0215)	.880	0.025 (-0.044, 0.094)	.472	0.004 (-0.082, 0.090)	.919
Pk Hip Abd	-0.003 (-0.022, 0.015)	.713	0.013 (-0.030, 0.055)	.564	0.0002 (-0.070, 0.070)	.996
Kinetics						
Pk HAM	0.00004 (-0.001, 0.001)	.930	**0.002 (0.0004, 0.004)**	**.015**	-0.001 (-0.004, 0.002)	.630
HAM Impulse	0.0003 (-0.0002, 0.001)	.210	**0.002 (0.0003, 0.003)**	**.015**	-0.0004 (-0.002, 0.003)	.929

Bold indicates statistical significance at $p < .05$. GMED, gluteus medius; GMIN, gluteus minimus; TFL, tensor fascia lata; LV, lean volume; Pk, peak; Add, adduction; Abd, abduction; HAM, external hip adduction moment.

Table 10.5. Results from generalized estimating equations for associations of muscle fat fraction with mean cartilage relaxation times adjusted for age, sex, and BMI.

	GMED FF		GMIN FF		TFL FF	
	β (95% CI)	*P*-Val	β (95% CI)	*P*-Val	β (95% CI)	*P*-Val
$T_{1\rho}$ Fem	-0.725 (-1.532, 0.081)	.078	-0.202 (-0.623, 0.218)	.345	-0.375 (-0.932, 0.181)	.190
$T_{1\rho}$ Ace	-0.503 (-1.374, 0.369)	.260	-0.237 (-0.612, 0.137)	.210	-0.312 (-0.843, 0.218)	.250
T_2 Fem	**-1.120 (-1.948, -0.291)**	**.008**	-0.402 (-0.867, 0.062)	.090	-0.574 (-1.199, 0.052)	.070
T_2 Ace	-0.607 (-1.486, 0.272)	.176	-0.294 (-0.655, 0.067)	.110	-0.428 (-0.962, 0.106)	.120

Bold indicates statistical significance at $P < .05$. GMED, gluteus medius; GMIN, gluteus minimus; TFL, tensor fascia lata; FF, fat fraction; Fem, femoral; Ace, acetabular.

Table 10.6. Results from generalized estimating equations for associations of muscle lean volume with mean cartilage relaxation times adjusted for age, sex, and BM**I.**

	GMED LV		GMIN LV		TFL LV	
	β (95% CI)	*P*-Val	β (95% CI)	*P*-Val	β (95% CI)	*P*-Val
$T_{1\rho}$ Fem	-0.003 (-0.034, 0.028)	.850	-0.022 (-0.104, 0.060)	.601	-0.040 (-0.173, 0.094)	.558
$T_{1\rho}$ Ace	0.005 (-0.019, 0.029)	.677	0.043 (-0.014, 0.100)	.140	0.068 (-0.027, 0.162)	.160
T_2 Fem	0.007 (-0.026, 0.039)	.683	-0.016 (-0.065, 0.098)	.694	0.012 (-0.150, 0.174)	.885
T_2 Ace	-0.004 (-0.307, 0.023)	.789	0.036 (-0.027, 0.100)	.260	0.054 (-0.028, 0.135)	.196

Bold indicates statistical significance at $P < .05$. GMED, gluteus medius; GMIN, gluteus minimus; TFL, tensor fascia lata; LV, lean volume; Fem, femoral; Ace, acetabular.

10.4 Discussion

This study presents novel evidence of relationships between muscle quality and size, strength, gait biomechanics, and cartilage composition. Our results indicate that GMED muscle quality may play an important role in hip abductor strength and frontal plane joint loading, as greater fatty infiltration was associated with decreased strength and increased HAM and HAM impulse. Additionally, LV of hip abductor muscles was evaluated in relation to gait kinematics and kinetics and showed significant associations of increased GMIN LV with increased frontal plane loading. These data indicate a potential compensation mechanism whereby GMIN may hypertrophy in the presence of increased GMED fatty infiltration, resulting in altered joint loading. Greater GMED fatty infiltration was also associated with decreased femoral T_2 relaxation times suggesting that cartilage composition may be sensitive to changes in GMED muscle quality, potentially due to altered joint loading.

Stability of the pelvis relative to the femur during the single-limb stance phase of gait is maintained by an internal hip abductor moment which counteracts the external HAM via forces generated by active and passive joint structures.[97,179] Larger external HAM has been shown to strongly correlate with increased joint contact forces.[180] Previous work has shown greater fatty infiltration of the GMED and GMIN is associated with greater in vivo hip joint contact forces after total hip arthroplasty.[117] The results of our study are in accordance with these findings and show that greater GMED fatty infiltration is associated with decreased strength and increased external peak HAM and HAM impulse suggesting greater peak and cumulative frontal plane joint loading. Given

that the GMED is the largest of the abductors and its distal and proximal attachments provide it with the largest abduction moment arm compared to GMIN and TFL,[103] it was not surprising that fatty infiltration of this muscle was associated with altered frontal plane joint loading. These findings are clinically relevant, as increased HAM has been observed in individuals with hip OA[164,166] and higher cumulative daily frontal plane hip moment impulse has been associated with progression of structural hip OA.[165] Our results provide evidence that even low levels of fatty infiltration in early-stage OA may significantly impact joint loading, particularly in the GMED which plays a critical role in frontal plane joint stability. Future interventional studies are needed to explore whether targeted therapies to improve GMED muscle quality may reduce frontal plane loads.

Additionally, we found that increased frontal plane joint loading indicated by the peak external HAM was associated with increased GMIN LV. These findings, combined with data indicating GMED FF is associated with increased frontal plane loading, suggest a possible compensation mechanism involving GMIN hypertrophy in the presence of GMED muscle dysfunction, as the primary hip abductor's capacity to stabilize the joint may be diminished. Our results are supported by recent work from Zacharias et al. which observed greater GMIN activity during gait measured using electromyography in individuals with hip OA compared to controls.[181] While muscle quality and size were associated with frontal plane hip joint loading in this study, we observed no associations with hip kinematics. This may be due to individuals in this study adopting varying, inconsistent kinematic patterns which contribute to altered frontal plane loading. Activities which place greater demand on the hip abductors than walking may be needed to observe more consistent kinematic patterns which contribute

to altered frontal plane loading. Overall, these findings support a possible mechanism by which dysfunction of the GMED may lead to greater demand placed on the GMIN to stabilize the pelvis during gait. Although previous work has shown decreased GMIN—and not GMED—LV was associated with greater in vivo joint contact forces after total hip arthroplasty,[117,182] the mechanism of atrophy and muscle dysfunction in an end-stage, post-surgical OA cohort may drastically differ from that of our early OA cohort.

Interestingly, GMED and TFL LV were not found to be associated with hip abduction strength. While increased GMIN LV was associated with greater hip abduction strength, the minimal associations observed indicate possible limitations in the analysis of lean volume. Previous studies have normalized muscle volume measures to body mass in order to account for body size related differences in muscle volume.[181] In the present study, we adjusted for BMI in statistical analyses in order to account for body size differences. However, these methods may not fully control for such differences, and more specific measures of pelvis or skeletal size may be needed to capture this information. These data highlight the utility of evaluating muscle quality rather than absolute muscle size, as FF is a relative value which provides information on the ratio of non-contractile to contractile tissue regardless of body size. Future studies should further investigate this topic and provide recommendations for standardized reporting of muscle volume, as this is currently lacking.[100]

Although few significant associations were found for cartilage relaxation times, greater GMED fatty infiltration was significantly associated with decreased femoral T_2 relaxation times and similar non-significant trends were observed. T_2 relaxation times have been shown to indirectly measure water content and collagen organization,[73] with

decreased T_2 relaxation times indicating denser, more organized collagen. The negative relationship observed between GMED fatty infiltration and femoral T_2 relaxation was unexpected, as greater fatty infiltration has been linked to OA[40–42,147,183] and increased T_2 relaxation is commonly observed in early-stage OA[171,172]. While these results were contrary to our hypothesis, they are in accordance with a previous study which similarly found that increased hip abductor fatty infiltration was associated with decreased T_2 relaxation times in individuals with mild-to-moderate hip OA.[118]

Though difficult to interpret, our findings of increased frontal plane joint loading in individuals with greater GMED fatty infiltration provide evidence of a possible mechanism of overloading-related changes to cartilage composition. At the knee, higher sagittal plane joint loads have been associated with decreased T_2 relaxation times[168] and greater compressive forces have been linked to decreased T_2 relaxation times.[169] The authors of these studies hypothesized possible chondroprotective mechanisms whereby cartilage adapts to resist greater compressive forces. At the hip, chronic overloading due to hip abductor muscle dysfunction appears to be associated with a denser collagen network and reduced water mobility. However, at the hip, greater daily cumulative HAM has been associated with radiographic progression of OA,[165] suggesting that this mechanism of chronic overloading may actually be detrimental to cartilage health and indicate some level of cartilage dehydration. Caution is needed when interpreting these results due to the magic angle effect of T_2 and varying collagen fiber orientation relative to B_0.[28] These data underscore the importance of joint loading evaluating in understanding the relationship between muscle dysfunction and cartilage

composition. Further research is needed to better understand the interplay between fatty infiltration, joint loading, and cartilage composition.

This study had several limitations. Our cohort was relatively high-functioning and consisted largely of hips without radiographic OA. Additionally, this cohort had a relatively healthy BMI and low levels of fatty infiltration. Thus, impacts of fatty infiltration on biomechanical patterns and cartilage composition may have been minimal in this cohort. An increased sample size of individuals with moderate severity hip OA may be needed to better understand how fatty infiltration impacts loading mechanics and cartilage composition. Another limitation of this study was the use of a fixed walking speed gait tasks for identifying kinematic and kinetic patterns associated with muscle quality and size. The fixed walk task may not place enough demand on the hip abductors during single-limb support to observe marked alterations in mechanics related muscle quality and size. Tasks which place greater demand on the support limb such as stair climbing, or single-leg balance may provide a greater ability to evaluate these relationships. Finally, sagittal and transverse kinematics and kinetics were not explored in this study. Although the primary role of the hip abductors is to stabilize the hip joint in the frontal plane, future studies should investigate the role of the hip abductors in these planes.

10.5 Conclusions

The results of this study demonstrate that increased GMED fatty infiltration is associated with increased peak and cumulative frontal plane joint loading, as well as decreased isometric strength. Additionally, patterns of decreased GMIN lean volume

were associated with increased frontal plane joint loads. Increased GMED fatty infiltration was also associated with decreased T_2 relaxation times, suggesting that cartilage composition may be sensitive to muscle quality, possibly due to increased joint loading association with greater fatty infiltration. These data suggest that targeted therapy aimed at reducing fatty infiltration may reduce frontal plane joint loads. Further research is needed to better understand the implications of muscle dysfunction and altered frontal plane joint loading on cartilage health.

11 Summary of Work

The work presented in this dissertation provides a comprehensive evaluation of the role of hip abductor muscle quality in the OA disease process using quantitative measures of muscle fatty infiltration and lean muscle volume. Joint health was evaluated on several scales which provide detailed information on both the composition and morphology of articular cartilage in relation to muscle quality. The role of muscle quality in hip OA was also investigated in the context of joint loading and various measures of physical function to provide a better understanding of the relationship between muscle quality and muscle function. Muscle quality was also explored in relation to the patient experience, as self-reported disability is known to have a disconnect with objective measures of OA-related degeneration. This body of work provides novel evidence to suggest that muscle quality plays an important role in disease severity, affecting cartilage health and physical function. The study design of the work presented here did not allow for causal analysis to determine whether muscle atrophy initiates disease onset or progression. However, the associations observed with various measures of disease severity suggest that muscle quality may be an important risk factor that could be targeted in the management and prevention of hip OA.

11.1 Gaps Filled

Previous studies have demonstrated a link between hip abductor muscle quality and presence or severity of radiographic OA.[40–43] However, no study to date has evaluated this relationship in a mild-to-moderate OA population using quantitative measures of muscle fat or lean volume. Additionally, the relationship of quantitatively evaluated muscle quality with patient-reported pain and disability has not been investigated in this population. While some studies have evaluated the relationship between semi-quantitatively evaluated hip abductor muscle quality and patient-reported pain and function,[147,156] objective measures of physical function have not been investigated in relation to hip abductor muscle quality in mild-to-moderate OA. Furthermore, the relationship between hip abductor muscle quality and joint loading has only been investigated in an end-stage, post-total hip arthroplasty cohort[117] despite the integral role muscle plays in forces transmitted across the joint. Lastly, the relationship between muscle quality and direct measures of cartilage health in hip OA have only been explored in a single study.[118] That study evaluated fatty infiltration across a small volume of the hip abductors and related those measures to cartilage relaxation times; their results showed mixed relationships between muscle quality and cartilage relaxation times and did not report on muscle volume. The work presented in this dissertation addresses these gaps in the literature and provides a better understanding of the role of muscle quality in joint health and physical function in individuals with mild-to-moderate hip OA.

11.2 Overall Findings

Due to the challenging, time-consuming nature of muscle quality evaluation, fatty infiltration of skeletal muscle has been minimally investigated in hip OA. To our knowledge, this is the first study to report relationships of quantitatively measured hip abductor fatty infiltration with patient-reported disability and physical function in individuals with mild-to-moderate hip OA. Previous studies have utilized semi-quantitative methods for evaluating hip abductor muscle quality in individuals mild-to-moderate hip OA, and have only evaluated relationships with patient function using self-reported measures of disability.[147,156] Our study utilized quantitative methods for muscle quality evaluation and demonstrated that not only was hip abductor fatty infiltration associated with worse self-reported symptoms and quality of life, but it was also associated with functional limitations and reduced mobility. These findings indicate that hip abductor fatty infiltration is an important factor in the patient experience, playing a significant role in both patient-perceived disability as well as objectively measured disability. Although previous work has reported mixed results for associations of hip abductor fatty infiltration with patient-reported disability in individuals with mild-to-moderate hip OA,[147,156] the more sensitive measures of fatty infiltration obtained by IDEAL-IQ imaging[84] in our study may better characterize these relationships. Additionally, the use of functional performance tests provides more concrete evidence of a link between hip abductor fatty infiltration and declining patient function.

A novel finding of this study was the relationship observed between hip abductor fatty infiltration and direct evidence of morphological cartilage degeneration. To date, relationships of hip abductor muscle quality with measures of joint degeneration have

been sparsely characterized. Previous studies have mainly focused on establishing increased levels of hip abductor fatty infiltration in hips with clinically-defined OA.[40–43] However, only one study has evaluated differences in muscle quality across a spectrum of varying degrees of radiographic OA and found greater differences in fatty infiltration with increasing radiographic severity.[42] These previous findings, however, only imply cartilage degeneration, as cartilage morphology is not visible on radiographs. Our data provide novel evidence of a direct link between increased hip abductor fatty infiltration and greater cartilage lesions evaluated using semi-quantitative MR grading. Additionally, we found evidence of localized patterns of degeneration in the superolateral aspect of the acetabulum and femoral head in individuals with greater hip abductor fatty infiltration.

Greater cartilage lesions associated with fatty infiltration would suggest that fatty infiltration may lead to muscle dysfunction and abnormal mechanical loads placed on the articular cartilage, particularly in the superolateral cartilage where joint contact forces have been shown to be highest during gait.[161] The influence of hip abductor muscle quality on gait biomechanics has previously only been investigated in a post-surgical total hip arthroplasty cohort in which fatty infiltration was shown to be associated with greater in vivo joint contact forces.[117] Our study similarly found that increased fatty infiltration was associated with increased frontal plane joint loading during gait, suggesting that fatty infiltration may lead to muscle dysfunction and reduced stabilization of the pelvis during gait. Increased hip abductor fatty infiltration was also associated with reduced isometric hip abduction strength indicating muscle weakness associated with increased fatty infiltration. Together with findings of decreased physical

function and mobility impairment, these data highlight the potential for adipose tissue stored within the muscle to affect muscle function and subsequently alter the mechanical loading environment of the joint.

A common finding in this dissertation was the importance of GMED muscle quality for OA outcomes. By far, fatty infiltration of GMED was associated with the greatest number of structural and functional OA outcomes compared to GMIN and TFL. This is likely due to the large size of the GMED and its importance as the primary hip abductor. However, these results may also be driven by the superior performance of the automatic segmentation network in segmenting this large muscle which may produce more accurate estimates of physiological fatty infiltration. Given that this muscle generates most of the frontal plane forces transmitted across the hip, even low levels of fatty infiltration appear to be related to significant symptoms and functional decline. Additionally, with its large size, a fat fraction of 5%, for example, corresponds to a larger fat volume stored in the muscle compared to a 5% fat fraction in the GMIN. This may impact surrounding tissues to a greater extent due to the inflammatory effects of adipose tissue. Further quantitative evaluations of hip abductor muscle quality in relation to muscle function are needed to confirm these findings.

With respect to lean volume, our results suggest a complex relationship between muscle structure and function. While fatty infiltration was often observed to be associated with various structural and functional indicators of OA severity, a loss of lean volume did not often accompany these findings indicating that fatty infiltration may occur without a concurrent loss of lean muscle mass. In fact, greater hip abductor lean volume was associated with worse patient-reported pain and quality of life and increased frontal

plane joint loading despite also being associated with increased isometric hip abduction strength. These results suggest a possible hypertrophy mechanism, particularly in the GMIN, during early-stage disease. As the primary abductor—the GMED—becomes increasingly dysfunctional due to fatty infiltration, the GMIN may hypertrophy and further contribute to abnormal frontal plane joint loading. However, the increased GMIN fatty infiltration observed in individuals with greater morphological cartilage lesions suggests that this mechanism may potentially lead to more severe degeneration. The authors of a previous study using fine-wire EMG hypothesized that increased GMIN activity may be a biomarker of abnormal muscle function in individuals with hip OA.[181] Together, these data point to increased demands placed on the GMIN due to GMED fatty infiltration as being pathological and a potential biomarker for OA degeneration. A more comprehensive evaluation of muscle quality, muscle activity, and joint loading may provide a better understanding of the role of each individual hip abductor muscle and patterns of degeneration in the OA disease process.

At the knee, it has been suggested that fat fraction may be more important in OA-related degeneration than lean muscle volume alone.[38,184] Our findings are consistent with this conclusion and suggest that adipose tissue may significantly impact the function of nearby lean muscle fibers, and a loss of lean muscle mass may not be required to elicit negative impacts on muscle function. However, these findings may also emphasize a very simple point: comparing lean volume in individuals with varying body sizes is challenging. Smaller muscle volumes measured in smaller individuals may be wrongly interpreted as muscle atrophy. While factors contributing to physiological muscle volume differences such as sex or BMI can be controlled for statistically, these

methods may not be able to fully capture differences in skeletal size or distribution of body mass. Fat fraction, however, provides an estimate of fat content relative to overall muscle size; therefore, it is not impacted by these limitations. Fat fraction may be more useful for gauging the level of atrophy of the muscle associated with disease severity, whereas measures of absolute volume may better describe within-subject features such as response to intervention or changes in muscle volume over time.

Although the etiology of adipose tissue stored within skeletal muscle is not well understood, it is primarily thought to arise from disuse-related atrophy and hormonal factors.[44] Our data suggest that fatty infiltration may precede a substantial decrease in lean muscle volume and may independently play a role in muscle function and joint health. In addition to contributing to a reduced ratio of lean contractile to non-contractile adipose tissue, fatty infiltration may reduce the force generating capacity of the muscle by altering the mechanical and metabolic properties of remaining muscle fibers. Fatty infiltration is thought to alter muscle fiber pennation angle, decrease elasticity, as well as induce local inflammation and reduced insulin sensitivity through the release of proinflammatory cytokines.[57–60] Our findings of increased hip abductor fatty infiltration associated with worse patient-reported outcomes, function, cartilage lesions, and increased joint loading point to adipose tissue as a contributing factor to joint degeneration through muscle dysfunction. However, it remains unclear whether an increase in fatty infiltration precedes functional decline in individuals with OA, as decreased physical activity levels associated with symptomatic disease may lead to secondary increases in fatty infiltration. This study did not measure physical activity or control for activity levels in our analyses. Future studies are needed to evaluate patterns

of physical activity in individuals with OA and determine whether increased fatty infiltration associated with disease severity may be due to lower activity levels.

While hip abductor fatty infiltration was linked to greater morphological cartilage degeneration, associations with bony changes and joint space narrowing evaluated by KL grading suggest that muscle quality may not increase linearly with radiographic disease severity. These results are contrary to previous studies which have demonstrated that hip abductor muscle quality is higher in individuals with hip OA,[40–43] and quadriceps fatty infiltration is associated with radiographic knee OA severity.[38] Few studies have evaluated these relationships in mild-to-moderate OA cohorts, thus previous findings may be largely driven by advanced disuse-related muscle atrophy in severe disease. However, a major limitation of our study was the evaluation of muscle quality at varying points in time relative to the initial KL assessment (up to 3 years after). Further investigation of this relationship in a cohort in which muscle quality and radiographic severity are evaluated concurrently is warranted given the observed association between fatty infiltration and cartilage lesions.

In early-stage disease, degenerative changes to the cartilage ECM include a loss of PG content and increased mobility of water associated with collagen network disruption.[28] These changes are expected to correlate with an increase in $T_{1\rho}$ and T_2 relaxation times. Our study found no significant association between hip abductor muscle quality and early degenerative changes to the composition of the cartilage ECM. Instead, we observed a decrease in T_2 relaxation times associated with greater hip abductor fatty infiltration—indicating a denser collagen network with reduced water mobility—and trends toward decreased $T_{1\rho}$ relaxation indicating lower PG content.

At the morphological level, hip abductor fatty infiltration was significantly associated with increased cartilage lesions. This finding may be important for interpreting the inverse relationship observed between fatty infiltration and cartilage relaxation. The superficial layer of cartilage is characterized by higher $T_{1\rho}$ and T_2 values due to differences in proteoglycan content, water content, and collagen fiber orientation and may be affected first in the degenerative process.[185–187] While degenerative changes to the deep cartilage layer after a loss of the superficial cartilage may lead to a further increase in relaxation times, the loss of the superficial layer with morphological degeneration may contribute to an overall decrease in mean relaxation in the remaining cartilage. This has been demonstrated by T_2 values at the knee measured in subjects with varying degrees of morphological degeneration evaluated using the whole-organ magnetic resonance imaging score (WORMS). Subjects with a WORMS score of 3 had lower T_2 relaxation times than subjects with a WORMS score of 2 or 2.5.[188] Additionally, there is evidence that the relationship between T_2 relaxation times and OA severity may not be linear.[189,190] These findings suggest an important role of muscle quality in morphological cartilage degeneration; however, whether muscle quality is associated with early compositional changes which precede morphological degeneration is unclear.

Increased joint loading associated with greater fatty infiltration may also contribute to further decreases in T_2 relaxation times as the cartilage adapts to withstand greater compressive loads. At the knee, overloading-related changes to cartilage composition have been observed with higher sagittal plane joint loads associated with decreased T_2 relaxation times[168] and greater compressive forces linked to decreased T_2 relaxation times[169]. Our study found that increased fatty infiltration was

associated with increased frontal plane joint loading and decreased T2 relaxation times, suggesting muscle quality may be related to loading-related adaptations of cartilage. Given that many factors may contribute to differences in measured cartilage relaxation times, the findings of decreased cartilage relaxation times in our study are difficult to interpret. Larger samples of individuals without morphological degeneration may be needed to better understand the role of muscle quality in early-stage cartilage degeneration relationships. Overall, our results highlight the importance of a comprehensively evaluating not only cartilage composition, but also mechanical and morphological factors which may affect the cartilage.

11.3 Clinical Significance

Overall, the findings of this dissertation are clinically significant, as reducing symptoms and functional limitations is critical to minimizing patient-perceived disability. These results indicate that muscle quality is a promising target for interventions aimed at improving disease outcomes. While the effects of muscle quality modification on structural progression of OA and functional decline have not been investigated, it has been shown that muscle quality can be improved through both aerobic and resistance training.[37,121–124] Specifically a 12-week strength training program which focused on progressive, isolated strengthening exercises for the hip abductors and other lower extremity muscle groups has been shown to elicit changes in hip abductor muscle quality and volume.[137] Our findings suggest that alteration of muscle quality may reduce frontal plane loads and normalize the mechanical loading environment of the joint; however, interventional studies are needed to confirm this hypothesis. Together, these

data highlight the role of muscle quality as an important factor in structural and symptomatic disease and support current recommendations for exercise in conservative treatment and management of hip OA.[15] Furthermore, our findings suggest the GMED may be preferentially targeted through exercise therapy to improve OA outcomes. These data also serve to inform the development of future therapeutic strategies and pharmacological treatments that may prevent or slow the progression of symptomatic and structural disease.

11.4 Future Directions

Longitudinal and interventional studies are needed to further explore the relationship of structural joint degeneration and functional decline with hip abductor muscle quality. This study identified patterns of lesions in superolateral cartilage regions associated with greater hip abductor fatty infiltration. Future work should evaluate these patterns using methods which characterize localized changes to cartilage composition such as voxel-based relaxometry (VBR).[172] Previous work that evaluated muscle quality in relation to cartilage composition using VBR was inconclusive.[118] Our work suggests that these types of analyses may need added context regarding cartilage morphology and joint loading to fully understand the effects of muscle quality on cartilage degradation. The GMED and GMIN are multipennate muscles with distinct functional segments which may be affected differently in aging and OA disease processes[191,192] and may respond differently to exercise intervention.[137] Therefore, advanced analyses such as statistical parametric mapping may be utilized to allow for an in-depth evaluation of localized fatty infiltration within the muscle and relationships with structural

degeneration and functional decline. Additionally, further investigation of mechanical and inflammatory properties of muscle in the presence of fatty infiltration is needed. Quantitative imaging techniques such as diffusion tensor imaging[193] or T_2 mapping[194] of muscle may provide information on the architecture and inflammatory environment of the muscle in the presence of fatty infiltration to better understand the structure-function relationship of muscle in OA.

References

1. Berenbaum F. Osteoarthritis as an inflammatory disease (osteoarthritis is not osteoarthrosis!). *Osteoarthritis Cartilage*. 2013;21(1):16-21. doi:10.1016/j.joca.2012.11.012

2. Neogi T. The epidemiology and impact of pain in osteoarthritis. *Osteoarthritis Cartilage*. 2013;21(9):1145-1153. doi:10.1016/j.joca.2013.03.018

3. Kim C, Nevitt MC, Niu J, Clancy MM, Lane NE, Link TM, Vlad S, Tolstykh I, Jungmann PM, Felson DT, Guermazi A. Association of hip pain with radiographic evidence of hip osteoarthritis: diagnostic test study. *BMJ*. Published online December 2, 2015:h5983. doi:10.1136/bmj.h5983

4. Felson DT, Naimark A, Anderson J, Kazis L, Castelli W, Meenan RF. The prevalence of knee osteoarthritis in the elderly. The Framingham Osteoarthritis Study. *Arthritis Rheum*. 1987;30(8):914-918. doi:10.1002/art.1780300811

5. Dieppe PA. Relationship between symptoms and structural change in osteoarthritis. what are the important targets for osteoarthritis therapy? *J Rheumatol Suppl*. 2004;70:50-53.

6. Hochberg MC, Lawrence RC, Everett DF, Cornoni-Huntley J. Epidemiologic associations of pain in osteoarthritis of the knee: data from the National Health and Nutrition Examination Survey and the National Health and Nutrition Examination-I

Epidemiologic Follow-up Survey. *Semin Arthritis Rheum*. 1989;18(4 Suppl 2):4-9. doi:10.1016/0049-0172(89)90008-5

7. Birrell F. Association between pain in the hip region and radiographic changes of osteoarthritis: results from a population-based study. *Rheumatology*. 2005;44(3):337-341. doi:10.1093/rheumatology/keh458

8. Salaffi F, Carotti M, Stancati A, Grassi W. Health-related quality of life in older adults with symptomatic hip and knee osteoarthritis: a comparison with matched healthy controls. *Aging Clin Exp Res*. 2005;17(4):255-263. doi:10.1007/BF03324607

9. Dawson J. Epidemiology of hip and knee pain and its impact on overall health status in older adults. *Rheumatology*. 2004;43(4):497-504. doi:10.1093/rheumatology/keh086

10. Mannoni A. Epidemiological profile of symptomatic osteoarthritis in older adults: a population based study in Dicomano, Italy. *Ann Rheum Dis*. 2003;62(6):576-578. doi:10.1136/ard.62.6.576

11. Zhao X, Shah D, Gandhi K, Wei W, Dwibedi N, Webster L, Sambamoorthi U. Clinical, humanistic, and economic burden of osteoarthritis among noninstitutionalized adults in the United States. *Osteoarthritis Cartilage*. 2019;27(11):1618-1626. doi:10.1016/j.joca.2019.07.002

12. Kotlarz H, Gunnarsson CL, Fang H, Rizzo JA. Osteoarthritis and Absenteeism Costs: Evidence From US National Survey Data. *J Occup Environ Med*. 2010;52(3):263-268. doi:10.1097/JOM.0b013e3181cf00aa

13. Buckwalter JA, Saltzman C, Brown T. The Impact of Osteoarthritis: Implications for Research. *Clin Orthop*. 2004;427:S6-S15. doi:10.1097/01.blo.0000143938.30681.9d

14. Griffin TM, Guilak F. The Role of Mechanical Loading in the Onset and Progression of Osteoarthritis: *Exerc Sport Sci Rev*. 2005;33(4):195-200. doi:10.1097/00003677-200510000-00008

15. Zhang W, Moskowitz RW, Nuki G, Abramson S, Altman RD, Arden N, Bierma-Zeinstra S, Brandt KD, Croft P, Doherty M, Dougados M, Hochberg M, Hunter DJ, Kwoh K, Lohmander LS, Tugwell P. OARSI recommendations for the management of hip and knee osteoarthritis, Part II: OARSI evidence-based, expert consensus guidelines. *Osteoarthritis Cartilage*. 2008;16(2):137-162. doi:10.1016/j.joca.2007.12.013

16. Man GS, Mologhianu G. Osteoarthritis pathogenesis - a complex process that involves the entire joint. *J Med Life*. 2014;7(1):37-41.

17. Mobasheri A, Batt M. An update on the pathophysiology of osteoarthritis. *Ann Phys Rehabil Med*. 2016;59(5-6):333-339. doi:10.1016/j.rehab.2016.07.004

18. Sophia Fox AJ, Bedi A, Rodeo SA. The Basic Science of Articular Cartilage: Structure, Composition, and Function. *Sports Health Multidiscip Approach*. 2009;1(6):461-468. doi:10.1177/1941738109350438

19. Kock L, van Donkelaar CC, Ito K. Tissue engineering of functional articular cartilage: the current status. *Cell Tissue Res*. 2012;347(3):613-627. doi:10.1007/s00441-011-1243-1

20. Cohen NP, Foster RJ, Mow VC. Composition and Dynamics of Articular Cartilage: Structure, Function, and Maintaining Healthy State. *J Orthop Sports Phys Ther*. 1998;28(4):203-215. doi:10.2519/jospt.1998.28.4.203

21. Li G, Yin J, Gao J, Cheng TS, Pavlos NJ, Zhang C, Zheng MH. Subchondral bone in osteoarthritis: insight into risk factors and microstructural changes. *Arthritis Res Ther*. 2013;15(6):223. doi:10.1186/ar4405

22. Şenol MS, Özer H. Architecture of cartilage tissue and its adaptation to pathological conditions. In: *Comparative Kinesiology of the Human Body*. Elsevier; 2020:91-100. doi:10.1016/B978-0-12-812162-7.00007-2

23. Goldring MB, Goldring SR. Osteoarthritis. *J Cell Physiol*. 2007;213(3):626-634. doi:10.1002/jcp.21258

24. Dijkgraaf LC, de Bont LGM, Boering G, Liem RSB. The structure, biochemistry, and metabolism of osteoarthritic cartilage: A review of the literature. *J Oral Maxillofac Surg*. 1995;53(10):1182-1192. doi:10.1016/0278-2391(95)90632-0

25. Martin JA, Buckwalter JA. Roles of articular cartilage aging and chondrocyte senescence in the pathogenesis of osteoarthritis. *Iowa Orthop J*. 2001;21:1-7.

26. Pritzker KPH, Gay S, Jimenez SA, Ostergaard K, Pelletier JP, Revell PA, Salter D, van den Berg WB. Osteoarthritis cartilage histopathology: grading and staging. *Osteoarthritis Cartilage*. 2006;14(1):13-29. doi:10.1016/j.joca.2005.07.014

27. van der Kraan PM, Buma P, van Kuppevelt T, van Den Berg WB. Interaction of chondrocytes, extracellular matrix and growth factors: relevance for articular cartilage tissue engineering. *Osteoarthritis Cartilage*. 2002;10(8):631-637. doi:10.1053/joca.2002.0806

28. Li X, Majumdar S. Quantitative MRI of articular cartilage and its clinical applications: Quantitative MRI of Articular Cartilage. *J Magn Reson Imaging*. 2013;38(5):991-1008. doi:10.1002/jmri.24313

29. Goldring SR. Alterations in periarticular bone and cross talk between subchondral bone and articular cartilage in osteoarthritis. *Ther Adv Musculoskelet Dis*. 2012;4(4):249-258. doi:10.1177/1759720X12437353

30. Lajeunesse D, Reboul P. Subchondral bone in osteoarthritis: a biologic link with articular cartilage leading to abnormal remodeling: *Curr Opin Rheumatol*. 2003;15(5):628-633. doi:10.1097/00002281-200309000-00018

31. Walker WT, Kawcak CE, Hill AE. Medial femoral condyle morphometrics and subchondral bone density patterns in Thoroughbred racehorses. *Am J Vet Res*. 2013;74(5):691-699. doi:10.2460/ajvr.74.5.691

32. Sharma AR, Jagga S, Lee SS, Nam JS. Interplay between cartilage and subchondral bone contributing to pathogenesis of osteoarthritis. *Int J Mol Sci*. 2013;14(10):19805-19830. doi:10.3390/ijms141019805

33. Frontera WR, Ochala J. Skeletal Muscle: A Brief Review of Structure and Function. *Calcif Tissue Int*. 2015;96(3):183-195. doi:10.1007/s00223-014-9915-y

34. Gillies AR, Lieber RL. Structure and function of the skeletal muscle extracellular matrix: Skeletal Muscle ECM. *Muscle Nerve*. 2011;44(3):318-331. doi:10.1002/mus.22094

35. Mukund K, Subramaniam S. Skeletal muscle: A review of molecular structure and function, in health and disease. *WIREs Syst Biol Med*. 2020;12(1). doi:10.1002/wsbm.1462

36. Kirkland JL, Tchkonia T, Pirtskhalava T, Han J, Karagiannides I. Adipogenesis and aging: does aging make fat go MAD? *Exp Gerontol*. 2002;37(6):757-767. doi:10.1016/S0531-5565(02)00014-1

37. Addison O, Marcus RL, LaStayo PC, Ryan AS. Intermuscular Fat: A Review of the Consequences and Causes. *Int J Endocrinol*. 2014;2014:1-11. doi:10.1155/2014/309570

38. Kumar D, Karampinos DC, MacLeod TD, Lin W, Nardo L, Li X, Link TM, Majumdar S, Souza RB. Quadriceps intramuscular fat fraction rather than muscle size is associated with knee osteoarthritis. *Osteoarthritis Cartilage*. 2014;22(2):226-234. doi:10.1016/j.joca.2013.12.005

39. Kumar D, Link TM, Jafarzadeh SR, LaValley MP, Majumdar S, Souza RB. Quadriceps adiposity is associated with increase in lesions of the knee cartilage, meniscus, or bone marrow over 3-years. *Arthritis Care Res*. Published online April 27, 2020:acr.24232. doi:10.1002/acr.24232

40. Momose T, Inaba Y, Choe H, Kobayashi N, Tezuka T, Saito T. CT-based analysis of muscle volume and degeneration of gluteus medius in patients with unilateral hip osteoarthritis. *BMC Musculoskelet Disord*. 2017;18(1):457. doi:10.1186/s12891-017-1828-2

41. Fukumoto Y, Ikezoe T, Tateuchi H, Tsukagoshi R, Akiyama H, So K, Kuroda Y, Yoneyama T, Ichihashi N. Muscle Mass and Composition of the Hip, Thigh and Abdominal Muscles in Women With and Without Hip Osteoarthritis. *Ultrasound Med Biol*. 2012;38(9):1540-1545. doi:10.1016/j.ultrasmedbio.2012.04.016

42. Zacharias A, Pizzari T, English DJ, Kapakoulakis T, Green RA. Hip abductor muscle volume in hip osteoarthritis and matched controls. *Osteoarthritis Cartilage*. 2016;24(10):1727-1735. doi:10.1016/j.joca.2016.05.002

43. Rasch A, Byström AH, Dalen N, Berg HE. Reduced muscle radiological density, cross-sectional area, and strength of major hip and knee muscles in 22 patients with

hip osteoarthritis. *Acta Orthop*. 2007;78(4):505-510. doi:10.1080/17453670710014158

44. Hamrick MW, McGee-Lawrence ME, Frechette DM. Fatty Infiltration of Skeletal Muscle: Mechanisms and Comparisons with Bone Marrow Adiposity. *Front Endocrinol*. 2016;7:69. doi:10.3389/fendo.2016.00069

45. Beasley LE, Koster A, Newman AB, Javaid MK, Ferrucci L, Kritchevsky SB, Kuller LH, Pahor M, Schaap LA, Visser M, Rubin SM, Goodpaster BH, Harris TB, The Health ABC study. Inflammation and Race and Gender Differences in Computerized Tomography-measured Adipose Depots. *Obesity*. 2009;17(5):1062-1069. doi:10.1038/oby.2008.627

46. Manini TM, Clark BC, Nalls MA, Goodpaster BH, Ploutz-Snyder LL, Harris TB. Reduced physical activity increases intermuscular adipose tissue in healthy young adults. *Am J Clin Nutr*. 2007;85(2):377-384. doi:10.1093/ajcn/85.2.377

47. Zoico E, Rossi A, Di Francesco V, Sepe A, Olioso D, Pizzini F, Fantin F, Bosello O, Cominacini L, Harris TB, Zamboni M. Adipose Tissue Infiltration in Skeletal Muscle of Healthy Elderly Men: Relationships With Body Composition, Insulin Resistance, and Inflammation at the Systemic and Tissue Level. *J Gerontol A Biol Sci Med Sci*. 2010;65A(3):295-299. doi:10.1093/gerona/glp155

48. Addison O, Drummond MJ, Lastayo PC, Dibble LE, Wende AR, McClain DA, Marcus RL. Intramuscular fat and inflammation differ in older adults: The impact of frailty and inactivity. *J Nutr Health Aging*. 2014;18(5):532-538. doi:10.1007/s12603-014-0019-1

49. Schaap LA, Pluijm SMF, Deeg DJH, Harris TB, Kritchevsky SB, Newman AB, Colbert LH, Pahor M, Rubin SM, Tylavsky FA, Visser M, for the Health ABC Study. Higher Inflammatory Marker Levels in Older Persons: Associations With 5-Year Change in Muscle Mass and Muscle Strength. *J Gerontol A Biol Sci Med Sci*. 2009;64A(11):1183-1189. doi:10.1093/gerona/glp097

50. Visser M, Pahor M, Taaffe DR, Goodpaster BH, Simonsick EM, Newman AB, Nevitt M, Harris TB. Relationship of Interleukin-6 and Tumor Necrosis Factor- With Muscle Mass and Muscle Strength in Elderly Men and Women: The Health ABC Study. *J Gerontol A Biol Sci Med Sci*. 2002;57(5):M326-M332. doi:10.1093/gerona/57.5.M326

51. Cesari M, Penninx BWJH, Pahor M, Lauretani F, Corsi AM, Williams GR, Guralnik JM, Ferrucci L. Inflammatory Markers and Physical Performance in Older Persons: The InCHIANTI Study. *J Gerontol A Biol Sci Med Sci*. 2004;59(3):M242-M248. doi:10.1093/gerona/59.3.M242

52. Sharma B, Dabur R. Role of Pro-inflammatory Cytokines in Regulation of Skeletal Muscle Metabolism: A Systematic Review. *Curr Med Chem*. 2020;27(13):2161-2188. doi:10.2174/0929867326666181129095309

53. Liu S, Deng Z, Chen K, Jian S, Zhou F, Yang Y, Fu Z, Xie H, Xiong J, Zhu W. Cartilage tissue engineering: From proinflammatory and anti-inflammatory cytokines to osteoarthritis treatments (Review). *Mol Med Rep*. 2022;25(3):99. doi:10.3892/mmr.2022.12615

54. Goldring SR, Goldring MB. The Role of Cytokines in Cartilage Matrix Degeneration in Osteoarthritis. *Clin Orthop*. 2004;427:S27-S36. doi:10.1097/01.blo.0000144854.66565.8f

55. Altajar S, Baffy G. Skeletal Muscle Dysfunction in the Development and Progression of Nonalcoholic Fatty Liver Disease. *J Clin Transl Hepatol*. 2020;8(4):1-10. doi:10.14218/JCTH.2020.00065

56. Urban H, Little CB. The role of fat and inflammation in the pathogenesis and management of osteoarthritis. *Rheumatology*. 2018;57(suppl_4):iv10-iv21. doi:10.1093/rheumatology/kex399

57. Rivas DA, McDonald DJ, Rice NP, Haran PH, Dolnikowski GG, Fielding RA. Diminished anabolic signaling response to insulin induced by intramuscular lipid accumulation is associated with inflammation in aging but not obesity. *Am J Physiol Regul Integr Comp Physiol*. 2016;310(7):R561-569. doi:10.1152/ajpregu.00198.2015

58. Mastrocola R, Collino M, Nigro D, Chiazza F, D'Antona G, Aragno M, Minetto MA. Accumulation of advanced glycation end-products and activation of the SCAP/SREBP Lipogenetic pathway occur in diet-induced obese mouse skeletal muscle. *PloS One*. 2015;10(3):e0119587. doi:10.1371/journal.pone.0119587

59. Meyer DC, Hoppeler H, von Rechenberg B, Gerber C. A pathomechanical concept explains muscle loss and fatty muscular changes following surgical tendon release. *J Orthop Res*. 2004;22(5):1004-1007. doi:10.1016/j.orthres.2004.02.009

60. Gerber C, Schneeberger AG, Hoppeler H, Meyer DC. Correlation of atrophy and fatty infiltration on strength and integrity of rotator cuff repairs: A study in thirteen patients. *J Shoulder Elbow Surg*. 2007;16(6):691-696. doi:10.1016/j.jse.2007.02.122

61. Gerber C, Meyer DC, Schneeberger AG, Hoppeler H, Von Rechenberg B. EFFECT OF TENDON RELEASE AND DELAYED REPAIR ON THE STRUCTURE OF THE MUSCLES OF THE ROTATOR CUFF: AN EXPERIMENTAL STUDY IN SHEEP. *J Bone Jt Surg-Am Vol*. 2004;86(9):1973-1982. doi:10.2106/00004623-200409000-00016

62. Kellgren JH, Lawrence JS. Radiological Assessment of Osteo-Arthrosis. *Ann Rheum Dis*. 1957;16(4):494-502. doi:10.1136/ard.16.4.494

63. Gold GE, Cicuttini F, Crema MD, Eckstein F, Guermazi A, Kijowski R, Link TM, Maheu E, Martel-Pelletier J, Miller CG, Pelletier JP, Peterfy CG, Potter HG, Roemer FW, Hunter DJ. OARSI Clinical Trials Recommendations: Hip imaging in clinical trials in osteoarthritis. *Osteoarthritis Cartilage*. 2015;23(5):716-731. doi:10.1016/j.joca.2015.03.004

64. Pooley RA. Fundamental Physics of MR Imaging. *RadioGraphics*. 2005;25(4):1087-1099. doi:10.1148/rg.254055027

65. Roemer FW, Hunter DJ, Winterstein A, Li L, Kim YJ, Cibere J, Mamisch TC, Guermazi A. Hip Osteoarthritis MRI Scoring System (HOAMS): reliability and associations with radiographic and clinical findings. *Osteoarthritis Cartilage*. 2011;19(8):946-962. doi:10.1016/j.joca.2011.04.003

66. Lee S. Scoring Hip Osteoarthritis with MRI (SHOMRI): a Whole Joint Osteoarthritis Evaluation System. *J Magn Reson Imaging*. 2015;41(6):1549-1557. doi:10.1002

67. Neumann J, Zhang AL, Schwaiger BJ, Samaan MA, Souza R, Foreman SC, Joseph GB, Grace T, Majumdar S, Link TM. Validation of scoring hip osteoarthritis with MRI (SHOMRI) scores using hip arthroscopy as a standard of reference. *Eur Radiol*. 2019;29(2):578-587. doi:10.1007/s00330-018-5623-8

68. Wáng YXJ, Zhang Q, Li X, Chen W, Ahuja A, Yuan J. T1ρ magnetic resonance: basic physics principles and applications in knee and intervertebral disc imaging. *Quant Imaging Med Surg*. 2015;5(6):858-885. doi:10.3978/j.issn.2223-4292.2015.12.06

69. Wang N, Xia Y. Dependencies of multi-component T2 and T1ρ relaxation on the anisotropy of collagen fibrils in bovine nasal cartilage. *J Magn Reson*. 2011;212(1):124-132. doi:10.1016/j.jmr.2011.06.031

70. Duvvuri U, Reddy R, Patel SD, Kaufman JH, Kneeland JB, Leigh JS. T1ρ-relaxation in articular cartilage: Effects of enzymatic degradation. *Magn Reson Med*. 1997;38(6):863-867. doi:10.1002/mrm.1910380602

71. Regatte RR, Akella SVS, Borthakur A, Kneeland JB, Reddy R. Proteoglycan Depletion–Induced Changes in Transverse Relaxation Maps of Cartilage. *Acad Radiol*. 2002;9(12):1388-1394. doi:10.1016/S1076-6332(03)80666-9

72. Regatte RR, Akella SVS, Lonner JH, Kneeland JB, Reddy R. T1ρ relaxation mapping in human osteoarthritis (OA) cartilage: Comparison of T1ρ with T2. *J Magn Reson Imaging*. 2006;23(4):547-553. doi:10.1002/jmri.20536

73. Xia Y. Relaxation anisotropy in cartilage by NMR microscopy (μMRI) at 14-μm resolution. *Magn Reson Med*. 1998;39(6):941-949. doi:10.1002/mrm.1910390612

74. Lüssea S, Claassen H, Gehrke T, Hassenpflug J, Schünke M, Heller M, Glüer CC. Evaluation of water content by spatially resolved transverse relaxation times of human articular cartilage. *Magn Reson Imaging*. 2000;18(4):423-430. doi:10.1016/S0730-725X(99)00144-7

75. Li X, Benjamin Ma C, Link TM, Castillo DD, Blumenkrantz G, Lozano J, Carballido-Gamio J, Ries M, Majumdar S. In vivo T1ρ and T2 mapping of articular cartilage in osteoarthritis of the knee using 3T MRI. *Osteoarthritis Cartilage*. 2007;15(7):789-797. doi:10.1016/j.joca.2007.01.011

76. Regatte RR, Akella SVS, Wheaton AJ, Lech G, Borthakur A, Kneeland JB, Reddy R. 3D-T1ρ-relaxation mapping of articular cartilage. *Acad Radiol*. 2004;11(7):741-749. doi:10.1016/j.acra.2004.03.051

77. Stahl R, Luke A, Li X, Carballido-Gamio J, Ma CB, Majumdar S, Link TM. T1rho, T2 and focal knee cartilage abnormalities in physically active and sedentary healthy subjects versus early OA patients—a 3.0-Tesla MRI study. *Eur Radiol*. 2009;19(1):132-143. doi:10.1007/s00330-008-1107-6

78. Boettcher M, Machann J, Stefan N, Thamer C, Häring HU, Claussen CD, Fritsche A, Schick F. Intermuscular adipose tissue (IMAT): Association with other adipose tissue compartments and insulin sensitivity. *J Magn Reson Imaging*. 2009;29(6):1340-1345. doi:10.1002/jmri.21754

79. Goutallier D, Postel JM, Bernageau J, Lavau L, Voisin MC. Fatty muscle degeneration in cuff ruptures. Pre- and postoperative evaluation by CT scan. *Clin Orthop*. 1994;(304):78-83.

80. Fuchs T, Immich H, Nedden R. [Quantitative relations between sero-chemical findings, fatty degeneration of the liver, alcohol drinking and body weight in a diabetic and non-diabetic collective with fatty degeneration of the liver]. *Med Welt*. 1971;10:392-399.

81. Fuchs B, Weishaupt D, Zanetti M, Hodler J, Gerber C. Fatty degeneration of the muscles of the rotator cuff: Assessment by computed tomography versus magnetic resonance imaging. *J Shoulder Elbow Surg*. 1999;8(6):599-605. doi:10.1016/S1058-2746(99)90097-6

82. Slabaugh MA, Friel NA, Karas V, Romeo AA, Verma NN, Cole BJ. Interobserver and Intraobserver Reliability of the Goutallier Classification Using Magnetic Resonance Imaging: Proposal of a Simplified Classification System to Increase Reliability. *Am J Sports Med*. 2012;40(8):1728-1734. doi:10.1177/0363546512452714

83. Nardo L, Karampinos DC, Lansdown DA, Carballido-Gamio J, Lee S, Maroldi R, Ma CB, Link TM, Krug R. Quantitative assessment of fat infiltration in the rotator cuff

muscles using water-fat MRI: Fat Infiltration in the Rotator Cuff Muscles. *J Magn Reson Imaging*. 2014;39(5):1178-1185. doi:10.1002/jmri.24278

84. Alizai H, Nardo L, Karampinos DC, Joseph GB, Yap SP, Baum T, Krug R, Majumdar S, Link TM. Comparison of clinical semi-quantitative assessment of muscle fat infiltration with quantitative assessment using chemical shift-based water/fat separation in MR studies of the calf of post-menopausal women. *Eur Radiol*. 2012;22(7):1592-1600. doi:10.1007/s00330-012-2404-7

85. Burakiewicz J, Sinclair CDJ, Fischer D, Walter GA, Kan HE, Hollingsworth KG. Quantifying fat replacement of muscle by quantitative MRI in muscular dystrophy. *J Neurol*. 2017;264(10):2053-2067. doi:10.1007/s00415-017-8547-3

86. Hines CDG, Yu H, Shimakawa A, McKenzie CA, Brittain JH, Reeder SB. T_1 independent, T_2* corrected MRI with accurate spectral modeling for quantification of fat: Validation in a fat-water-SPIO phantom. *J Magn Reson Imaging*. 2009;30(5):1215-1222. doi:10.1002/jmri.21957

87. Hines CDG, Frydrychowicz A, Hamilton G, Tudorascu DL, Vigen KK, Yu H, McKenzie CA, Sirlin CB, Brittain JH, Reeder SB. T1 independent, T2* corrected chemical shift based fat-water separation with multi-peak fat spectral modeling is an accurate and precise measure of hepatic steatosis. *J Magn Reson Imaging*. 2011;33(4):873-881. doi:10.1002/jmri.22514

88. Meisamy S, Hines CDG, Hamilton G, Sirlin CB, McKenzie CA, Yu H, Brittain JH, Reeder SB. Quantification of Hepatic Steatosis with T1-independent, T2*-corrected

MR Imaging with Spectral Modeling of Fat: Blinded Comparison with MR Spectroscopy. *Radiology*. 2011;258(3):767-775. doi:10.1148/radiol.10100708

89. Yokoo T, Shiehmorteza M, Hamilton G, Wolfson T, Schroeder ME, Middleton MS, Bydder M, Gamst AC, Kono Y, Kuo A, Patton HM, Horgan S, Lavine JE, Schwimmer JB, Sirlin CB. Estimation of Hepatic Proton-Density Fat Fraction by Using MR Imaging at 3.0 T. *Radiology*. 2011;258(3):749-759. doi:10.1148/radiol.10100659

90. Reeder SB, Cruite I, Hamilton G, Sirlin CB. Quantitative assessment of liver fat with magnetic resonance imaging and spectroscopy. *J Magn Reson Imaging*. 2011;34(4):729-749. doi:10.1002/jmri.22580

91. Reeder SB, Pineda AR, Wen Z, Shimakawa A, Yu H, Brittain JH, Gold GE, Beaulieu CH, Pelc NJ. Iterative decomposition of water and fat with echo asymmetry and least-squares estimation (IDEAL): Application with fast spin-echo imaging. *Magn Reson Med*. 2005;54(3):636-644. doi:10.1002/mrm.20624

92. Yu H, McKenzie CA, Shimakawa A, Vu AT, Brau ACS, Beatty PJ, Pineda AR, Brittain JH, Reeder SB. Multiecho reconstruction for simultaneous water-fat decomposition and T2* estimation. *J Magn Reson Imaging*. 2007;26(4):1153-1161. doi:10.1002/jmri.21090

93. Reeder SB, McKenzie CA, Pineda AR, Yu H, Shimakawa A, Brau AC, Hargreaves BA, Gold GE, Brittain JH. Water–fat separation with IDEAL gradient-echo imaging. *J Magn Reson Imaging*. 2007;25(3):644-652. doi:10.1002/jmri.20831

94. Johnson BL, Schroeder ME, Wolfson T, Gamst AC, Hamilton G, Shiehmorteza M, Loomba R, Schwimmer JB, Reeder S, Middleton MS, Sirlin CB. Effect of flip angle on the accuracy and repeatability of hepatic proton density fat fraction estimation by complex data-based, T1-independent, T2*-corrected, spectrum-modeled MRI: Effect of Flip Angle on PDFF Estimation. *J Magn Reson Imaging*. 2014;39(2):440-447. doi:10.1002/jmri.24153

95. Hu HH, Li Y, Nagy TR, Goran MI, Nayak KS. Quantification of Absolute Fat Mass by Magnetic Resonance Imaging: a Validation Study against Chemical Analysis. *Int J Body Compos Res*. 2011;9(3):111-122.

96. Schmeel FC, Vomweg T, Träber F, Gerhards A, Enkirch SJ, Faron A, Sprinkart AM, Schmeel LC, Luetkens JA, Thomas D, Kukuk GM. Proton density fat fraction MRI of vertebral bone marrow: Accuracy, repeatability, and reproducibility among readers, field strengths, and imaging platforms. *J Magn Reson Imaging*. 2019;50(6):1762-1772. doi:10.1002/jmri.26748

97. Gottschalk F, Kourosh S, Leveau B. The functional anatomy of tensor fasciae latae and gluteus medius and minimus. *J Anat*. 1989;166:179-189.

98. Winter D. Human balance and posture control during standing and walking. *Gait Posture*. 1995;3(4):193-214. doi:10.1016/0966-6362(96)82849-9

99. Amaro A, Amado F, Duarte J, Appell HJ. Gluteus Medius Muscle Atrophy is Related to Contralateral and Ipsilateral Hip Joint Osteoarthritis. *Int J Sports Med*. 2007;28(12):1035-1039. doi:10.1055/s-2007-965078

100. Loureiro A, Mills PM, Barrett RS. Muscle weakness in hip osteoarthritis: A systematic review. *Arthritis Care Res*. 2013;65(3):340-352. doi:10.1002/acr.21806

101. Flack NAMS, Nicholson HD, Woodley SJ. The anatomy of the hip abductor muscles: Hip Abductor Anatomy. *Clin Anat*. 2014;27(2):241-253. doi:10.1002/ca.22248

102. Pfirrmann CWA, Chung CB, Theumann NH, Trudell DJ, Resnick D. Greater Trochanter of the Hip: Attachment of the Abductor Mechanism and a Complex of Three Bursae—MR Imaging and MR Bursography in Cadavers and MR Imaging in Asymptomatic Volunteers. *Radiology*. 2001;221(2):469-477. doi:10.1148/radiol.2211001634

103. Neumann DA. Kinesiology of the Hip: A Focus on Muscular Actions. *J Orthop Sports Phys Ther*. 2010;40(2):82-94. doi:10.2519/jospt.2010.3025

104. Correa TA, Crossley KM, Kim HJ, Pandy MG. Contributions of individual muscles to hip joint contact force in normal walking. *J Biomech*. 2010;43(8):1618-1622. doi:10.1016/j.jbiomech.2010.02.008

105. Hinterwimmer S, Krammer M, Krötz M, Glaser C, Baumgart R, Reiser M, Eckstein F. Cartilage atrophy in the knees of patients after seven weeks of partial load bearing: Knee Cartilage Atrophy After Partial Load Bearing. *Arthritis Rheum*. 2004;50(8):2516-2520. doi:10.1002/art.20378

106. Souza RB, Baum T, Wu S, Feeley BT, Kadel N, Li X, Link TM, Majumdar S. Effects of Unloading on Knee Articular Cartilage T1rho and T2 Magnetic Resonance Imaging

Relaxation Times: A Case Series. *J Orthop Sports Phys Ther*. 2012;42(6):511-520. doi:10.2519/jospt.2012.3975

107. Martin JA, Brown T, Heiner A, Buckwalter JA. Post-traumatic osteoarthritis: the role of accelerated chondrocyte senescence. *Biorheology*. 2004;41(3-4):479-491.

108. Recnik G, Kralj-Iglič V, Iglič A, Antolič V, Kramberger S, Rigler I, Pompe B, Vengust R. The role of obesity, biomechanical constitution of the pelvis and contact joint stress in progression of hip osteoarthritis. *Osteoarthritis Cartilage*. 2009;17(7):879-882. doi:10.1016/j.joca.2008.12.006

109. Valente G, Taddei F, Jonkers I. Influence of weak hip abductor muscles on joint contact forces during normal walking: probabilistic modeling analysis. *J Biomech*. 2013;46(13):2186-2193. doi:10.1016/j.jbiomech.2013.06.030

110. Allison K, Wrigley TV, Vicenzino B, Bennell KL, Grimaldi A, Hodges PW. Kinematics and kinetics during walking in individuals with gluteal tendinopathy. *Clin Biomech*. 2016;32:56-63. doi:10.1016/j.clinbiomech.2016.01.003

111. Hurley MV. THE ROLE OF MUSCLE WEAKNESS IN THE PATHOGENESIS OF OSTEOARTHRITIS. *Rheum Dis Clin N Am*. 1999;25(2):283-298. doi:10.1016/S0889-857X(05)70068-5

112. Goodpaster BH, Carlson CL, Visser M, Kelley DE, Scherzinger A, Harris TB, Stamm E, Newman AB. Attenuation of skeletal muscle and strength in the elderly: The

Health ABC Study. *J Appl Physiol*. 2001;90(6):2157-2165. doi:10.1152/jappl.2001.90.6.2157

113. Tuttle LJ, Sinacore DR, Mueller MJ. Intermuscular Adipose Tissue Is Muscle Specific and Associated with Poor Functional Performance. *J Aging Res*. 2012;2012:1-7. doi:10.1155/2012/172957

114. Addison O, Young P, Inacio M, Bair WN, Prettyman M, Beamer B, Ryan A, Rogers M. Hip but Not Thigh Intramuscular Adipose Tissue is Associated with Poor Balance and Increased Temporal Gait Variability in Older Adults. *Curr Aging Sci*. 2014;7(2):137-143. doi:10.2174/1874609807666140706150924

115. Grimaldi A, Richardson C, Stanton W, Durbridge G, Donnelly W, Hides J. The association between degenerative hip joint pathology and size of the gluteus medius, gluteus minimus and piriformis muscles. *Man Ther*. 2009;14(6):605-610. doi:10.1016/j.math.2009.07.004

116. Grimaldi A, Richardson C, Durbridge G, Donnelly W, Darnell R, Hides J. The association between degenerative hip joint pathology and size of the gluteus maximus and tensor fascia lata muscles. *Man Ther*. 2009;14(6):611-617. doi:10.1016/j.math.2008.11.002

117. Damm P, Zonneveld J, Brackertz S, Streitparth F, Winkler T. Gluteal muscle damage leads to higher in vivo hip joint loads 3 months after total hip arthroplasty. Williams JL, ed. *PLOS ONE*. 2018;13(1):e0190626. doi:10.1371/journal.pone.0190626

118. Tibrewala R, Pedoia V, Lee J, Kinnunen C, Popovic T, Zhang AL, Link TM, Souza RB, Majumdar S. Automatic hip abductor muscle fat fraction estimation and association with early OA cartilage degeneration biomarkers. *J Orthop Res*. 2021;39(11):2376-2387. doi:10.1002/jor.24974

119. Chopp-Hurley JN, Wiebenga EG, Bulbrook BD, Keir PJ, Maly MR. Evaluating the relationship between quadriceps muscle quality captured using ultrasound with clinical severity in women with knee osteoarthritis. *Clin Biomech*. 2020;80:105165. doi:10.1016/j.clinbiomech.2020.105165

120. Raynauld JP, Pelletier JP, Roubille C, Dorais M, Abram F, Li W, Wang Y, Fairley J, Cicuttini FM, Martel-Pelletier J. Magnetic Resonance Imaging-Assessed Vastus Medialis Muscle Fat Content and Risk for Knee Osteoarthritis Progression: Relevance From a Clinical Trial: Association Between Muscle Fat Content and Cartilage Volume Loss. *Arthritis Care Res*. 2015;67(10):1406-1415. doi:10.1002/acr.22590

121. Santanasto AJ, Glynn NW, Newman MA, Taylor CA, Brooks MM, Goodpaster BH, Newman AB. Impact of weight loss on physical function with changes in strength, muscle mass, and muscle fat infiltration in overweight to moderately obese older adults: a randomized clinical trial. *J Obes*. 2011;2011:516576. doi:10.1155/2011/516576

122. Ryan AS, Ivey FM, Prior S, Li G, Hafer-Macko C. Skeletal Muscle Hypertrophy and Muscle Myostatin Reduction After Resistive Training in Stroke Survivors. *Stroke*. 2011;42(2):416-420. doi:10.1161/STROKEAHA.110.602441

123. Taaffe DR, Henwood TR, Nalls MA, Walker DG, Lang TF, Harris TB. Alterations in muscle attenuation following detraining and retraining in resistance-trained older adults. *Gerontology*. 2009;55(2):217-223. doi:10.1159/000182084

124. Goodpaster BH, Chomentowski P, Ward BK, Rossi A, Glynn NW, Delmonico MJ, Kritchevsky SB, Pahor M, Newman AB. Effects of physical activity on strength and skeletal muscle fat infiltration in older adults: a randomized controlled trial. *J Appl Physiol*. 2008;105(5):1498-1503. doi:10.1152/japplphysiol.90425.2008

125. Teichtahl AJ, Wluka AE, Wang Y, Wijethilake PN, Strauss BJ, Proietto J, Dixon JB, Jones G, Forbes A, Cicuttini FM. Vastus medialis fat infiltration – a modifiable determinant of knee cartilage loss. *Osteoarthritis Cartilage*. 2015;23(12):2150-2157. doi:10.1016/j.joca.2015.06.016

126. Carballido-Gamio J, Link TM, Li X, Han ET, Krug R, Ries MD, Majumdar S. Feasibility and reproducibility of relaxometry, morphometric, and geometrical measurements of the hip joint with magnetic resonance imaging at 3T. *J Magn Reson Imaging*. 2008;28(1):227-235. doi:10.1002/jmri.21411

127. Bennell K, Dobson F, Hinman R. Measures of physical performance assessments: Self-Paced Walk Test (SPWT), Stair Climb Test (SCT), Six-Minute Walk Test (6MWT), Chair Stand Test (CST), Timed Up & Go (TUG), Sock Test, Lift and Carry

Test (LCT), and Car Task. *Arthritis Care Res*. 2011;63(S11):S350-S370. doi:10.1002/acr.20538

128. Gill S, McBurney H. Reliability of performance-based measures in people awaiting joint replacement surgery of the hip or knee. *Physiother Res Int*. 2008;13(3):141-152. doi:10.1002/pri.411

129. Hansen H, Beyer N, Frølich A, Godtfredsen N, Bieler T. Intra- and inter-rater reproducibility of the 6-minute walk test and the 30-second sit-to-stand test in patients with severe and very severe COPD. *Int J Chron Obstruct Pulmon Dis*. 2018;13:3447-3457. doi:10.2147/COPD.S174248

130. Unver B, Kahraman T, Kalkan S, Yuksel E, Karatosun V, Gunal I. Test-Retest Reliability of the Stair Test in Patients with Total Hip Arthroplasty. *HIP Int*. 2015;25(2):160-163. doi:10.5301/hipint.5000217

131. Chiari L, Croce UD, Leardini A, Cappozzo A. Human movement analysis using stereophotogrammetry. *Gait Posture*. 2005;21(2):197-211. doi:10.1016/j.gaitpost.2004.04.004

132. Widler KS, Glatthorn JF, Bizzini M, Impellizzeri FM, Munzinger U, Leunig M, Maffiuletti NA. Assessment of Hip Abductor Muscle Strength. A Validity and Reliability Study: *J Bone Jt Surg*. 2009;91(11):2666-2672. doi:10.2106/JBJS.H.01119

133. Nilsdotter AK, Lohmander LS, Klässbo M, Roos EM. Hip disability and osteoarthritis outcome score (HOOS) – validity and responsiveness in total hip replacement. *BMC Musculoskelet Disord*. 2003;4(1):10. doi:10.1186/1471-2474-4-10

134. de Groot IB, Reijman M, Terwee CB, Bierma-Zeinstra SMA, Favejee M, Roos EM, Verhaar JAN. Validation of the Dutch version of the Hip disability and Osteoarthritis Outcome Score. *Osteoarthritis Cartilage*. 2007;15(1):104-109. doi:10.1016/j.joca.2006.06.014

135. Ornetti P, Parratte S, Gossec L, Tavernier C, Argenson JN, Roos EM, Guillemin F, Maillefert JF. Cross-cultural adaptation and validation of the French version of the Hip disability and Osteoarthritis Outcome Score (HOOS) in hip osteoarthritis patients. *Osteoarthritis Cartilage*. 2010;18(4):522-529. doi:10.1016/j.joca.2009.12.007

136. Nilsdotter A, Bremander A. Measures of hip function and symptoms: Harris Hip Score (HHS), Hip Disability and Osteoarthritis Outcome Score (HOOS), Oxford Hip Score (OHS), Lequesne Index of Severity for Osteoarthritis of the Hip (LISOH), and American Academy of Orthopedic Surgeons (A. *Arthritis Care Res*. 2011;63(S11):S200-S207. doi:10.1002/acr.20549

137. Koch K, Semciw AI, Commean PK, Hillen TJ, Fitzgerald GK, Clohisy JC, Harris-Hayes M. Comparison between movement pattern training and strengthening on muscle volume, muscle fat, and strength in patients with hip-related groin pain: An exploratory analysis. *J Orthop Res*. Published online August 18, 2021:jor.25158. doi:10.1002/jor.25158

138. Belzunce MA, Henckel J, Di Laura A, Hart AJ. Reference values for volume, fat content and shape of the hip abductor muscles in healthy individuals from Dixon MRI. *NMR Biomed*. 2022;35(2). doi:10.1002/nbm.4636

139. LeCun Y, Bengio Y, Hinton G. Deep learning. *Nature*. 2015;521(7553):436-444. doi:10.1038/nature14539

140. Milletari F, Navab N, Ahmadi SA. V-Net: Fully Convolutional Neural Networks for Volumetric Medical Image Segmentation. *ArXiv160604797 Cs*. Published online June 15, 2016. Accessed February 18, 2022. http://arxiv.org/abs/1606.04797

141. Akkus Z, Galimzianova A, Hoogi A, Rubin DL, Erickson BJ. Deep Learning for Brain MRI Segmentation: State of the Art and Future Directions. *J Digit Imaging*. 2017;30(4):449-459. doi:10.1007/s10278-017-9983-4

142. Yu H, Shimakawa A, McKenzie CA, Brodsky E, Brittain JH, Reeder SB. Multiecho water-fat separation and simultaneous *R 2** estimation with multifrequency fat spectrum modeling. *Magn Reson Med*. 2008;60(5):1122-1134. doi:10.1002/mrm.21737

143. Zou KH, Warfield SK, Bharatha A, Tempany CMC, Kaus MR, Haker SJ, Wells WM, Jolesz FA, Kikinis R. Statistical validation of image segmentation quality based on a spatial overlap index1. *Acad Radiol*. 2004;11(2):178-189. doi:10.1016/S1076-6332(03)00671-8

144. Martin Bland J, Altman DouglasG. STATISTICAL METHODS FOR ASSESSING AGREEMENT BETWEEN TWO METHODS OF CLINICAL MEASUREMENT. *The Lancet*. 1986;327(8476):307-310. doi:10.1016/S0140-6736(86)90837-8

145. Pataky TC. Generalized n-dimensional biomechanical field analysis using statistical parametric mapping. *J Biomech*. 2010;43(10):1976-1982. doi:10.1016/j.jbiomech.2010.03.008

146. Marcon M, Berger N, Manoliu A, Fischer MA, Nanz D, Andreisek G, Ulbrich EJ. Normative values for volume and fat content of the hip abductor muscles and their dependence on side, age and gender in a healthy population. *Skeletal Radiol*. 2016;45(4):465-474. doi:10.1007/s00256-015-2325-z

147. Zacharias A, Green RA, Semciw A, English DJ, Kapakoulakis T, Pizzari T. Atrophy of hip abductor muscles is related to clinical severity in a hip osteoarthritis population: Muscle Atrophy and Clinical Severity in Hip OA. *Clin Anat*. 2018;31(4):507-513. doi:10.1002/ca.23064

148. Murphy LB, Helmick CG, Schwartz TA, Renner JB, Tudor G, Koch GG, Dragomir AD, Kalsbeek WD, Luta G, Jordan JM. One in four people may develop symptomatic hip osteoarthritis in his or her lifetime. *Osteoarthritis Cartilage*. 2010;18(11):1372-1379. doi:10.1016/j.joca.2010.08.005

149. Zhang W, Moskowitz RW, Nuki G, Abramson S, Altman RD, Arden N, Bierma-Zeinstra S, Brandt KD, Croft P, Doherty M, Dougados M, Hochberg M, Hunter DJ, Kwoh K, Lohmander LS, Tugwell P. OARSI recommendations for the management of

hip and knee osteoarthritis, Part I: Critical appraisal of existing treatment guidelines and systematic review of current research evidence. *Osteoarthritis Cartilage*. 2007;15(9):981-1000. doi:10.1016/j.joca.2007.06.014

150. Arokoski MH, Arokoski JPA, Haara M, Kankaanpää M, Vesterinen M, Niemitukia LH, Helminen HJ. Hip muscle strength and muscle cross sectional area in men with and without hip osteoarthritis. *J Rheumatol*. 2002;29(10):2185-2195.

151. Marshall AR, Noronha M de, Zacharias A, Kapakoulakis T, Green R. Structure and function of the abductors in patients with hip osteoarthritis: Systematic review and meta-analysis. *J Back Musculoskelet Rehabil*. 2016;29(2):191-204. doi:10.3233/BMR-150614

152. Lawrenson PR, Crossley KM, Vicenzino BT, Hodges PW, James G, Croft KJ, King MG, Semciw AI. Muscle size and composition in people with articular hip pathology: a systematic review with meta-analysis. *Osteoarthritis Cartilage*. 2019;27(2):181-195. doi:10.1016/j.joca.2018.10.008

153. Rahemi H, Nigam N, Wakeling JM. The effect of intramuscular fat on skeletal muscle mechanics: implications for the elderly and obese. *J R Soc Interface*. 2015;12(109):20150365. doi:10.1098/rsif.2015.0365

154. Liang KY, Zeger SL. Longitudinal data analysis using generalized linear models. *Biometrika*. 1986;73(1):13-22. doi:10.1093/biomet/73.1.13

155. Engelken F, Wassilew GI, Köhlitz T, Brockhaus S, Hamm B, Perka C, Diederichs und G. Assessment of Fatty Degeneration of the Gluteal Muscles in Patients With THA Using MRI: Reliability and Accuracy of the Goutallier and Quartile Classification Systems. *J Arthroplasty*. 2014;29(1):149-153. doi:10.1016/j.arth.2013.04.045

156. Peiris WL, Cicuttini FM, Constantinou M, Yaqobi A, Hussain SM, Wluka AE, Urquhart D, Barrett R, Kennedy B, Wang Y. Association between hip muscle cross-sectional area and hip pain and function in individuals with mild-to-moderate hip osteoarthritis: a cross-sectional study. *BMC Musculoskelet Disord*. 2020;21(1):316. doi:10.1186/s12891-020-03348-5

157. Kivle K, Lindland ES, Mjaaland KE, Svenningsen S, Nordsletten L. Gluteal atrophy and fatty infiltration in end-stage osteoarthritis of the hip: a case-control study. *Bone Jt Open*. 2021;2(1):40-47. doi:10.1302/2633-1462.21.BJO-2020-0179.R1

158. Goodpaster BH, Park SW, Harris TB, Kritchevsky SB, Nevitt M, Schwartz AV, Simonsick EM, Tylavsky FA, Visser M, Newman AB, for the Health ABC Study. The Loss of Skeletal Muscle Strength, Mass, and Quality in Older Adults: The Health, Aging and Body Composition Study. *J Gerontol A Biol Sci Med Sci*. 2006;61(10):1059-1064. doi:10.1093/gerona/61.10.1059

159. Yoshiko A, Tomita A, Ando R, Ogawa M, Kondo S, Saito A, Tanaka NI, Koike T, Oshida Y, Akima H. Effects of 10-week walking and walking with home-based resistance training on muscle quality, muscle size, and physical functional tests in

healthy older individuals. *Eur Rev Aging Phys Act*. 2018;15(1):13. doi:10.1186/s11556-018-0201-2

160. Pedroso MG, de Almeida AC, Aily JB, de Noronha M, Mattiello SM. Fatty infiltration in the thigh muscles in knee osteoarthritis: a systematic review and meta-analysis. *Rheumatol Int*. 2019;39(4):627-635. doi:10.1007/s00296-019-04271-2

161. De Pieri E, Friesenbichler B, List R, Monn S, Casartelli NC, Leunig M, Ferguson SJ. Subject-Specific Modeling of Femoral Torsion Influences the Prediction of Hip Loading During Gait in Asymptomatic Adults. *Front Bioeng Biotechnol*. 2021;9:679360. doi:10.3389/fbioe.2021.679360

162. Arokoski JPA, Jurvelin JS, Väätäinen U, Helminen HJ. Normal and pathological adaptations of articular cartilage to joint loading: Articular cartilage and joint loading. *Scand J Med Sci Sports*. 2000;10(4):186-198. doi:10.1034/j.1600-0838.2000.010004186.x

163. Saxby DJ, Lloyd DG. Osteoarthritis year in review 2016: mechanics. *Osteoarthritis Cartilage*. 2017;25(2):190-198. doi:10.1016/j.joca.2016.09.023

164. Constantinou M, Loureiro A, Carty C, Mills P, Barrett R. Hip joint mechanics during walking in individuals with mild-to-moderate hip osteoarthritis. *Gait Posture*. 2017;53:162-167. doi:10.1016/j.gaitpost.2017.01.017

165. Tateuchi H, Koyama Y, Akiyama H, Goto K, So K, Kuroda Y, Ichihashi N. Daily cumulative hip moment is associated with radiographic progression of secondary hip

osteoarthritis. *Osteoarthritis Cartilage*. 2017;25(8):1291-1298. doi:10.1016/j.joca.2017.02.796

166. Liao TC, Samaan MA, Popovic T, Neumann J, Zhang AL, Link TM, Majumdar S, Souza RB. Abnormal Joint Loading During Gait in Persons With Hip Osteoarthritis Is Associated With Symptoms and Cartilage Lesions. *J Orthop Sports Phys Ther*. 2019;49(12):917-924. doi:10.2519/jospt.2019.8945

167. Souza RB, Stehling C, Wyman BT, Hellio Le Graverand MP, Li X, Link TM, Majumdar S. The effects of acute loading on T1rho and T2 relaxation times of tibiofemoral articular cartilage. *Osteoarthritis Cartilage*. 2010;18(12):1557-1563. doi:10.1016/j.joca.2010.10.001

168. Souza RB, Fang C, Luke A, Wu S, Li X, Majumdar S. Relationship between knee kinetics during jumping tasks and knee articular cartilage MRI T1rho and T2 relaxation times. *Clin Biomech*. 2012;27(4):403-408. doi:10.1016/j.clinbiomech.2011.10.015

169. Van Rossom S, Smith CR, Zevenbergen L, Thelen DG, Vanwanseele B, Van Assche D, Jonkers I. Knee Cartilage Thickness, T1ρ and T2 Relaxation Time Are Related to Articular Cartilage Loading in Healthy Adults. Kellermayer MS, ed. *PLOS ONE*. 2017;12(1):e0170002. doi:10.1371/journal.pone.0170002

170. Li X, Han ET, Busse RF, Majumdar S. In vivoT1ρ mapping in cartilage using 3D magnetization-prepared angle-modulated partitionedk-space spoiled gradient echo

snapshots (3D MAPSS). *Magn Reson Med*. 2008;59(2):298-307. doi:10.1002/mrm.21414

171. Gallo MC, Wyatt C, Pedoia V, Kumar D, Lee S, Nardo L, Link TM, Souza RB, Majumdar S. T1ρ and T2 relaxation times are associated with progression of hip osteoarthritis. *Osteoarthritis Cartilage*. 2016;24(8):1399-1407. doi:10.1016/j.joca.2016.03.005

172. Pedoia V, Gallo MC, Souza RB, Majumdar S. Longitudinal study using voxel-based relaxometry: Association between cartilage $T_{1\rho}$ and T_2 and patient reported outcome changes in hip osteoarthritis: Voxel-Based Relaxometry in Hip Cartilage. *J Magn Reson Imaging*. 2017;45(5):1523-1533. doi:10.1002/jmri.25458

173. Li X, Wyatt C, Rivoire J, Han E, Chen W, Schooler J, Liang F, Shet K, Souza R, Majumdar S. Simultaneous acquisition of $T_{1\rho}$ and T_2 quantification in knee cartilage: Repeatability and diurnal variation: $T_{1\rho}$ and T_2 Quantification in Cartilage. *J Magn Reson Imaging*. 2014;39(5):1287-1293. doi:10.1002/jmri.24253

174. Samaan MA, Zhang AL, Popovic T, Pedoia V, Majumdar S, Souza RB. Hip joint muscle forces during gait in patients with femoroacetabular impingement syndrome are associated with patient reported outcomes and cartilage composition. *J Biomech*. 2019;84:138-146. doi:10.1016/j.jbiomech.2018.12.026

175. Perry J, Burnfield JM. *Gait Analysis: Normal and Pathological Function*. 2nd ed. SLACK; 2010.

176. Spoor CW, Veldpaus FE. Rigid body motion calculated from spatial co-ordinates of markers. *J Biomech*. 1980;13(4):391-393. doi:10.1016/0021-9290(80)90020-2

177. Grood ES, Suntay WJ. A Joint Coordinate System for the Clinical Description of Three-Dimensional Motions: Application to the Knee. *J Biomech Eng*. 1983;105(2):136-144. doi:10.1115/1.3138397

178. Schache AG, Baker R. On the expression of joint moments during gait. *Gait Posture*. 2007;25(3):440-452. doi:10.1016/j.gaitpost.2006.05.018

179. Pandy MG, Lin YC, Kim HJ. Muscle coordination of mediolateral balance in normal walking. *J Biomech*. 2010;43(11):2055-2064. doi:10.1016/j.jbiomech.2010.04.010

180. Wesseling M, de Groote F, Meyer C, Corten K, Simon JP, Desloovere K, Jonkers I. Gait alterations to effectively reduce hip contact forces: GAIT ALTERATIONS REDUCE CONTACT FORCES. *J Orthop Res*. 2015;33(7):1094-1102. doi:10.1002/jor.22852

181. Zacharias A, Pizzari T, Semciw AI, English DJ, Kapakoulakis T, Green RA. Comparison of gluteus medius and minimus activity during gait in people with hip osteoarthritis and matched controls. *Scand J Med Sci Sports*. 2019;29(5):696-705. doi:10.1111/sms.13379

182. Damm P, Brackertz S, Streitparth F, Perka C, Bergmann G, Duda GN, Winkler T. ESB Clinical Biomechanics Award 2018: Muscle atrophy-related increased joint

loading after total hip arthroplasty and their postoperative change from 3 to 50 months. *Clin Biomech*. 2019;65:105-109. doi:10.1016/j.clinbiomech.2019.04.008

183. Rasch A. Reduced muscle radiological density, crosssectional area, and strength of major hip and knee muscles in 22 patients with hip osteoarthritis. Published online 2009.

184. Kumar D, Wyatt CR, Lee S, Nardo L, Link TM, Majumdar S, Souza RB. Association of cartilage defects, and other MRI findings with pain and function in individuals with mild–moderate radiographic hip osteoarthritis and controls. *Osteoarthritis Cartilage*. 2013;21(11):1685-1692. doi:10.1016/j.joca.2013.08.009

185. Li X, Kuo D, Theologis A, Carballido-Gamio J, Stehling C, Link TM, Ma CB, Majumdar S. Cartilage in Anterior Cruciate Ligament–Reconstructed Knees: MR Imaging T1 $_{\rho}$ and T2—Initial Experience with 1-year Follow-up. *Radiology*. 2011;258(2):505-514. doi:10.1148/radiol.10101006

186. Nozaki T, Kaneko Y, Yu HJ, Kaneshiro K, Schwarzkopf R, Hara T, Yoshioka H. T1rho mapping of entire femoral cartilage using depth- and angle-dependent analysis. *Eur Radiol*. 2016;26(6):1952-1962. doi:10.1007/s00330-015-3988-5

187. Takao S, Nguyen TB, Yu HJ, Hagiwara S, Kaneko Y, Nozaki T, Iwamoto S, Otomo M, Schwarzkopf R, Yoshioka H. T1rho and T2 relaxation times of the normal adult knee meniscus at 3T: analysis of zonal differences. *BMC Musculoskelet Disord*. 2017;18(1):202. doi:10.1186/s12891-017-1560-y

188. Jungmann PM, Kraus MS, Nardo L, Liebl H, Alizai H, Joseph GB, Liu F, Lynch J, McCulloch CE, Nevitt MC, Link TM. T $_2$ relaxation time measurements are limited in monitoring progression, once advanced cartilage defects at the knee occur: Longitudinal data from the osteoarthritis initiative: Analysis of T $_2$ Value Progression. *J Magn Reson Imaging*. 2013;38(6):1415-1424. doi:10.1002/jmri.24137

189. Crema MD, Roemer FW, Marra MD, Burstein D, Gold GE, Eckstein F, Baum T, Mosher TJ, Carrino JA, Guermazi A. Articular Cartilage in the Knee: Current MR Imaging Techniques and Applications in Clinical Practice and Research <sup/>. *RadioGraphics*. 2011;31(1):37-61. doi:10.1148/rg.311105084

190. Koff MF, Amrami KK, Kaufman KR. Clinical evaluation of T2 values of patellar cartilage in patients with osteoarthritis. *Osteoarthritis Cartilage*. 2007;15(2):198-204. doi:10.1016/j.joca.2006.07.007

191. Pfirrmann CWA, Notzli HP, Dora C, Hodler J, Zanetti M. Abductor Tendons and Muscles Assessed at MR Imaging after Total Hip Arthroplasty in Asymptomatic and Symptomatic Patients. *Radiology*. 2005;235(3):969-976. doi:10.1148/radiol.2353040403

192. Chi AS, Long SS, Zoga AC, Read PJ, Deely DM, Parker L, Morrison WB. Prevalence and pattern of gluteus medius and minimus tendon pathology and muscle atrophy in older individuals using MRI. *Skeletal Radiol*. 2015;44(12):1727-1733. doi:10.1007/s00256-015-2220-7

193. Heemskerk AM, Damon BM. Diffusion Tensor MRI Assessment of Skeletal Muscle Architecture. *Curr Med Imaging Rev*. 2007;3(3):152-160. doi:10.2174/157340507781386988

194. Maillard SM. Quantitative assessment of MRI T2 relaxation time of thigh muscles in juvenile dermatomyositis. *Rheumatology*. 2004;43(5):603-608. doi:10.1093/rheumatology/keh130

Publishing Agreement

It is the policy of the University to encourage open access and broad distribution of all theses, dissertations, and manuscripts. The Graduate Division will facilitate the distribution of UCSF theses, dissertations, and manuscripts to the UCSF Library for open access and distribution. UCSF will make such theses, dissertations, and manuscripts accessible to the public and will take reasonable steps to preserve these works in perpetuity.

I hereby grant the non-exclusive, perpetual right to The Regents of the University of California to reproduce, publicly display, distribute, preserve, and publish copies of my thesis, dissertation, or manuscript in any form or media, now existing or later derived, including access online for teaching, research, and public service purposes.

DocuSigned by:
Alyssa Bird
D03AD556FA78451...
Author Signature

4/6/2022
Date